2018

Synthesis and kinetic activity analysis of substituted pyrazole, pyrazoline, and pyrazolidine alcohol dehydrogenase inhibitors

Meagan E. Hackey
mhackey003@g.rwu.edu

Synthesis and kinetic activity analysis of substituted pyrazole, pyrazoline, and pyrazolidine alcohol dehydrogenase inhibitors.

Meagan E. Hackey

Bachelor of Science Biochemistry

Department of Chemistry and Physics

Feinstein College of Social and Natural Sciences

Roger Williams University

May 2018

The thesis of *Meagan E. Hackey* was reviewed and approved by the following:

_____ Date _____
Dr. Lauren Rossi
Associate Professor of Chemistry
Thesis advisor

_____ Date _____
Dr. Avelina Espinosa
Professor of Biology

_____ Date _____
Dr. Cliff Timpson
Professor of Chemistry

Acknowledgements

I would first like to thank my advisor Dr. Rossi for all of her support and guidance in this project. I would also like to thank my committee, Dr. Espinosa and Dr. Timpson for their support throughout this process. I would also like to extend my gratitude to Hiba Wakidi and the MNS Stockroom staff for their continued support in lab. I would also like to thank my funding sources as well which include the RWU chemistry department, the CEED and Senior Thesis Grant program, and the provost fund for student research. Additionally, I would like to thank my family, friends, and faculty that have been an essential support through the entirety of my undergraduate career.

Table of Contents

List of Figures

List of Tables

List of Schemes

Abstract

Alcohol dehydrogenase inhibitors may be employed for the treatment of parasitic infection in humans. A series of substituted pyrazoline derivatives were synthesized to elucidate the pharmacophore for the inhibition of ADH. Targeted structure modification was used to alter the electronic and steric interactions associated with the enzyme active site. This study identified several effective *N*-aryl-carboxamide derivatives with horse liver ADH inhibition, comparable to that of 4-methylpyrazole, a known ADH inhibitor. The identification of pharmacophoric regions will allow for the methodological modification of these compounds to improve enzyme affinity and targeted inhibition. Future research may include additional solubility, toxicity and docking analysis of these compounds.

Chapter 1: Introduction

1.1: Introduction

Alcohol dehydrogenase (ADH) enzymes, present in both prokaryotes and eukaryotes, are responsible for alcohol metabolism and rely upon the reversible conversion between NADH (nicotinamide adenine dinucleotide) and NAD^+ for anaerobic metabolism (Scheme 1). Alcohol dehydrogenases are essential for the growth and survival of many bacteria and eukaryotic parasites through fermentation metabolism. In humans, alcohol dehydrogenases are required for the breakdown of alcohol into acetaldehyde and acetate.[1] Humans possess several enzymes capable of metabolizing alcohol through oxidative (alcohol dehydrogenase, cytochrome P450 isoxymes, and catalase) and non-oxidative pathways (fatty acid ethyl ester synthase and phospholipase D)[1]. As ADHs are present but nonessential in humans, therapeutics can be designed to inhibit anaerobic parasite metabolism via ethanol fermentation.

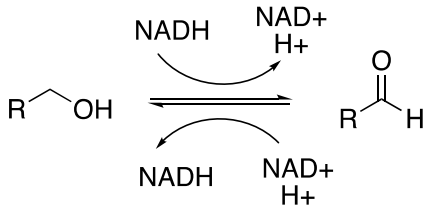

Scheme 1. Interconversion between alcohol and aldehyde by alcohol dehydrogenases.

Drug design relies heavily upon the identification of highly effective compounds with low toxicity in humans. Enzyme inhibitors are designed specifically to optimize binding efficiency at the active site of a target enzyme often of medicinal or therapeutic interest. An understanding of the enzyme active site characteristics may allow for optimization of cooperative interactions, thus increasing binding efficiency and enzyme inhibition.

Protein amino acid sequences, crystal structures, and modeling software are commonly used to understand likely binding interactions with target molecules. Most effective inhibitors will have a low inhibitory concentration (K_i)[a] required to significantly decrease function. At these low concentrations, the inhibitory compounds ought to have low toxicity as well. Inhibitors are commonly screened for drug properties including toxicity, carcinogenicity, and metabolic stability with LD_{50}[b], AMES (mutagenic potential determination), and LC-MS serum monitoring assays.

Fomepizole, 4-methylpyrazole (Figure 1), is an effective ADH inhibitor (K_i of 0.013 μM for horse liver ADH)[2] and subsequent structural modifications have been done to assess it as an anti-parasitic and anti-inflammatory agent[3–5]. This compound has been used as a therapeutic agent for the treatment of methanol poisoning since 1997[3–5]. 4-Methylpyrazole exhibits an ADH binding affinity greater than 8,000 times that of ethanol with no significant toxicity identified at concentrations required for methanol poisoning treatment[6]. The effectiveness of this small substructure has sparked interest in other nitrogen heterocycles, such as pyrazolines.

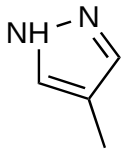

Figure 1. 4-Methylpyrazole

[a] The Inhibitor constant (K_i) of a compound is equal to the concentration of inhibitor that results in half maximal inhibition. Low K_i values are associated with effective inhibitors and stronger binding affinity.
[b] The LC_{50} for pharmaceuticals is equivalent to the treatment dose required for death in 50% of subjects. This value is directly correlated with drug toxicity.

Several pyrazoline and triazole derivatives are currently under investigation as therapeutic agents for inflammation, tumor suppression, and parasitic infection management[7–12]. Pyrrole and pyrazoles are the structural units for many natural products, including withasomnine and pyrazomycin (Figure 2)[10,13,14]. Pyrazomycin, (pyrazofurin), was isolated as a fermentation product of *Streptomyces candidus* and has proven to be an extremely effective monophosphate decarboxylase inhibitor (K_i 5.0 nM)[10]. The diverse applications of these derivatives in current pharmaceutics also indicates that these may be effective as inhibitors for a wide range of enzyme families including monoamine oxidases, NADPH oxidases, ipoxygenases and cyclooxygenases[15–17].

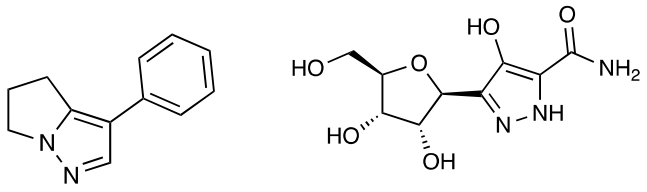

Withasomnine **Pyrazomycin**

Figure 2. "Withasomnine" (3-phenyl-5,6-dihydro-4*H*-pyrrolo[1,2-b]pyrazole) and "Pyrazomycin" ((1S)-1,4-Anhydro-1-(5-carbamoyl-4-hydroxy-1*H*-pyrazol-3-yl)-D-ribitol).

Pyrazoline derivatives specifically have been identified as effective anti-tubercular agents, which provide an alternative approach for the treatment of multi-drug resistant infections[18]. Additionally, several 1,3-disubstituted, 1,3,4-trisubstituted, and 1,3,5-trisubstituted pyrazolines have been identified as successful inhibitors of anaerobic growth in the parasitic protist *Entamoeba histolytica*. The mode of inhibition by these compounds has yet to be elucidated[8,19–21].

The thiocarbamoyl substituent (adjacent to the pyrazoline) may potentially be the pharmacophore for these molecules[22]. Carbamates and thiocarbamates have been shown to provide significant anti-fungal, anti-cancer, and anti-protozoal properties[22–24]. Thiocarbamoyl derivatives have exhibited an increased efficiency, relative to carbamoyl derivatives for *E. histolytica* trophozoite growth inhibition, which relies upon ADH function (*Eh*ADH2) for anaerobic growth and survival[25–28]. It is presumed that inhibition of the alcohol dehydrogenase function of this bifunctional enzyme will eliminate trophozoite growth.

The current treatment for *E. histolytica* infection is the antiprotozoal drug metronidazole. Metronidazole acts as a DNA replication inhibitor and has been proven to be effective for *E. histolytica* growth inhibition at an IC_{50}[c] value of 9.5 μM (Figure 3)[7,25,27]. This treatment is associated with significant neural toxicity and morbidity. As such, alternative treatments are desirable. The identification of alternative treatments for parasitic and bacterial infections are also necessary as current treatments are toxic and drug resistance is increasing.

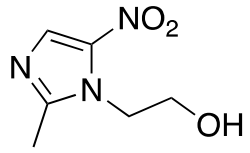

Figure 3. "Metronidazole", 2-methyl-5-nitroimidazole-1-ethanol.

[c] The IC_{50} value of a compound is equivalent to the concentration required to reduce substrate binding by 50%. Low IC_{50} values are associated with strong competitive inhibitors.

As ADH is nonessential to human health, the identification of effective ADH inhibitors may allow for the improved treatment of several bacterial and parasitic infections[25,28,29]. Additionally, the identification of pharmacophoric regions of substituted pyrazolines may allow for the targeted modification of known inhibitors for improved function and more effective drug treatments. Therefore, this research project may be directly applied to drug screening and subsequent pharmaceutical development.

The compounds synthesized in this study will be evaluated for their inhibitory efficiency in order to determine alternative therapeutic target scaffolds for the management of bacterial and parasitic infection. A goal of this study is to identify pyrazoline inhibitors with inhibition comparable to or better than that of 4-methylpyrazole. The identification of the potential pharmacophoric regions of substituted pyrazoline and/or pyrazole derivatives may then allow for further methodological modification for improved ADH affinity and targeted inhibition.

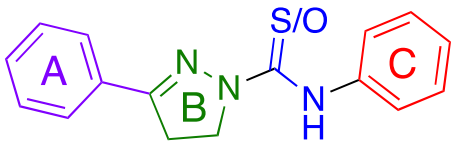

Figure 4. 1,3-diaryl substituted carbamoyl pyrazoline structure.

We propose to probe the carbamoyl pyrazoline structure through modification of regions **A**, **B**, and **C** (Figure 4). Rings **A** and **C** will be modified through the investigation of aryl substituents with varied electron donating and withdrawing properties, as well as modifying the aryl ring to alkyl groups. The pyrazoline heterocycle, **B**, will also be

investigated through oxidation and reduction. The importance of the carbamoyl region will be investigated with elimination of the carbonyl and nitrogen of the carbamoyl group. Additionally, alkylation of the secondary nitrogen will be explored. These structure-activity investigations ought to then elucidate the structural requirements for alcohol dehydrogenase inhibition.

Synthesized inhibitors will be screened as inhibitors of horse liver ADH. Enzyme activity, converting aldehyde to alcohol with NADH as a co-factor, will be monitored. (This is the reaction direction required for fermentative metabolism in many anaerobic pathogens.) Successful inhibitors will be those that significantly decrease the observed enzyme activity monitored through a change in absorbance at 340 nm resulting from the conversion of the coenzyme NADH to NAD^+ (Scheme 1). The assessment of a compound's inhibition activity will be relative to that of the blank, which contains all components of the assay except the proposed inhibitor compound.

Horse liver ADH was selected for all enzyme assays and modeling studies. Horse liver ADH is commonly used to model human ADH as it is homologous to the structure of human ADH at its active site. This enzyme is a eukaryotic ADH, which resembles the tertiary structure of many parasitic ADHs. Additionally, this enzyme is a zinc metalloenzyme requiring the coordination of two zinc cations for enzymatic activity[30]. The two zinc cations are tetracoordinated at the active site with two cysteines, a histidine, and one water molecule[30]. The substrates for horse liver ADH include benzaldehyde, acetaldehyde, ethanol, and benzyl alcohol[31]. Horse liver ADH also requires

NADH/NAD^+ as a cofactor for activity. NADH binds to an NADH binding domain before substrate coordinates/binds, thus closing the active site to its active form[30]. A methionine residue (position 141) buried in the active site pocket of human ADH is known to play an essential role in substrate binding as well as binding 4-methylpyrazole, a known ADH inhibitor[3]. This methionine residue lines the substrate binding pocket near the docking site of the methyl group of 4-methylpyrazole[3]. Horse liver ADH used in this study lacks methionine at the substrate binding region but other hydrophobic amino acids line the substrate binding site which may engage in similar interactions (Valine-52,53,58,63, Glycine-55,66, Leucine-57,61, Proline-60,62, Isoleucine-64, Alanine-65)[31].

The positive inhibition control compound within this study will be 4-methylpyrazole (Figure 1)[2,5,32]. This compound has previously been identified as a competitive inhibitor of alcohol dehydrogenases (K_i 0.013 μM for horse liver ADH) and our reported experimental enzymatic inhibition activity will be in relation to this this known value[2]. Enzyme assays will be performed with no pyrazoline inhibitor present as a positive control to ensure that the enzyme is functional under the given conditions. Additionally, control assays will be performed in the presence of NADH and inhibitor (without enzyme) to determine if there is any interaction between the pyrazoline compounds and NADH coenzyme that would perturb the spectrophotometric data analysis.

1.2: Synthesis

The reactions central to the synthetic efforts of this project are outlined below. The synthesis of 3-aryl 2-pyrazolines was required for all described herein. Substituents on

rings **A** and **C** were assessed in the *para* position for all derivatives to maximize the impact of the net electronic dipole of the aryl ring. The *para* substituent modifications focus upon the role of electron density within the ring (electron donating or withdrawing groups) rather than steric factors. Varied substituents at the *meta* position would likely target mainly inductive influences while the *ortho* position would likely target a substituent- dependent combination of electronic and steric influences.

1.2.1: Modification of Ring A:

In order to assess the role of the **A** ring, *para* substituents of varied electron donating or withdrawing character were synthesized and evaluated for their ADH inhibition (Scheme 2). Additionally, the influence of electronic and steric hindrance upon ADH inhibition at this pyrazoline position was assessed with a methyl group at this position in place of the 3-aryl group.

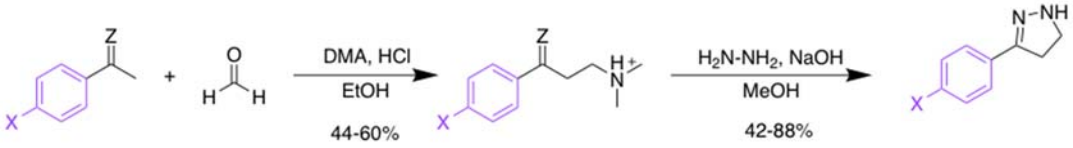

Scheme 2. Synthesis of 3-aryl 2-pyrazoline. Modifications of ring **A** including *para* substituents.

1.2.2: Modification of Ring B:

In order to assess the role of ring **B**, the pyrazoline ring, it will be either reduced or oxidized (Scheme 3 and Scheme 4, respectively). These modifications will affect most directly the electronic structure of the compounds, and minimally steric considerations.

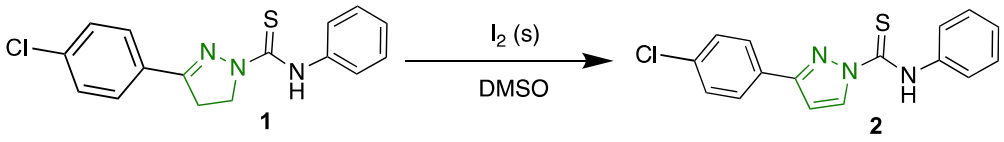

Scheme 3. Synthetic route to oxidize **1** to form 3-(4-chlorophenyl)-1-(phenylthiocarbamoyl)-2-pyrazole **2**.

Oxidation of pyrazoline **1** to pyrazole **2** has been successfully performed and will be used to evaluate the effects of increased electron density at ring **B** (Scheme 3)[18]. This transformation decreases the net dipole of the molecule and adds additional aromatic character to the molecule. This transformation alters proposed hydrogen bonding and stacking interactions the compounds may have within the enzyme active site.

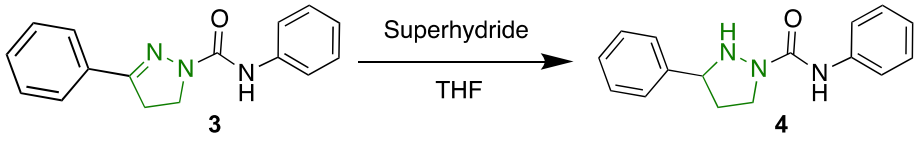

Scheme 4. Reduction of *N*,3-diphenyl-4,5-dihydro-1*H*-pyrazole-1-carboxamide **3** to *N*,3-diphenylpyrazolidine-1-carboxamide **4**.

Reduction of pyrazoline **3** via Superhydride® (lithium triethylborohydride) to pyrazolidine **4** (Scheme 4) probes the effects of decreased electron density at the pyrazoline position. This modification also shortens the overall conjugated system within the molecule. This modification thus would aid in the identification of the essential elements of the pyrazoline moiety for enzyme binding and inhibition.

1.2.3: Modification of Ring C:

In order to assess the role of ring **C** ring in ADH inhibition, a series of derivatives with *para* substituents of varied electron donating/withdrawing character were prepared (Scheme 5). Additionally, several *N*-propyl derivatives were synthesized to evaluate the importance and role aromatic character at this position may have upon ADH inhibition.

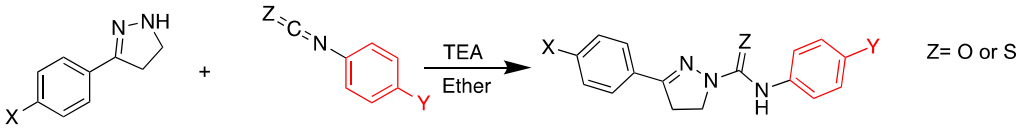

Scheme 5. Synthesis of 1,3-diaryl carbamoyl 2-pyrazoline with varied substituents on the **C** ring.

1.2.4: Modification of the carbamoyl region:

In order to assess the role of electronics at the carbamoyl region on ADH inhibition, several carbamoyl and thiocarbamoyl derivatives were synthesized (Scheme 6). The net dipole difference between carbamoyl and thiocarbamoyl derivatives probes primarily the role of electronics at this position. Additionally, an amide derivative was prepared to probe the role of the carbamoyl group upon ADH inhibition (Scheme 7). Alkylation of the carbamoyl or thiocarbamoyl region was also investigated to understand the role of a large net dipole at this position, and to a lesser extent steric considerations (Scheme 8, Scheme 9).

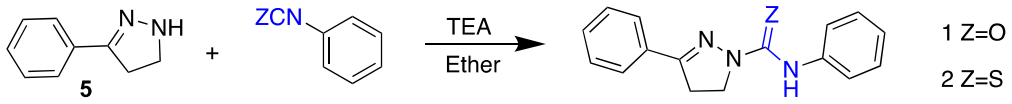

Scheme 6. Synthesis of 1,3-diaryl carbamoyl/thiocarbamoyl derivatives.

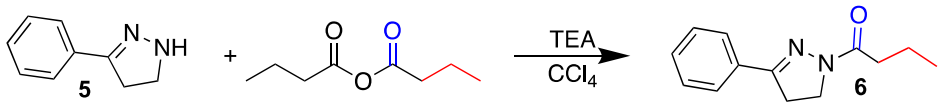

Scheme 7. Synthesis of compound **6**, 1-(3-phenyl-4,5-dihydro-1*H*-pyrazol-1-yl)butan-1-one.

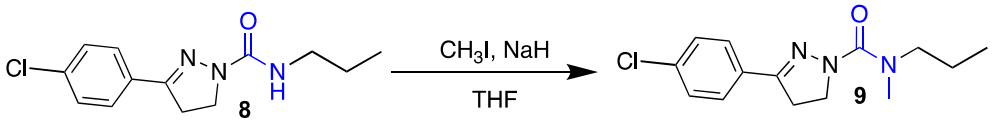

Scheme 8. Synthesis of compound **9**, *N*-methyl-3-phenyl-*N*-propyl-4,5-dihydro-1*H*-pyrazole-1-carboxamide.

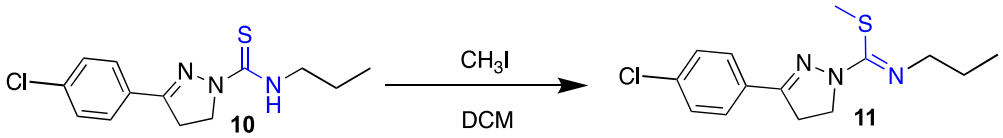

Scheme 9. Synthesis of compound **11**, (1Z)-1-(methylsulfanyl)-*N*-propyl-1-(3-(4-chlorophenyl-4,5-dihydro-1*H*-pyrazol-1-yl)methanimine.

1.3: AutoDock Visualization

AutoDock modeling software will be employed in this study to visualize potential binding modes for 1,3-disubstituted 2-pyrazolines with the horse liver ADH crystal structure. AutoDock is an open source, three-dimensional modeling software that is commonly employed for ligand docking analysis and protein visualization[33]. AutoDock

was selected over other modeling programs because it is an open source software with user interface that does not require coding and it is a common method for calculating various protein-ligand docking interactions (where ligand may be substrate, cofactor, inhibitor, or activator)[33]. This program performs a series of Lamarckian genetic algorithms to determine likely binding configurations based upon approximations of favorable ligand docking interactions[33].

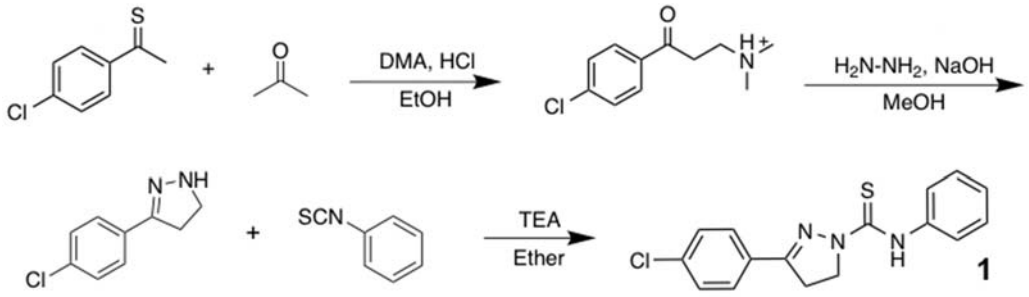

Scheme 10 Synthesis of compound **1**, 3-(4-chlorophenyl)-1-(phenylthiocarbamoyl)-2-pyrazoline.

Compound **1** has been successfully synthesized and used for the evaluation of inhibitory ability of 1,3-disubstituted 2-pyrazoline against ADH (Scheme 10). This compound was selected for AutoDock modeling as it was the only completed compound at the time of modeling analysis.

The protein crystal structure of horse liver ADH was utilized to mathematically compute one possible enzyme conformation and inhibitor binding site, based upon common ligand-binding interactions (PDB 1HLD) (Figure 5)[31]. The crystal structure of the synthesized pyrazoline compounds are unknown and solvent influences may further alter

the conformation of horse liver ADH in screening assays. This analysis is thus an estimate utilized to visualize potential binding sites. Experimental data will be used to determine modes of inhibition and to evaluate inhibitor efficiency.

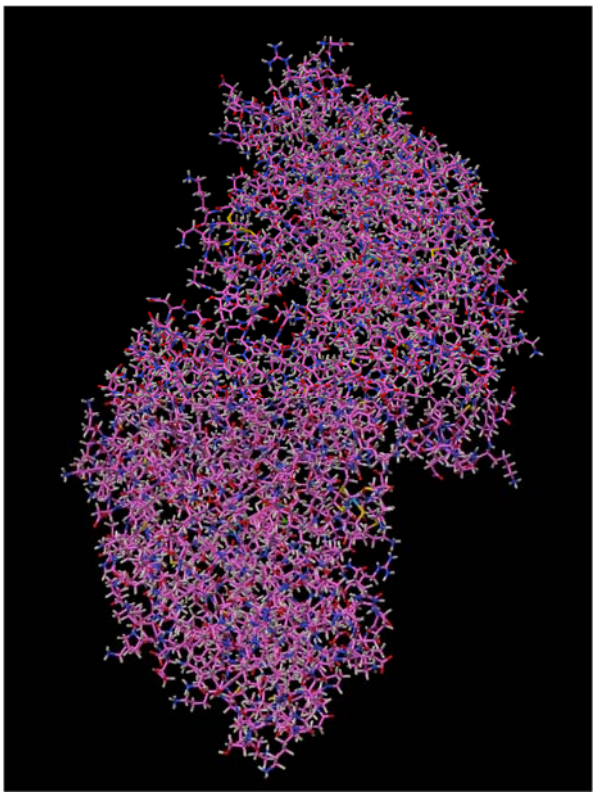

Figure 5. Crystal structure of horse liver ADH with NADH and benzyl alcohol bound (PDB 1HLD) used for all AutoDock visualization in this study[31].

The pyrazoline **1** structure was evaluated with AutoDock software to visualize a likely mode of binding to the horse liver ADH-NADH-benzyl alcohol complex (PDB 1HLD, Protein Data Bank ID 4XD2, the same enzyme complex proposed for kinetics assays). Additional studies would be required to determine the most likely binding modes for other synthesized compounds with the horse liver ADH crystal structure.

1.4: Description of Project

The overall goal of the studies described herein has been to elucidate structural attributes responsible for pyrazoline-based inhibition of alcohol dehydrogenases. This aim will be accomplished through the synthesis of 1,3-disubstituted carbamoyl- 2-pyrazoline derivatives. Targeted and systematic structural modifications will be used to probe the pharmacophoric region of 1,3-diaryl pyrazoline carbamates by assessing enzyme activity in response to these structural and electronic changes. The steric and electronic influences of the pyrazoline structure upon bioactivity will be assessed through the systematic alteration of each of the three rings (Figure 4). Electronics are anticipated to play a significant role with the binding and coordination of these molecule with the enzyme complex or active site[22]. The thionyl and pyrazoline regions are proposed to play an essential role in binding efficiency due to the highly electrophilic character of the ADH binding domain[31]. Modification of the electronics and sterics at these positions ought to allow for the identification of essential structural components for optimal ADH binding.

Chapter 2: Research Methods and Procedures

2.1: Materials and Methods

All reagents used for this study were purchased from Sigma Aldrich or Alfa Aesar and were used in their commercial state without further purification. Concentrations of reagents used were as follows, unless otherwise indicated: hydrazine hydrate (60% reagent grade), absolute ethanol, and paraformaldehyde (95% reagent grade, powder). The derivatives were characterized using ^{1}H NMR, ^{13}C NMR, FT-IR spectroscopy, UV-Vis spectroscopy, and/or melting point analysis. All NMR measurements were recorded using a JEOL EXQ 300 MHz FT-NMR Spectrometer. Deuterated solvents used for NMR were sourced from Sigma Aldrich and ampules were used for samples analyzed in dmso-d_6. All IR measurements were recorded using a Perkin Elmer Spectrum Two FT-Infrared Spectroscopy instrument. A BUCHI M-565 melting point instrument was used for all melting point analysis. Abbreviations used for common solvents and reagents include dimethylsulfoxide (DMSO), tetrahydrofuran (THF), dimethylformamide (DMF), nicotinamide adenine dinucleotide (NAD^+), nicotinamide adenine dinucleotide reduced disodium salt (NADH), and dimethylamine (DMA).

IUPAC refers to the common 2-pyrazoline structure as 4,5-dihydro-*1H*-pyrazole. The common nomenclature will be used henceforth in this study.

2.1.1: Modification of Ring **A**:[20]

All derivatives probing the influence of ring **A** on ADH inhibition were synthesized as described (Table 1, Scheme 3, Scheme 5). Phenone (83 mmol, 1

equiv.), dimethylamine hydrochloride (108 mmol, 1.3 equiv.), and paraformaldehyde (108 mmol, 1.3 equiv.), and four drops of 0.4 M hydrochloric acid was refluxed in a stirred solution of 13.5 mL ethanol. This solution was cooled after 1.5 hours and 100 mL of acetone was added. The resulting solid was washed and vacuum dried. A warm solution of 26.4 mL methanol and this product was added over 10 minutes to a solution of 5 mL hydrazine hydrate and 2.70 mL 50% sodium hydroxide in 6.70 mL methanol. This solution was refluxed for 45 minutes after which the methanol was evaporated under reduced pressure to yield the product as an oil. This product (12.0 mmol, 1.00 equiv.) was dissolved in 40.0 mL dry ether with three drops of triethylamine and isocyanate (12.0 mmol, 1.00 equiv.). This solution was stirred for three days at room temperature and the resulting solid was filtered and vacuum dried.

Table 1. Synthesis of derivatives with modifications of the ring **A** position.

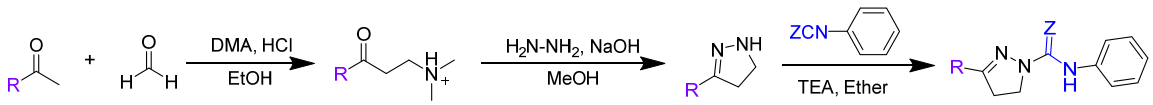

Compound #	R	Z	Yield
3	H	O	42.8%
12	H	S	54.5%
13	*p*-chlorophenyl	O	40.0%
14	*p*-methoxyphenyl	O	32.0%
15	*p*-tolyl	O	58.0%
16	*p*-fluorophenyl	O	97.0%
17	CH_3	O	69.0%
1	*p*-chlorophenyl	S	39.0%

2.1.2: Modification of Ring **B**:[18]

All derivatives probing the influence of oxidation of ring **B** were prepared as described (Scheme 11). Pyrazoline **13** (0.079 mmol, 0.025 g, 1.0 equiv.) and an iodine crystal (0.0373 g) was dissolved in 0.50 mL of DMSO[18]. This solution was refluxed for two hours before cooling to ambient temperature. A thick paste resulted with an orange-brown liquid supernatant. The liquid was decanted and the solid was washed twice with aqueous 10% sodium thiosulfate. The washes were combined with the decanted liquid. Ethanol (2 mL) was added with two drops of 0.60 M acetic acid resulting in the precipitation of black solid. The supernatant was decanted, and a small quantity of ice was added to the supernatant which induced immediate precipitation.

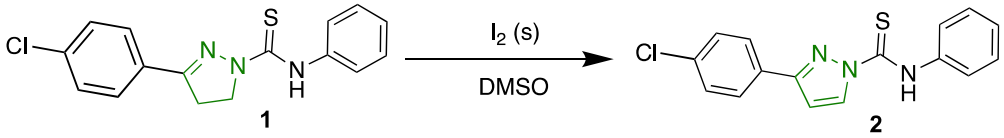

Scheme 11. Oxidation of compound **1**, 1,3-disubstituted thiocarbamoyl 2-pyrazoline to compound **2**, 1,3-disubstituted thiocarbamoyl pyrazole.

The reduction of ring **B** was attempted several times without isolation of the desired pyrazolidine product (Scheme 12). A Schlenck flask was oven and flame dried and pyrazoline was desiccated. Pyrazoline (0.21 mmol, 0.08 g, 1.00 equiv.) and 6 mL anhydrous THF were added and three cycles of freeze-pump-thaw were performed (liquid nitrogen and ethanol bath). The solution was warmed to 0 °C and Superhydride® (0.51 mmol, 0.52 mL, 2.50 equiv.) was added dropwise[12]. This solution was stirred two hours at 0 °C before quenching with 2 M NaOH (2.5

mL) slowly. The resulting liquid was concentrated, washed with 2 M NaOH, and back extracted in DCM. The organic layer was dried over magnesium sulfate and concentrated. Starting pyrazoline reactant was recovered as a white solid. This synthesis was repeated with longer reaction time (8 hours) and additional Superhydride® equivalents, as well as warming to ambient temperature. Neither modification resulted in successful synthesis of this derivative.

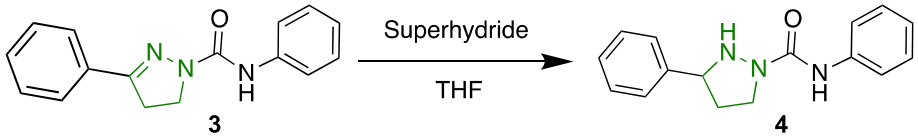

Scheme 12. Attempted reduction of compound **3**, 1,3-disubstituted carbamoyl 2-pyrazoline to compound **4**, 1,3-disubstituted carbamoyl pyrazolidine.

2.1.3: Modification of Ring **C**:[20]

All derivatives probing the influence of ring **C** upon ADH inhibition were synthesized as described (Table 2). Ketone (83 mmol, 1.0 equiv.), dimethylamine hydrochloride (108 mmol, 1.30 equiv.), and paraformaldehyde (108 mmol, 1.3 equiv.), and four drops of 0.4M hydrochloric acid was refluxed in a stirred solution of 13.5 mL ethanol. This solution was cooled after 1.5 hours and 100 mL of acetone was added. The resulting solid was washed and vacuum dried. A warm solution of 26.4 mL methanol and this product was added over 10 minutes to a solution of 5 mL hydrazine hydrate and 2.70 mL 50% sodium hydroxide in 6.70 mL methanol. This solution was refluxed for 45 minutes after which the methanol was evaporated under reduced pressure to yield the 3-aryl substituted 2-pyrazoline

product **5** as an oil. This product (**5**, 12.0 mmol, 1.00 equiv.) was dissolved in 40.0 mL dry ether with three drops of triethylamine and isocyanate (12.0 mmol, 1.00 equiv.). This solution was stirred for three days at room temperature and the resulting solid was filtered and vacuum dried.

Table 2. Synthesis of derivatives with modification at the ring **C** position.

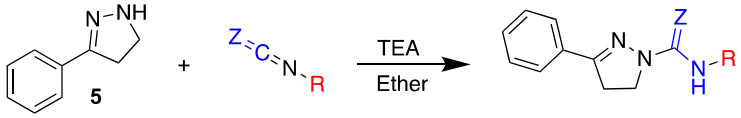

Compound #	R	Z	Yield
18	n-propyl	O	39.2%
19	n-propyl	S	6.90%
20	4-methoxyphenyl	O	80.0%
21	4-chlorophenyl	O	94.0%
22	4-nitrophenyl	O	83.2%

2.1.4: Modification of the Carbamoyl Region:[21,34,35]

The *N*- substituted 2-pyrazoline was prepared as described in the modification of ring **A** and **C** (Scheme 13). 3-aryl substituted 2-pyrazoline (**5**, 12.5 mmol, 1 equiv.) was dissolved in 50 mL chloroform and cooled to 0°C. Triethylamine (12.5 mmol, 1 equiv.) was added gradually to the solution. Butyric anhydride (12.5 mmol, 1 equiv.) was added and the solution was stirred for three hours while warming to room temperature. Solid precipitate resulted, which was isolated via vacuum filtration and dried.

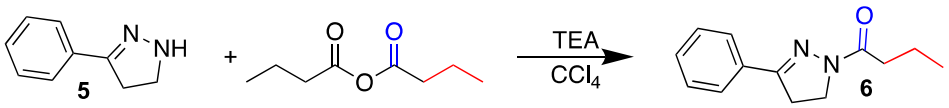

Scheme 13. Synthesis of amide derivative **6** for investigation of the carbamoyl region of *N*-substituted 2-pyrazolines.

Alkylation of a carbamoyl derivative was also investigated (Scheme 14)[21]. 3-(4-chlorophenyl)-*N*-propyl-4,5-dihydro-1*H*-pyrazole-carboxamide **8** (20.0 mg, 0.075 mmol, 1.00 equiv.), prepared previously was dissolved in 0.40 mL anhydrous THF, under nitrogen. Sodium hydride (60.0%) (0.23 mmol, 3.00 equiv.) was added to the solution and stirred one hour on ice. Methyl iodide (0.08 mmol, 1.00 equiv.) was added to the stirring solution dropwise and stirred. The reaction was monitored by TLC with a 50% ethyl acetate: hexanes mobile phase. After two hours the solution was cooled on ice and an additional equivalent of NaH was added followed by an additional 1.50 equivalents of methyl iodide. After another four hours an additional equivalent of methyl iodide was added. After another 24 hours stirring at room temperature under nitrogen, ice was added to the solution and the resulting precipitate was filtered. The resulting crude yellow oil and solid white precipitate was purified via gradient silica flash column chromatography (12-52% ethyl acetate: hexanes) to isolate 6.3 mg of an off-white solid **9**, in 29% yield. (Recovered pyrazoline reactant, 15.6 mg).

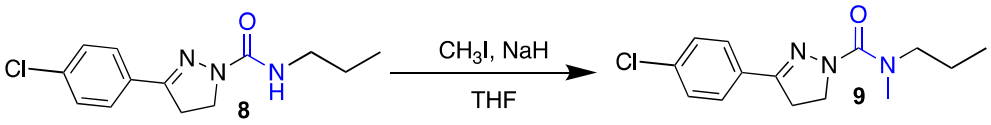

Scheme 14. Synthesis of an alkylated *N*-propyl carbamoyl 2-pyrazoline derivative.

Synthesis of the *N*- alkylated thiocarbamoyl derivative was also performed (Scheme 15)[35]. 3-(4-chlorophenyl)-*N*-propyl-4,5-dihydro-1*H*-pyrazole-carbothiamide **10** (25.0 mg, 0.089 mmol, 1.00 equiv.) was dissolved in 1 mL DCM. This solution was chilled on ice before the gradual addition of methyl iodide (0.14 mL, 2.3 mmol, 25 equiv.). This stirring solution was warmed to room temperature and stirred at ambient temperature for 68 hours. The reaction was monitored by TLC with a 4:1 hexanes: ethyl acetate mobile phase. This solution was concentrated under reduced pressure, reconstituted in DCM, and washed with 10% NaOH. The organic layer was dried over $MgSO_4$, filtered, and concentrated to yield a crude yellow viscous oil (21.6 mg, 81% yield). This oil was purified via silica flash column chromatography (4:1 hexanes: ethyl acetate) to yield **11** as a white solid (8.8 mg, 33% yield).

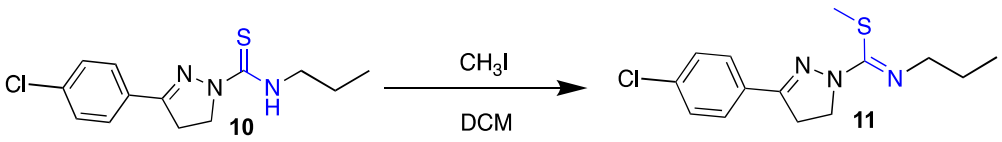

Scheme 15. Synthesis of an alkylated *N*-propyl thiocarbamoyl 2-pyrazoline derivative **11**.

2.2: Enzyme Assays

Horse liver alcohol dehydrogenase sourced from Sigma Aldrich (A9589) was used for all enzymatic kinetics assays. High-throughput enzyme kinetics screens were performed with 0.25 mM NADH (cofactor), 0.25 μM horse liver ADH, and 3 mM benzaldehyde (substrate) in 50 mM triethanolamine (TEA) buffer pH 7.2. High-throughput enzyme

kinetics assays were performed using a Spectro STAR Omega plate reader at 340 nm with UV-Transparent polystyrene 96 well plates. The plate reader was set in plate mode with a positioning delay of 0.2 seconds, a kinetic window of 1, 10 cycles, with 10 flashes per well and cycle, and a cycle time of 15 seconds. The orbital shaking frequency was set at 500 rpm with five seconds shaking before each cycle. The temperature of the plate reader was maintained at 30 °C for all readings. Each kinetics assay trial was monitored for a 5-minute time interval and temperature was maintained at 30 °C. A maximum of six wells were used per trial assay to minimize error associated with mixing time. A positive control and DMSO control were included for each assay trial to compare consistency between individual runs. Prepared NADH and ADH stock solutions were stored at 4 °C for long term storage (two months NADH, two weeks ADH).

Several method conditions were employed for enzyme assay optimization, positive inhibition controls, and inhibitor trials. All assay conditions monitored the decrease in absorbance at 340 nm resulting from the conversion of NADH (absorbs at 340 nm) and NAD+ (minimal absorbance at 340 nm) cofactors accompanying the conversion of benzaldehyde substrate to benzyl alcohol (Scheme 16). All enzyme activity slopes reported are measured in units of M sec^{-1}.

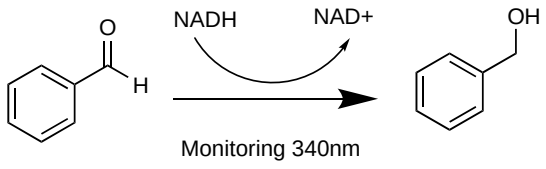

Scheme 16. Conversion of benzaldehyde to benzyl alcohol performed by ADH and monitored in enzyme assays with decrease in absorbance at 340 nm.

2.2.1: Method A

This method was employed for high throughput enzyme screens with substrate added last and readings using an incubated plate reader. Plates were prepared with NADH, ADH, DMSO or diluted samples (1, 10, and 100μM final inhibitor concentration), and buffer at room temperature and incubated five minutes in the plate reader at 30 °C, with shaking every 10 seconds at 500 rpm. After incubation, benzaldehyde was added, mixed by pipetting, and immediately inserted for kinetic readings at 340 nm. The average time between benzaldehyde addition and the initial reading was approximately 15 seconds.

2.2.2: Method B

This method was employed for high throughput enzyme screens with cofactor added last and readings using an incubated plate reader. Plates were prepared with NADH, benzaldehyde, DMSO or diluted samples (1, 10, and 100 μM final concentration), and buffer at room temperature and incubated 5 minutes in the plate reader at 30 °C, with shaking every 10 seconds at 500 rpm. After incubation, ADH was added, mixed by pipetting, and immediately inserted for kinetic readings at 340 nm. The average time between ADH addition and the initial reading was approximately 15 seconds.

2.2.3: Method C

This method was employed for assay verification using a double beam UV-Vis spectrophotometer and quartz cuvettes. Following Method A described above

except performed using a Cary 5000 spectrophotometer with 1 cm quartz cuvettes. The same concentration of reagents was used, with benzaldehyde added post incubation at 30 °C. This instrument does not feature temperature control, so cuvettes were incubated in a water bath at 30 °C and ambient temperature was approximately 27 °C.

2.2.4: Method D

This method was employed to identify interference at the monitoring wavelength for assay components. Several assays were also performed using a Cary 5000 UV-Vis-NIR spectrophotometer with 1 cm quartz cells. These assays verified that the enzyme initial rate was appropriately monitored under these assay conditions. For several trials, the same concentration of reagents was used from Method A and the volume was adjusted to a cuvette final volume of 600 μL. Additional trials including double substrate (i.e. 6 mM benzaldehyde) or double co-factor (i.e. 0.5 mM NADH) concentration were included.

2.2.5: Method E

This method was employed to identify interfering absorbencies near the monitoring wavelength for assay components. Wavelength scans from 280- 400 nm were also done to determine if interactions between assay components influenced absorbance readings. These assays used the same reagent concentrations as Method A but some assay components were omitted in each trial. The final cuvette volume was adjusted to 600 μL for all combinations. All

trials were performed with 3 μL DMSO added and measurements were taken immediately after reagent addition using the Cary 5000 instrument at ambient temperature.

2.2.6: Method F

This method was employed to monitor the change in absorbance of tested inhibitor derivatives at different buffer pH conditions to assess any compound degradation at the pH employed. Trials were performed with 100 μM of compound **6** in TEA buffer ranging from pH 4.19 to 8.90. Buffer pH was adjusted using a Fisherbrand™ Accumet™ AB150 pH meter and the addition of 1 N sodium hydroxide or 1 N hydrochloric acid. Wavelength scans were recorded for only buffer and compound **6** from 280 to 400 nm over five minutes to monitor the stability of assay components at varied buffer pH. These measurements were recorded at room temperature using the Cary 5000 instrument and 1 cm quartz cuvettes.

A minimum of three trials were performed for each compound or control. Reported slopes represent the average of all slopes from all trials at a given concentration. Reported remaining activity was calculated using the ratio of the average slope for each concentration over the average of all DMSO control runs. The average and standard deviation was calculated for each compound and percent remaining activity was calculated as the ratio between the average slope of each compound trial and the average of all DMSO standard runs. Outliers were determined and eliminated if they fell outside

of the lower 25% and upper 75% bounds of the data set determined by the first and third quartile calculations. Outliers were determined as those that lie outside of 1.5 times the inner quartile range.

2.3: Ternary Complex Fluorescence Analysis

Fluorescence spectroscopy analysis was performed on combinations of assay components to monitor ternary complexation between ADH and NADH with DMSO as a co-solvent. Previous studies identified a ternary complex for NADH bound to ADH with fluorescence emission at approximately 420 nm for an excitation wavelength of 328 nm at pH 7.2[36]. The following combinations of assay components were analyzed for their fluorescence emission intensity at the concentrations used in Method A: (1) NADH, ADH, ADH and DMSO scanned immediately upon addition, (2) NADH and ADH scanned immediately upon addition, (3) NADH and ADH incubated for five minutes at 30 °C, and (4) ADH, NADH, and DMSO incubated for five minutes at 30 °C. 1 cm quartz fluorescence spectroscopy cells were used for all measurements. A Horiba Fluorolog 3 spectrofluorometer with FluorEssence 3.0.0 software was used for all fluorescence measurements. The excitation wavelength used for all scans was 328 nm with a slit width of 1 nm and an increment of 1 nm for a monitoring frame of 338- 550 nm.

2.4: AutoDock Docking Analysis

ChemDraw 15.0 Professional MM2 Minimization calculations were used to determine the lowest energy conformation of pyrazoline **1** based upon computation of the

conformation with the fewest steric interactions based upon free rotation about sigma bonds. The default parameters were used for MM2 minimization in ChemDraw3D with a step interval of 2 fs, frame interval of 10 fs and 10,000 iterations. AutoDock Version 1.5.6 with AutoDock tools and an X-Quartz X11 display server was used for all analyses. Standard AutoGrid ligand docking analysis was performed with the system default parameters.

Chapter 3: Results

3.1: AutoDock Docking Analysis

ChemDraw Professional 15.0 MM2 Minimization was used to generate the lowest energy conformer for pyrazoline **1** which was used for docking analysis (Figure 6).

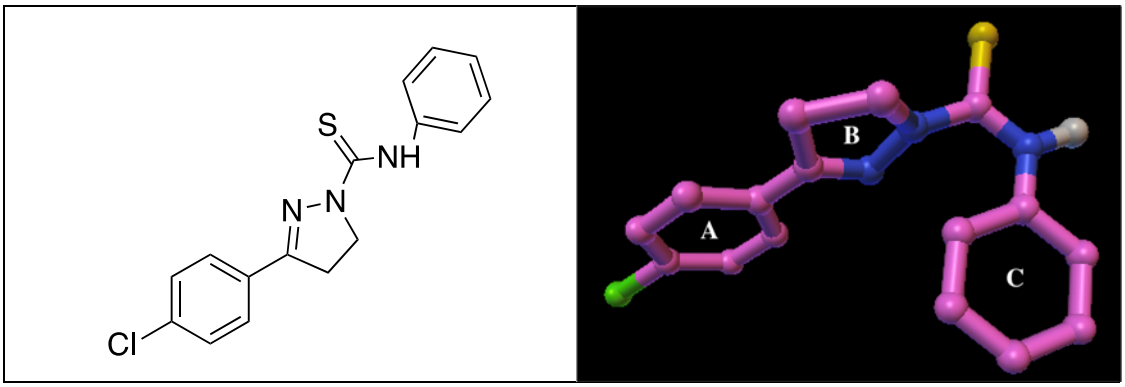

Figure 6. Three-dimensional representation (right) of the lowest energy conformation of compound **1** (left) in AutoDock as determined by ChemDraw Professional 15.0 MM Minimization calculation.

Autodock software was used to visualize a possible binding site for pyrazoline **1** if it was to behave as a competitive inhibitor (Figure 7)[33]. Figure 7 illustrates a theoretical mode of binding for pyrazoline **1** with the horse liver ADH active site (PDB 1HLD, Protein Data Bank ID 4XD2, cofactor and substrate bound, assumed competitive inhibition) based upon the minimized steric interactions. This theoretical model was generated with the lowest energy conformation of **1** assuming the maximum number of rotational modes. Figure 7 provides a topological representation of this binding interaction and is indicative of a likely shallow binding interaction. A potential binding region for compound **1** is the

active site for the alcohol dehydrogenase, which is a highly electrophilic region with many hydrogen-bonding residues. The bent conformation of pyrazoline **1** overall may orient the thiocarbamate group to face into the active site of the horse liver ADH with phenyl groups facing outwards (Figure 7). These model approximations indicate a shallow potential binding site that is available to water, which increases the number of possible inhibitor conformations.

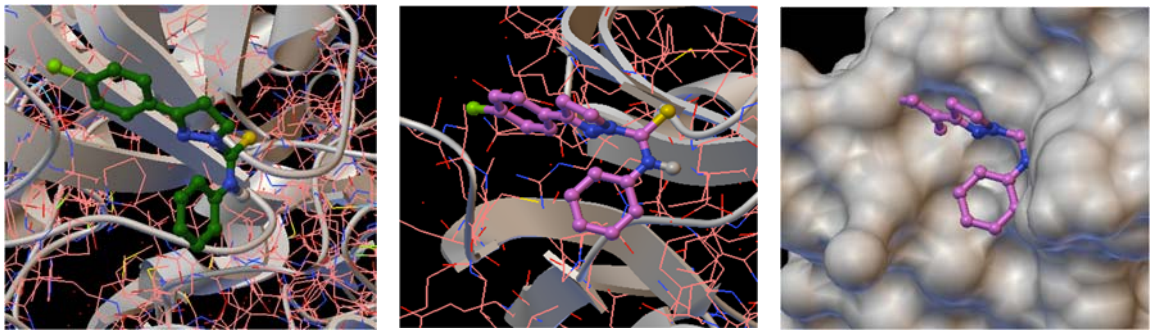

Figure 7. AutoDock modeling of the interaction between compound **1** and horse liver ADH protein secondary structure, top/side view (left), top view (middle), and topological representation (right).

The AutoDock viewing of the protein secondary structure identified a nonpolar active site with several hydrogen bonding residues that may interact with inhibitors (Figure 7). Residues at the substrate binding site include several polar residues (Serine-54 and Threonine-56,59), many nonpolar residues (Valine-52,53,58,63, Glycine-55,66, Leucine-57,61, Proline-60,62, Isoleucine-64, Alanine-65), and several positively charged residues (Aspartic acid-49,50 and Histidine-51,67)[31].

3.2: Initial Enzyme Assay Optimization

Several modified assays were performed to verify that the assay was effective at monitoring enzyme activity within the initial rate window. In the absence of enzyme, benzaldehyde or NADH, a significant decrease in activity was observed (Table 3). Only 3.24±1.35 percent remaining activity was observed when NADH was removed relative to the positive control containing all assay components. A greater change in absorbance readings (at 340 nm) was observed in the absence of enzyme or benzaldehyde (Table 3). This high change in absorbance in the absence of substrate or enzyme suggests auto-reduction of the cofactor under the assay conditions. All enzyme activity slopes reported are measured in units of M sec^{-1}.

Table 3. Enzyme activity control assays. All assays performed according to Method C.

	Slope	St. Dev.	RSD	Average Remaining Activity ±STD
Positive Control	-3.85E-04	4.44E-05	-0.12	100±0.00 (n=9)
No ADH	-1.40E-04	2.01E-04	-1.44	36.3±5.22 (n=3)
No Benzaldehyde	-1.73E-04	4.24E-05	-0.24	45.0±1.10 (n=3)
No NADH	-1.25E-05	5.20E-05	-4.16	3.24±1.35 (n=8)

The role of enzyme concentration was investigated, and 60.8% activity was observed with half enzyme concentration relative to the positive control (Table 4). This assay was performed to verify that enzyme concentration was rate limiting with substrate and cofactor in excess. This ensures that the assay exists under steady state conditions with the concentrations of substrate and cofactor changing negligibly. This drives the equilibrium to position in the desired direction, ensuring that the enzyme initial rate is being monitored. An increase in activity was observed with double the enzyme

concentration relative to the positive control (Table 4). The role of substrate concentration was also investigated and a minimal increase in activity was observed when the concentration of benzaldehyde was doubled (Table 5).

Table 4. Enzyme concentration assays. Assay performed according to Method C, with indicated modification.

Enzyme	Slope	Percent Activity Relative to Positive Control
Positive Control (0.25 μM ADH)	-8.23E-04	100% (n=1)
Half ADH (0.13 μM)	-5.01E-04	60.8% (n=1)
Double ADH (0.5 μM)	-1.01E-03	122% (n=1)

Table 5. Substrate concentration assays. Assay performed according to Method C with indicated modification.

Substrate	Slope	Percent Activity Relative to Positive Control
3 mM Benzaldehyde	-6.91E-04	100% (n=1)
6 mM Benzaldehyde	-8.32E-04	120% (n=1)

3.3: Solvent Controls

All derivatives were screened with DMSO as a co-solvent. DMSO is a known competitive ADH inhibitor with a K_i of 5 mM for horse liver ADH[36]. DMSO is the standard solvent for high throughput screens and has been used up to 3% in screens of acetaldehyde dehydrogenase activity[37]. Other suggested solvents included DMF which also exhibits ADH inhibition and ethanol which is a substrate for the reverse reaction and would influence kinetics readings[38]. Assays were performed to determine the optimal

DMSO concentration for screening. The ideal volume of DMSO resulted in a maximum remaining enzyme activity and minimal dispensing error. The greatest volume of DMSO having the minimal impact upon ADH enzymatic activity was 3 μL with 34.6% remaining activity relative to the positive control without DMSO (Figure 8). This volume of DMSO was used for all DMSO standard controls and derivative screenings. Stock solutions were adjusted to maintain the same volume of DMSO in all assay trials for reduced error associated with dispensing/ mixing. Significant inhibition was observed upon the addition of DMSO likely resulting from inhibition of the enzyme by the solvent as DMSO is a known ADH inhibitor[36]. Smaller volumes of DMSO exhibited similar activity and were associated with pipet delivery error.

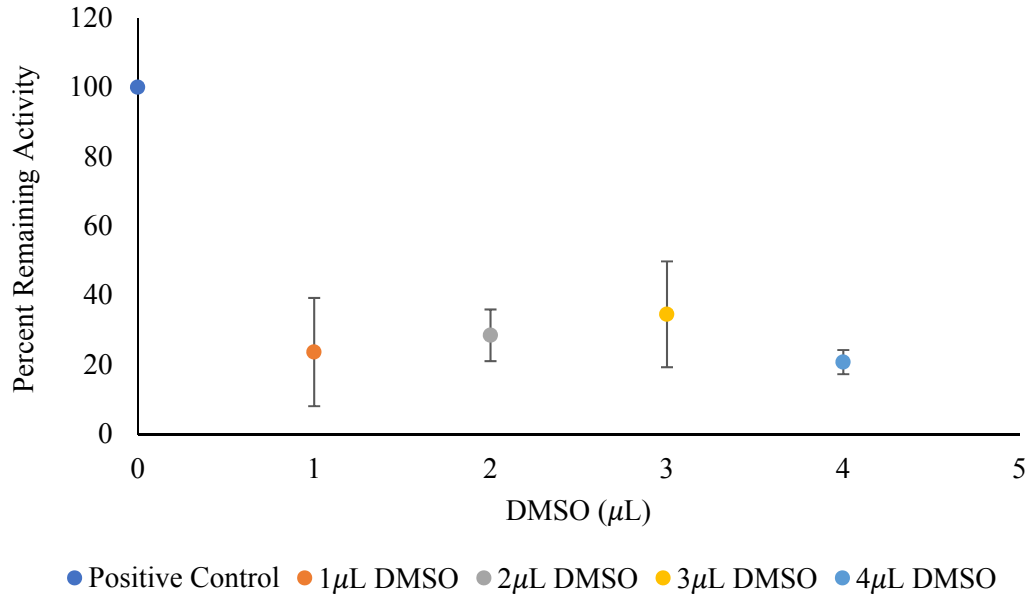

Figure 8. Percent remaining ADH activity with DMSO added to enzyme assay conditions (Method C).

3.4: Reagent Stability Assays

The change in absorbance over time was measured for various combinations of assay components to ensure that non-enzyme interactions are not contributing to measured activity monitored at 340 nm (Figure 9). An increase in absorbance was observed for enzyme and NADH over time in the absence of substrate. A decrease in absorbance was recorded for all other combinations including the positive control, which exhibited a large drop in absorbance within 70 seconds (Figure 9). This suggests that the positive control had the greatest decrease in absorbance at this wavelength. Other assay components do influence measurements at this wavelength and these influences ought to be considered in the calculation of enzyme activity within the screen assays.

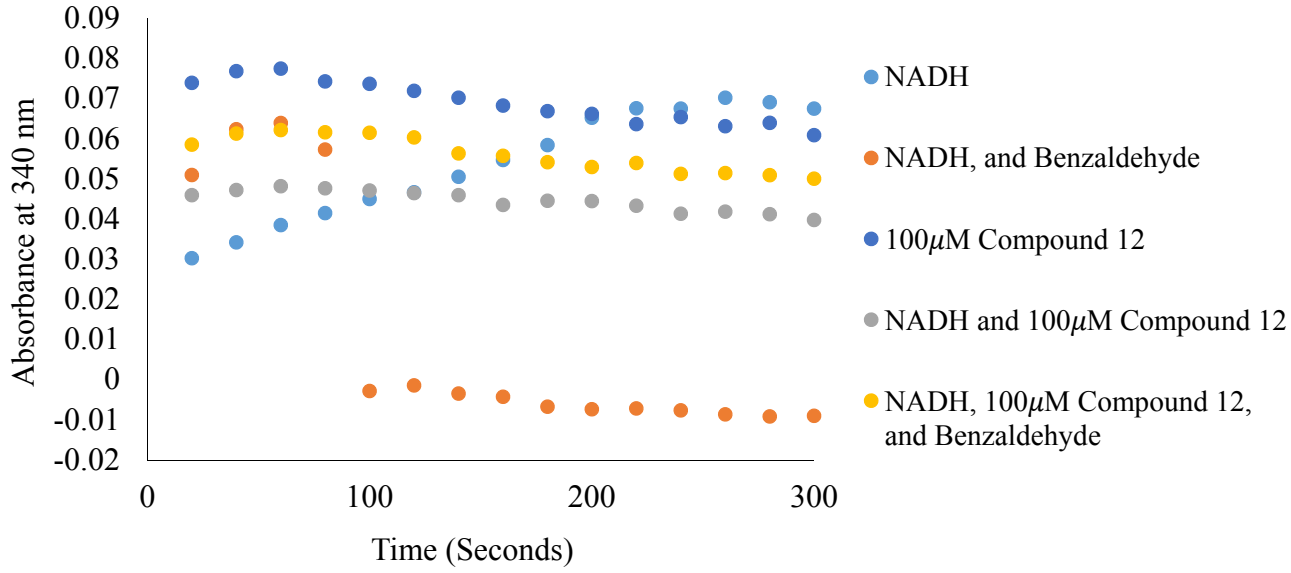

Figure 9. Enzymatic assays monitoring the change in absorbance over time at 340 nm for varied combinations of assay components including ADH (Horse liver) and DMSO. Compound **12** at 100 μM, in pH 7.21 TEA buffer was assessed (with 3 μL DMSO for combinations without 100 μM compound **12**). Assays performed according to Method C with the indicated modifications.

The stability of these compounds at pH 7.21 (assayed pH) was of concern due to the lack of dose dependence observed (1, 10, 100 μM). One of the derivatives (compound **12**, *N*-3-diphenyl-4,5-dihydro-1*H*-pyrazole-1-carbothioamide), was examined at 100 μM in TEA buffer. The pH was varied from 4.19 to 8.90 while monitoring any change in absorbance at 340 nm (Figure 10). This compound was selected and screened at this concentration as an example of the 1,3-disubstituted 2-pyrazoline carboxamide derivatives. Further studies would be required to determine the effects of pH upon other derivatives. The slopes of the line of best fit for each of these conditions did not vary greatly but the slope of the highest magnitude was observed at pH 5.71 (Table 6). This suggests that there is not a significant decomposition of this or other screened compounds. As some absorbance was observed across all pHs, this compound specific absorbance must be accounted for in the background readings of the assay.

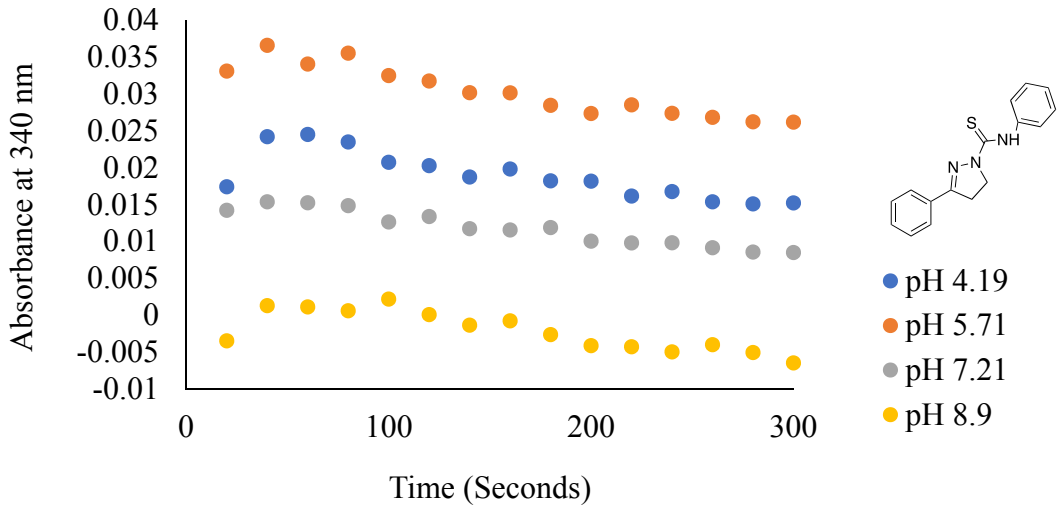

Figure 10. Change in absorbance at 340 nm for 100 μM compound **12** in TEA buffer adjusted to pH ranging from 4.19 to 8.90. Assays were prepared according to Method C with buffer pH adjusted as indicated.

Table 6. Slope of the best fit line for the change in absorbance at 340 nm over time of 100 μM compound **12** in TEA buffer, adjusted pH to range from 4.19 to 8.90.

TEA Buffer pH	Slope
4.19	-2.87E-05
5.71	-3.60E-05
7.21	-2.61E-05
8.90	-2.43E-05
Average	-2.88E-05
St. Dev.	5.15E-06

3.5: Positive Inhibition Control

4-Methylpyrazole was employed as the positive inhibition control compound for this assay. DMSO was used as a solvent for 4-methylpyrazole and percent inhibition values were calculated relative to the average of all DMSO standard trials. Dose dependent inhibition of horse liver ADH activity was observed for Method A and B (Table 7 and Table 8). The sequence of addition order within this screen assay does appear to matter at the inhibitor concentrations employed in this study.

Table 7. Average screen inhibition assay trials for 4-methylpyrazole. Assays performed according to Method A.

		Slope	St. Dev.	RSD	Average Remaining Activity ±STD
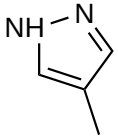	1 μM	-4.04E-05	8.21E-06	-0.20	66.1±21.2% (n=6)
	10 μM	-2.33E-05	2.55E-06	-0.11	39.8±6.73% (n=5)
	100 μM	-2.08E-05	7.71E-07	-0.04	36.4±1.14% (n=4)

Table 8. Average screen inhibition assay trials for 4-methylpyrazole. Assays performed according to Method B.

		Slope	St. Dev.	RSD	Average Remaining Activity ±STD
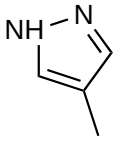	1 μM	-7.84E-05	1.92E-05	-0.24	107±33.4% (n=7)
	10 μM	-5.46E-05	1.18E-05	-0.22	74.5±20.5% (n=6)
	100 μM	-4.88E-05	5.67E-06	-0.12	66.7±9.86% (n=6)

3.6: Inhibition Comparison

For all enzyme assays, "significant inhibition" activity was (arbitrarily) defined as 80-100% inhibitory efficiency relative to the positive inhibition control, 4-methylpyrazole with benzaldehyde added last (Table 7). "Moderate activity" was defined as 60-80% inhibitory efficiency relative to 4-methylpyrazole. "Minimal activity" was defined as 0-60% inhibitory efficiency relative to 4-methylpyrazole. The importance of addition order was investigated with either benzaldehyde (Method A) or enzyme added after incubation (Method B) for 5 minutes. The most consistent results were identified with benzaldehyde added after incubation. All compounds were screened with benzaldehyde added last but the data for several compounds with enzyme added last are also included for comparison.

3.6.1: Modification of the carbamoyl region

The 1,3-diaryl pyrazoline base structure (compound **3**, *N*,3-diphenyl-4,5-dihydro-1*H*-pyrazole-1-carboxamide) exhibited the highest ADH inhibition at 10 μM (Method A, Table 9). No significant inhibition was observed for this compound with enzyme added after incubation and minimal increase in enzyme activity was observed relative to the average of all DMSO controls. Modification of the carbamoyl of the base structure to a

thiocarbamoyl functional group (compound **12**) resulted in no significant enzyme inhibition at any of the screened concentrations. Modification of the carbamoyl region of the pyrazoline base structure to an amide functional group (compound **6**) resulted in no significant ADH inhibition for neither Method A nor B (Table 9 and Table 10). No significant inhibition was observed in response to changes in addition order for compound **3** or **6**. Alkylation of the nitrogen of the carbamoyl region for a 3-*p*-chlorophenyl-*N*-propyl-carbamoyl 2-pyrazoline derivative (compound **9**) resulted in poor ADH inhibition for all concentrations screened and no dose dependent inhibition was measured. Alkylation of the sulfur of a 3-*p*-chlorophenyl-*N*-propyl-thiocarbamoyl 2-pyrazoline derivative (compound **11**) resulted in significant inhibition at all concentrations screened and dose dependent inhibition was measured.

Table 9. Average screen inhibition assay trials for compounds (**3**, **6**, **9**, **11**, and **12**) synthesized to probe role of carbamoyl moiety for ADH inhibition by 1,3-disubstituted carbamoyl 2-pyrazolines. Assays performed according to Method A.

Compound		Slope	St. Dev.	RSD	Average Remaining Activity ±STD
3 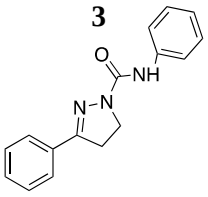	1 μM	-6.86E-05	1.55E-05	-0.23	119±29.6% (n=6)
	10 μM	-5.03E-05	1.31E-05	-0.26	85.6±31.6% (n=6)
	100 μM	-7.50E-05	1.78E-05	-0.24	131±25.1% (n=6)
6 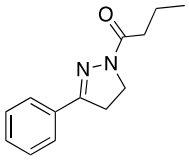	1 μM	-5.67E-05	5.79E-06	-0.10	98.6±10.1% (n=6)
	10 μM	-6.30E-05	2.69E-06	-0.04	110±4.68% (n=4)
	100 μM	-6.62E-05	9.65E-06	-0.15	115±16.8% (n=6)
9 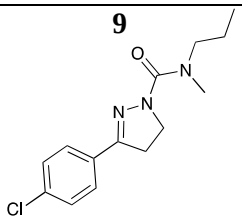	1 μM	-6.17E-05	1.76E-06	-0.28	107±30.7% (n=4)
	10 μM	-4.89E-05	7.79E-06	-0.16	85.1±13.6% (n=4)
	100 μM	-9.18E-05	3.14E-05	-0.34	159±54.6% (n=2)
11 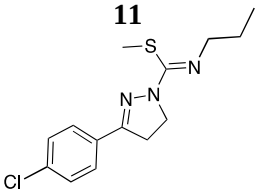	1 μM	-3.46E-05	2.96E-05	-0.85	60.2±51.5% (n=4)
	10 μM	-3.43E-05	9.27E-06	-0.27	59.7±16.1% (n=4)
	100 μM	-2.57E-05	1.05E-05	-0.47	44.8±18.2% (n=4)
12 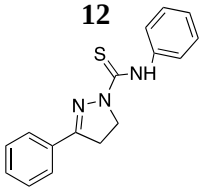	1 μM	-5.41E-05	6.87E-06	-0.13	83.0±17.1% (n=3)
	10 μM	-6.56E-05	2.07E-05	-0.32	108±36.0% (n=6)
	100 μM	-6.24E-05	3.36E-05	-0.54	330±18.5% (n=4)

Table 10. Screen inhibition assay trials for compounds (**3** and **6**) synthesized to probe role of the carbamoyl moiety for ADH inhibition by 1,3-disubstituted carbamoyl 2-pyrazolines. Assays performed according to Method B.

Compound		Slope	St. Dev.	RSD	Average Remaining Activity ±STD
3 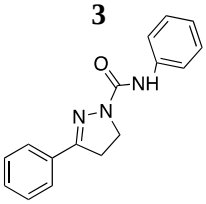	1 μM	-7.06E-05	4.76E-06	-0.07	96.4±8.29% (n=3)
	10 μM	-7.78E-05	7.89E-06	-0.10	106±13.7% (n=3)
	100 μM	-8.23E-05	1.11E-05	-0.14	112±19.4% (n=3)
6 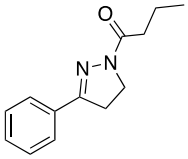	1 μM	-7.06E-05	4.76E-06	-0.07	102±29.0% (n=3)
	10 μM	-7.78E-05	7.89E-06	-0.10	97.4±17.5% (n=3)
	100 μM	-8.23E-05	1.11E-05	-0.14	111±29.3% (n=3)

3.6.2: Modification of Ring **A**

The role of ring **A** in 1,3-disubstituted carbamoyl 2-pyrazoline inhibition activity was investigated through enzyme inhibition screening assays (Table 11). The aryl ring was modified to a methyl group and this derivative exhibited only minimal ADH inhibition at 10 μM (compound **17**). The electron donating *p*-methoxyphenyl group resulted in moderate enzyme inhibition at 1 and 10 μM concentrations (compound **14**). A *p*-methylphenyl group resulted in moderate enzyme inhibition for all concentrations screened (compound **15**). The electron withdrawing *p*-chlorophenyl group resulted in moderate enzyme inhibition at 1 and 10 μM but regained activity at 100 μM (compound **13**). Additionally, *p*-fluorophenyl substituent resulted in significant enzyme inhibition for all concentrations screened with the highest inhibition observed at 10 μM (compound **16**). The *p*-chlorophenyl thiocarbamoyl 2-pyrazoline derivative was also screened and resulted in only minimal enzyme inhibition at 1 μM (compound **1**). None of these derivatives exhibited dose dependent inhibition across all three screened concentrations.

Table 11. Screen inhibition assay trials for compounds (**1**, **13- 17**) synthesized to probe role of ring **A** for ADH inhibition by 1,3-disubstituted carbamoyl 2-pyrazolines. Assays performed according to Method A.

Compound		Slope	St. Dev.	RSD	Average Remaining Activity ±STD
1 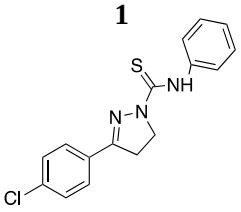	1 μM	-5.01E-05	1.48E-05	-0.29	87.1±25.7% (n=3)
	10 μM	-6.36E-05	3.98E-05	-0.63	111±69.3% (n=4)
	100 μM	-7.94E-05	8.05E-06	-0.10	138±14.0% (n=4)
13 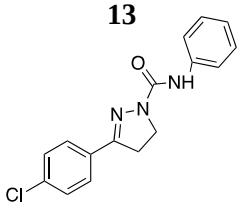	1 μM	-3.59E-05	7.25E-06	-0.20	62.6±12.6% (n=4)
	10 μM	-4.46E-05	1.93E-05	-0.43	77.7±33.6% (n=4)
	100 μM	-6.88E-05	1.38E-06	-0.02	120±2.41% (n=3)
14 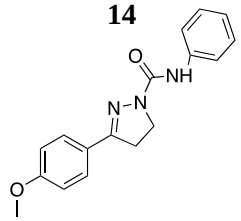	1 μM	-4.33E-05	1.74E-05	-0.40	75.3±30.3% (n=3)
	10 μM	-3.27E-05	7.64E-06	-0.23	57.0±13.3% (n=4)
	100 μM	-5.95E-05	1.98E-05	-0.33	104±34.5% (n=4)
15 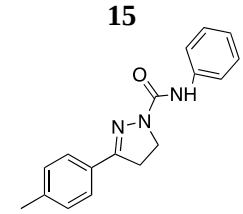	1 μM	-3.82E-05	2.67E-05	-0.70	66.5±46.5% (n=4)
	10 μM	-4.38E-05	1.71E-05	-0.39	76.3±29.8% (n=4)
	100 μM	-4.16E-05	9.44E-06	-0.23	72.3±16.4% (n=3)
16 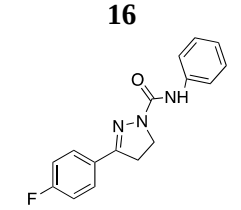	1 μM	-3.95E-05	6.04E-06	-0.15	68.7±10.5% (n=3)
	10 μM	-2.58E-05	8.63E-05	-3.34	45.0±150% (n=4)
	100 μM	-3.46E-05	1.73E-05	-0.50	60.2±30.0% (n=4)
17 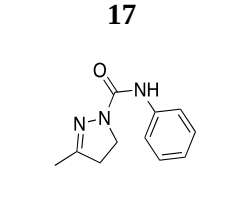	1 μM	-7.41E-05	1.58E-05	-0.21	109±31.5% (n=6)
	10 μM	-4.81E-05	1.76E-05	-0.37	95.2±30.6% (n=6)
	100 μM	-6.28E-05	4.62E-06	-0.07	104±21.3% (n=6)

3.6.3: Modification of ring **C**

The role of the ring **C** moiety was also investigated through screening assays (Table 12). The *N*-propyl carbamoyl 2-pyrazoline derivative investigated exhibited no significant ADH inhibition at the concentrations screened (compound **18**). The *N*-propyl thiocarbamoyl 2-pyrazoline derivative investigated also exhibited no significant ADH inhibition at the concentrations screened (compound **19**).

Substituents at the *para* position of the *N*-phenyl ring were introduced with substituents of varying electron donating or withdrawing character. None of these derivatives exhibited dose dependent inhibition over the screened concentrations. The electron donating *p*-methoxyphenyl group resulted in moderate enzyme inhibition at 1 and 10 μM concentrations (compound **20**). The strong electron withdrawing *p*-nitrophenyl group resulted in minimal enzyme inhibition at 1 and 10 μM concentrations but significant inhibition at 100 μM (compound **22**). A *p*-chlorophenyl group resulted in moderate ADH inhibition at all concentrations, with the highest enzyme inhibition observed at 1 μM (compound **21**).

Table 12. Screen inhibition assay trials for compounds (**18- 22**) synthesized to probe role of ring **C** for ADH inhibition by 1,3-disubstituted carbamoyl 2-pyrazolines. Assays performed according to Method A.

Compound		Slope	St. Dev.	RSD	Average Remaining Activity ±STD
18 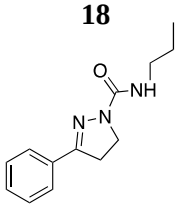	1 μM	-4.73E-05	2.61E-05	-0.55	82.4±45.5% (n=4)
	10 μM	-5.63E-05	9.95E-06	-0.18	98.0±17.3% (n=4)
	100 μM	-5.65E-05	6.20E-06	-0.11	98.4±10.8% (n=3)
19 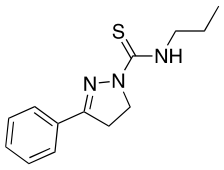	1 μM	-5.41E-05	6.87E-06	-0.13	94.1±12.0% (n=4)
	10 μM	-6.56E-05	2.07E-05	-0.32	114±36.0% (n=6)
	100 μM	-6.25E-05	3.36E-05	-0.54	109±58.5% (n=5)
20 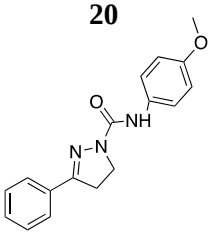	1 μM	-3.63E-05	1.84E-05	-0.51	63.1±32.1% (n=4)
	10 μM	-4.02E-05	9.82E-06	-0.24	70.0±17.1% (n=4)
	100 μM	-6.85E-05	5.58E-06	-0.08	119±9.7% (n=4)
21 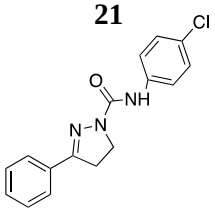	1 μM	-1.88E-05	2.24E-05	-1.19	32.7±38.9% (n=4)
	10 μM	-3.34E-05	1.21E-05	-0.36	58.2±21.0% (n=4)
	100 μM	-3.95E-05	1.61E-05	-0.41	68.8±28.0% (n=4)
22 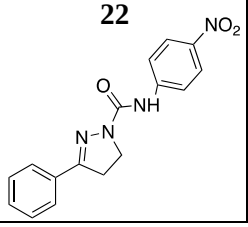	1 μM	-4.62E-05	1.16E-05	-0.25	80.5±20.2% (n=4)
	10 μM	-5.53E-05	7.67E-06	-0.14	96.3±13.3% (n=3)
	100 μM	-2.51E-05	3.99E-05	-1.59	89.0±69.4% (n=4)

3.7: Ternary Complex Analysis

Florescence spectroscopy analysis was performed with various combinations of the assay components to monitor ternary complexation between ADH and NADH in the presence of DMSO. Previous studies identified increased fluorescence emission intensity at approximately 420 nm with NADH binding to ADH[39]. An increase in emission intensity at 455 nm was observed for all assay component combinations investigated, except for ADH alone. ADH alone did not exhibit significant emission with this excitation wavelength and a minor peak was observed at 370 nm (Figure 11). The incubated sample of NADH and ADH exhibited lower fluorescence emission intensity at 455 nm relative to the other samples analyzed (Figure 11).

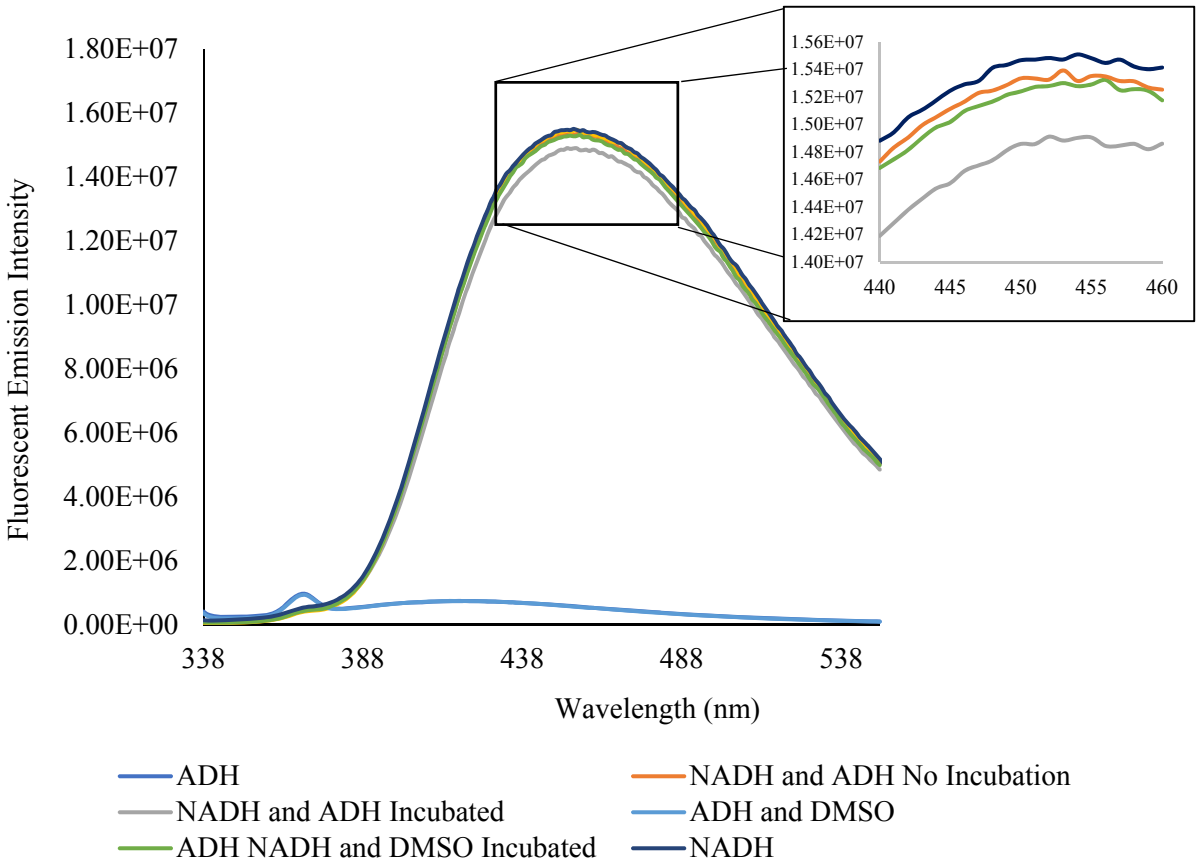

Figure 11. Fluorescence emission scans for assay components excited at 328 nm.

Chapter 4: Discussion and Conclusions

4.1: Discussion

This study evaluated the inhibitory efficiency of 1,3-disubstituted carbamoyl 2-pyrazoline derivatives as horse liver alcohol dehydrogenase inhibitors. The assay used in this study was effective for high throughput screening of inhibitors, but further assay optimization would allow for more accurate activity determination. The high throughput assay performed allowed for rapid determination of inhibitory activity with a larger sample size than standard 1 cm cuvette trials would allow. However, this method introduced additional error with mixing and dispensing such small volumes. Further optimization of the assay conditions is necessary to minimize error associated with solvent influences and background change in absorbance at the monitoring wavelength for assay components.

Positive control trials including all assay components (ADH, NADH, benzaldehyde, and buffer) were included with every screen to monitor experimental variation between trials. Minimal variation was observed for all positive controls with an average change in absorbance of -2.57E-04± 9.99E-05 (n=63) with a relative standard deviation of 0.38 using Method A. These assay conditions exhibited measurable change in absorbance within the instrument detection limit and this method was deemed suitable for high throughput screens. Several modifications of assay concentrations were used to verify that kinetics readings fall within the initial rate for horse liver ADH (Table 3, Table 4, Table 5). Double enzyme concentration resulted in 122% activity relative to the positive control indicating that substrate was in excess at the concentration used for screening (Table 4). However, since this value was not directly correlated with enzyme

concentration, the concentrations used may be nearing the end of the enzyme kinetics initial rate region.

This study offered an effective method for rapid screening of derivatives and approximate inhibitory efficiency. Optimization of the enzyme kinetics assay in response to these finding is necessary to decrease error associated with measurement and to validate inhibition results. Kinetics assays monitoring the change in absorbance of assay components over time at the wavelength of interest identified changes that may contribute to error associated with measured inhibition values (Figure 9, Table 6). A decrease in absorbance with enzyme and 100 μM compound **12** suggested possible metabolism of the compound as a substrate or cofactor analog (Figure 9).

The addition order of assay components also influenced absorbance values with benzaldehyde added last exhibiting lower variation between runs. Adding enzyme last did not allow for incubation of the enzyme with cofactor and addition of the smaller volume (3 μL) may have contributed to mixing and pipet dispensing error. The difference in activity in response to addition order suggests that time required for co-factor binding is important for accurately monitoring enzyme activity.

Dimethylsulfoxide, DMSO, was used as a co-solvent for screening. Other suggested solvents include ethanol and methanol, but as these alcohol solvents closely resemble the substrate for the reverse reaction, an alternative solvent was necessary. DMSO is the standard solvent for high-throughput screenings in pharmaceutics and biotechnology but

there are known effects of DMSO on alcohol dehydrogenase activity[40]. DMSO is a known competitive inhibitor of ADH with a K_i of 0.005M.[39] This solvent is known to react with the enzyme and NADH complex to form a ternary complex with fluorescent properties.[39] A mixed solvent system may be investigated if solubility within these inhibition assays continues to be a challenge. The small 3 μL volume (2%) of DMSO was selected for all assays because it exhibited the highest percent remaining activity relative to the positive control and this volume was associated with our lowest pipet delivery error (Figure 8).

Percent remaining activity for all derivative screens were compared to the DMSO standard runs to account for enzyme inhibition by the co-solvent. The significant inhibition of ADH activity by DMSO has been of concern due to error associated with monitoring a small fraction of total enzyme activity and potential conformational changes resulting from the co-solvent. Inhibition due to the DMSO co-solvent may result from conformational changes with DMSO- coordination which would alter ligand docking and these screens may not be representative of natural ADH activity/ inhibition. Ligand coordination in the presence of DMSO may influence the binding of these compounds and measured inhibition values[41].

Solubility of the screened inhibitors may cause the observed absorbance interference at higher screen concentrations. Several derivatives precipitated out of solution at higher assay concentrations (250 μM and 1 mM). Fine particulates not visible to the eye within the 10 and 100 μM assay wells may contribute to increased enzyme activity observed for

several compounds. Alternative co-solvents should be investigated to address issues with solubility and ADH inhibition.

4-Methylpyrazole was employed as the positive inhibitor control compound for this study due to its demonstrated ADH inhibition[2]. ADH inhibition by this compound was used to evaluate the efficiency of synthesized derivatives as horse liver ADH inhibitors. A linear dose dependent response was not observed for 4-methylpyrazole trials which it suggestive that additional assay optimization may be required for this assay to replicate literature results (Table 7 and Table 8).

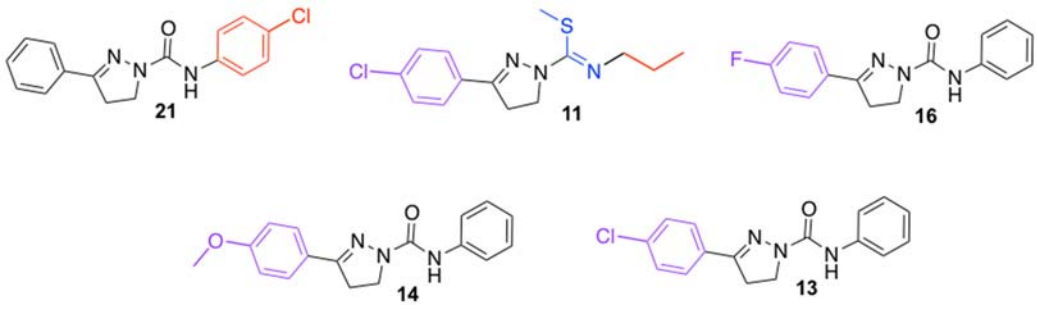

Figure 12. Horse liver ADH inhibitors identified through high throughput inhibition screening assays of 1,3-disubstituted carbamoyl 2-pyrazoline derivatives.

The systematic modification of electronic and steric factors surrounding the carbamoyl 2-pyrazoline scaffold identified several effective horse liver ADH inhibitors at the concentrations screened. The synthesized 1,3-disubstituted carbamoyl 2-pyrazoline derivatives that resulted in horse liver ADH inhibition are shown in Figure 12.

This discussion of compound structural attributes will follow the observed ADH inhibition potency of the screened compounds.

The compound with the greatest inhibition was compound **21**, *N*-(4-chlorophenyl)-3-phenyl-4,5-dihydro-1*H*-pyrazole-1-carboxamide, with 32.7± 38.2% remaining activity at 1 μM (Table 12). However, this ring **C** modification derivative was only moderately effective at higher concentrations and did not exhibit a dose dependent response. The success of this compound at a low concentration suggested that decreased electron density with ring **C** may contribute to ADH inhibition. Strong electron withdrawing or electron donating groups on ring **C** (compound **22** and **20**, respectively) failed at ADH inhibition which suggested that the net dipole of this region may not be an important factor for ADH inhibition. Removal of ring **C**, as with 3-phenyl-*N*-propyl carbamoyl and thiocarbamoyl 2-pyrazoline derivatives (compounds **18** and **19**) resulted in minimal inhibition at all concentrations screened (Table 12). This suggested that aromatic character at ring **C** may be an important factor for ADH inhibition.

Derivatives investigating the role of the carbamoyl region of 1,3-disubstituted carbamoyl 2-pyrazolines within ADH inhibition (Table 9) only identified successful inhibition with the alkylated thiocarbamoyl derivative (compound **11**). This derivative exhibited 44.8± 18.2% remaining activity at 100 μM. The ADH inhibition of this compound was comparable to that of 4-methylpyrazole at 100 μM (36.4± 1.14%, Table 7). The 3-phenyl-2-pyrazoyl butanamide (compound **6**), the *N*,3-diphenyl thiocarbamoyl 2-pyrazoline (compound **11**) and the *N*,3-diphenyl carbamoyl 2-pyrazoline (compound **9**)

derivatives did not exhibit any ADH inhibition at the concentrations screened (Table 9). The ADH inhibition for these modifications suggested that non-polar interactions with the active site may be involved with ADH inhibition and the acyclic nitrogen of the carbamoyl group plays a minimal role within ADH inhibition.

Modifications of the electronic character of ring **A** also exhibited significant ADH inhibition for several of the concentrations screened (Table 11). Many ring **A** modification derivatives provided ~60% inhibition activities at the 1 μM concentration (compounds **13**,**15** and **16**). The most effective derivative of ring **A** modification derivatives at 1 μM was identified as compound **13**, 3-(4-chlorophenyl)-*N*-phenyl-4,5-diphenyl-1*H*-pyrazole-1-carboxamide. This derivative exhibited 62.6± 12.6% remaining activity at 1 μM and 77.7± 33.6% at 10 μM. Compound **16**, 3-(4-fluorophenyl)-*N*-phenyl-4,5-dihydro-1*H*-pyrazole-1-carboxamide, was also identified as an effective horse liver ADH inhibitor with 45.0± 15.0% remaining activity at 10 μM. The inhibitory activity of compound **16** was similar to that of 4-methylpyrazole at this concentration (39.8±17.0%) at 10μM (Table 7). The inhibition by ring A derivatives having electron withdrawing substituents suggested the importance of electronic character of this ring for ADH inhibition. However, an electron donating *para*- methoxyphenyl group (compound **14**) also exhibited ADH inhibition with 57.0± 13.3% remaining activity at 10 μM (Table 18). Thus, the lack of change in ADH inhibition with varied ring **A** modifications implied that, other than having the aryl ring itself, its electronic properties may play a minor role in ADH inhibition.

Comparing the enzyme inhibition results from all of these structural modifications does not highlight an essential role of any single structural position for horse liver ADH inhibition. Thus, a combination of electronic and steric influences at these multiple positions are likely to be responsible for ADH inhibition. Thus, there was not a single pharmacophore with 1,3-disubstituted 2-pyrazolines and multiple factors influence their ADH inhibitory activity.

The lack of dose dependence for all of these derivatives suggested errors with the assay, compound degradation/ metabolism, solubility issues, or an atypical mode of inhibition. The cause of the dose independent response was not identified for these derivatives. These results highlight the need for experimental optimization of a high- throughput inhibition screens for ADHs and the need to elucidate the operative mechanism of inhibition/ action of 1,3- disubstituted carbamoyl 2-pyrazoline compounds.

The stability of compounds at the buffer pH used for screening assays was investigated through absorbance changes over a wide pH range (4.19- 8.90) (Figure 10). Compound **12** exhibited the greatest absorbance at pH 5.71 at 340 nm and the lowest absorbance at pH 8.90 at 340 nm. Degradation may then be occurring under these extreme pH conditions. In order to confirm/ discredit metabolism or degradation of substituted 2-pyrazoline derivatives at these pH conditions and under the assay conditions, NMR and/or GC/MS analysis may be pursued.

Limitations of this study included inhibition of ADH activity by DMSO, insolubility of derivatives at higher concentrations, and ternary complex formation. Given the inhibition of the target ADH enzyme by the co-solvent, only minimal enzyme activity was available to monitor and inhibit. Solubility challenges with pyrazoline compounds at higher concentrations also may introduce errors associated with absorbance measurements. Ternary complex formation was required for activity with the coordination of NADH co-factor with ADH; ternary complex formation was anticipated between NADH and ADH as monitored by an increase in absorbance at 420 nm. Minimal ternary complex formation was detected under the assay conditions that included the DMSO, indicating that co-factor binding, or lack thereof, may be contributing to error associated with screen assays (Figure 11).

4.2: Conclusion

This study was aimed at identifying effective ADH inhibitors for their potential application as anti-parasitic and anti-bacterial agents. A series of 1,3-disubstituted carbamoyl 2-pyrazoline derivatives were synthesized with variable steric and electronic properties to investigate and identify the pharmacophore required for ADH inhibition. Several compounds synthesized and screened in this study exhibited moderate horse liver ADH inhibition, with few compounds exhibiting inhibition similar to 4-methylpyrazole. This study suggests that some 1,3-disubstituted 2-pyrazolines are effective horse liver ADH inhibitors but the mode of inhibition (competitive/ uncompetitive/ noncompetitive/ mixed) of these compounds remains to be determined.

Electronic and steric interactions at the carbamoyl position were anticipated to play a major role in enzyme inhibition given the performed computational modeling studies. Alkylation of the sulfur of the 3-chlorophenyl-*N*-propyl thiocarbamoyl derivative resulted in significant inhibition. Activity observed with the alkylated thiocarbamoyl derivative suggested that the exocyclic nitrogen (of the thiocarbamoyl group) does not play an essential role in ADH inhibition and nonpolar interactions may increase ADH inhibition. Derivatives with substituents at the *para* position on rings **A** and **C** were shown to effect ADH inhibition. This study illustrated that *para* electron donating groups on ring **A** increased ADH inhibition. Thus, the electronics of ring **A** (and greater electron density contributing to the pyrazoline ring) contribute to ADH inhibition. Additionally, decreased electron density at ring **C** was associated with increased ADH inhibition. Overall, there was not a single pharmacophore identified through our described studies and multiple factors influence ADH inhibition by 1,3-disubstituted carbamoyl 2-pyrazoline compounds. The assay used to screen inhibitors must be further optimized to verify the activity of these compounds and to eliminate extraneous variables, including solubility, decomposition, or substrate analog metabolism.

Chapter 5: Future Studies

5.1: Assay Optimization

Additional studies are required to optimize the inhibition screen assay employed within this study. Additional trials of each inhibitor and standards would minimize error associated with measurement and improve accuracy. The source of positive inhibition values should be investigated to determine the mechanism of action behind any enzyme activity enhancement. The error associated with DMSO inhibition should be investigated and, in the event, that this error cannot be minimized another co-solvent or colorimetric assay should be attempted[42]. An alternative solvent system may also increase compound water solubility and decrease the observed error associated with DMSO as the co-solvent, avoiding ADH inhibition. A colorimetric assay could also be employed. One such as that monitoring the reduction of nitroblue tetrazolium (NBT) with the reduction of NADH in the presence of phenazine methosulphate (PMS) with the change in absorbance at 590 nm may offer an alternative to monitoring directly the cofactor conversion at 340 nm[42]. This method would also allow for high throughput screening of derivatives avoiding background absorbances of assay components.

Several studies were performed investigating the role of addition order on enzyme activity and inhibition. Additional trials would help to minimize error and identify the optimal addition order. pH dependent effects were investigated for one compound, but studies of additional compounds would help to establish a relationship between pH and compound stability. Structure identification of the compounds at different pH values would help to determine if the derivatives are metabolized or decomposed at the assay

pH. Further assays and studies would be needed to determine if these pyrazoline derivatives behave as substrate or co-factor analogs for ADH.

5.2: Mode of Action

The mode of inhibition for these compounds remains unknown and classic Lineweaver Burke kinetics analysis should be used to determine the mode of inhibition for successful compounds. At this time, solubility of the compounds at high concentrations preclude such measurements. The determination of K_i and IC_{50} values would improve comparisons of compound efficiency and determine the mode of inhibition.

5.3: AutoDock Modeling

AutoDock modeling may be used for successful inhibitors to understand potential competitive binding interactions between the enzyme and the derivatives. Modeling with the crystal structure of horse liver ADH with substrate, cofactor, and DMSO bound (assuming competitive inhibition) would increase the accuracy of these approximations. The crystal structure of successful inhibitors may also allow for more appropriate AutoDock modeling analysis. AutoDock analysis with the crystal structure of human or bacterial ADH would also allow for an approximation of the binding modes of these compounds for different targets and applications.

5.4: Additional Derivatives

Future studies should also include the screening of additional derivatives. Several other compounds are of interest have yet to be synthesized that probe the pyrazole core and

sterics surrounding the carbamoyl position (Figure 13). A pyrazolidine derivative would probe the role of aromaticity and electron density at ring **B** in ADH inhibition. This reduction was attempted several times with Superhydride® as a reducing agent with no conversion. Alternative reduction conditions will be investigated to achieve this transformation.

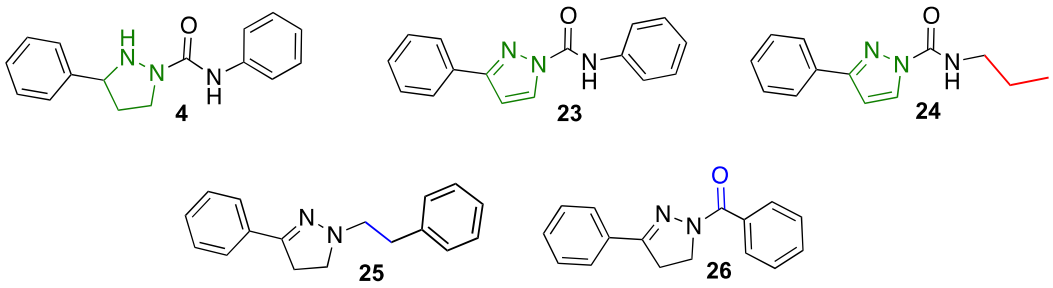

Figure 13. Several proposed derivatives probing the pyrazole core and sterics surrounding the carbamoyl position.

Additionally, oxidation of the pyrazoline ring to a pyrazole would probe the role of increased electron density at ring **B** in ADH inhibition. Investigation of *N*-phenyl and *N*-propyl pyrazole derivatives would investigate the influences of aromaticity and steric interactions at ring **C**. This oxidation has been achieved for three pyrazole derivatives (compounds **2**, **23**, and **24**) but time did not permit for adequate purification and high throughput screening to determine inhibitory activity of these derivatives.

Furthermore, a 1,3-diphenyl 2-pyrazolylcarbamide derivative (**26**) was synthesized to target the role of the exocyclic nitrogen of the carbamoyl region. Additionally, a derivative completely lacking the carbamoyl moiety (**25**) would investigate the

importance of the carbamyl dipole. Both of the latter derivatives were synthesized but time did not permit for adequate purification and high throughput screening to determine their ADH inhibition. Investigation of this series of derivatives would identify the role of the pyrazoline and carbamoyl regions in ADH inhibition.

References

(1) Zakhari, S. Overview: How Is Alcohol Metabolized by the Body. *Alcohol Res. Heal.* **2006**, *29* (4), 245–254.

(2) Dahlbom, R.; Tolf, B. .; Akeson, A.; Lundquist, G.; Theorell, H. On the Inhibtory Power of Some Further Pyrazole Derivatives of Horse Liver Alcohol Dehydrogenase. *Biochem. Biophys. Res. Commun.* **1974**, *57* (3), 549–553.

(3) P Xie, T. H. Methionine-141 Directly Influences the Binding of 4-Methylpyrazole in Human Sigma Sigma Alcohol Dehydrogenase. *Protein Sci.* **1999**, *8* (12), 2639–2644.

(4) Brent, J.; McMartin, K.; Phillips, S.; Aaron, C.; Kulig, K. Fomepizole for the Treatment of Methanol Poisoning. *N. Engl. J. Med.* **2001**, *344* (6), 424–429.

(5) Chen, W.-J.; West, J.; McAlhany, R. 4-Methylpyrazole, an Alcohol Dehydrogenase Inhibitor, Exacerbates Alcohol-Induced Microencephaly During the Brain Growth Spurt. *Alcohol* **1994**, *12* (4), 351–355.

(6) AFT Pharmaceuticals. *Australian Pblic Assessment Report for Fomepizole*; 2017.

(7) Zhou, Y. W. Recent Researches in Triazole Compounds as Medicinal Drugs. *Curr. Med. Chem.* **2012**, *19* (2), 239–280.

(8) Wani, M. Y.; Azam, A.; Choi, I.; Athar, F.; Bhat, A. R. Probing the Antiamoebic and Cytotoxicity Potency of Novel Tetrazole and Triazine Derivatives. *Eur. J. Med. Chem.* **2012**, *48*, 313–320.

(9) Reddy, N.; Sistla, V. R.; Uppuluri, M.; Kota, A. Synthesis and Anti-Inflammatory Activity of Novel Triazole Hybrids of (+)-Usnic Acid, the Major Dibenzofuran Metabolite of the Lichen *Usnea Longissima*. *Mol. Divers.* **2017**, *27* (2), 273–282.

(10) Dix, D. E.; Jakubowski, A.; Moyer, J. D.; Handschumacher, R. E.; Lehman, C. P. Pyrazofurin Metabolism, Enzyme Inhibition, and Resistance in L5178Y Cells. *Cancer Res.* **1979**, *39*, 4485–4490.

(11) Chen, W.; Wang, Y.; Cao, L. Syntheses,Characterizations and Antifungal Activities of Thiocarbamates and Oxamates. *Chemistry (Easton).* **2015**, *20* (7), 29–36.

(12) de los Santos, J. M.; Aparicio, D.; Palacios, F.; Lopez, Y. A Convenient Synthesis of Substituted Pyrazolidines and Azaproline Derivatives through Highly Regio- and Diastereoselective Reduction of 2-Pyrazolines. *J. Org. Chem.* **2007**, *2008* (73), 550–557.

(13) Ansari, A.; Asif, M.; Shamsuzzaman, A. A. Review: Biologically Active Pyrazole Derivatives. *New J. Chem.* **2017**, *41*, 16–41.

(14) Lachlan, B.; Sperry, J. Natural Products Containing a Nitrogen-Nitrogen Bond. *J. Nat. Prod.* **2013**, *76*, 794–812.

(15) Badavath, V. N.; Ucar, G.; Sinha, B. N.; Jayaprakash, V. Monoamine Oxidase Inhibitory Activity of Novel Pyrazoline Analogues: Curcumin Based Design and Synthesis. *ACS Med. Chem. Lett.* **2016**, *7* (1), 56–61.

(16) Gould, E. R.; Menzies, S. K.; Fraser, A. L.; Tulloch, L. B.; K.Zacharova, M.; Smith, T. K.; Florence, G.; King, E. F. B. Simplifying Nature: Towards the Design of Broad Spectrum Kinetoplastid Inhibitors, Inspired by Acetogenins. *Bioorganic Med. Chem.* **2017**, *25* (22), 6126–6136.

(17) Smith, P.; Howes, P.; Cherry, P.; Starkey, I.; Cobley, K.; Weston, H.; Scicinski, J.; Merritt, A.; Whittington, A.; Wyatt, P.; et al. Dihydropyrancarboxamides Related to Zanamivir: A New Series of Inhibitors of Influenza Virus Sialidases. Discovery, Synthesis, Biological Activity, and Structure-Activity Relationships of 4-Guanidino- and 4-Amino-4H-Pyran-6-Carboxamides. *J. Med. Chem.* **1998**, *41* (6), 787–797.

(18) Khobragade, B. P.; Kosankar, P. T. Synthesis, Antimicrobial and Antifungal Study of 2-(5-Aryl-1-Substituted-Pyrazol-3-yl)-Substituted Naphthalene-1-ol by Dehydrogenation Method. *Int. J. Chem. Sci.* **2013**, *11* (1), 569–572.

(19) Van Hes, R.; Grosscurt, A. C.; Wellinga, K. 1-Phenylcarbamoyl-2-Pyrazolines: A New Class of Insecticides 3. Synthesis and Insecticidal Properties of 3,4-Diphenyl-1-Phenylcarbamoyl-2-Pyrazolines. *J. Agric. Food Chem.* **1978**, *26* (4), 915–918.

(20) Grosscurt, A. C.; Wellinga, K.; Van Hes, R. 1-Phenylcarbamoyl-2-Pyrazolines, a New Class of Insecticides. 3. Synthesis and Insecticidal Properties of 3,4-Diphenyl-1-Phenylcarbamoyl-2-Pyrazolines. *J. Agric. Food Chem.* **1979**, *27* (2), 406–409.

(21) Wellinga, K.; VanHes, R.; Grosscurt, A. 1-Phenylcarbamoyl-2-Pyrazolines: A New Class of Insecticides 1. Synthesis and Insecticidal Properties of 3-Phenyl-1-Phenylcarbamoyl-2-Pyrazolines. *J. Agric. Food Chem.* **1977**, *25* (5), 987–992.

(22) Nishimura, K.; Shimizu, R.; Ohoka, A.; Tada, T. Effects of Alkyl Groups Attached to the Carbamoyl Nitrogen Atom of an *N*-Arylcarbamoylpyrazoline on Insecticidal Activity. *Pestic. Sci.* **1999**, *55*, 446–451.

(23) Brindisi, A. K. G. and M. Organic Carbamates in Drug Design and Medicinal Chemistry. *J. Med. Chem.* **2015**, *58*, 2895–2940.

(24) Karabacak, M.; Altıntop, M. D.; Çiftçi, H. İ.; Koga, R.; Otsuka, M.; Fujita, M.; Özdemir, A. Synthesis and Evaluation of New Pyrazoline Derivatives as Potential Anticancer Agents. *Molecules* **2015**, *20* (10), 19066–19084.

(25) Espinosa, A.; Zhang, Z.; Foster, L.; Clark, D.; Li, E.; Stanley, S. L.; Yan, L. The Bifunctional *Entamoeba Histolytica* Alcohol Dehydrogenase 2 (EhADH2) Protein Is Necessary for Amebic Growth and Survival and Requires an Intact C-Terminal Domain for Both Alcohol Dehydrogenase and Acetaldehyde Dehydrogenase Activity. *J. Biol. Chem.* **2001**, *276* (23), 20136–20143.

(26) Espinosa, A.; Stanley, S. J.; Clark, D. *Entamoeba Histolytica* Alcohol Dehydrogenase 2 (EhADH2) as a Target for Anti-Amoebic Agents. *J. Antimicrob. Chemother.* **2004**, *54*, 56–59.

(27) Bansal, D.; Chawla, Y.; Mahajan, R. C.; Malla, N.; Sehgal, R. In Vitro Activity of Antiamoebic Drugs against Clinical Isolates of *Entamoeba Histolytica* and Entamoeba Dispar. *Ann. Clin. Microbiol. Antimicrob.* **2004**, *3* (27), 1–5.

(28) Pineda, E.; Encalada, R.; Olivos-garcía, A.; Néquiz, M.; Moreno-sánchez, R.; Saavedra, E. The Bifunctional Aldehyde – Alcohol Dehydrogenase Controls Ethanol and Acetate Production in *Entamoeba Histolytica* under Aerobic Conditions. *FEBS Lett.* **2013**, *587* (2), 178–184.

(29) Azam, A.; Peerzada, M. N.; Ahmad, K. Parasitic Diarrheal Disease : Drug Development and Targets. **2015**, *6* (October), 1–12.

(30) Plapp, B. V.; Savarimuthu, B. R.; Ferraro, D. J.; Rubach, J. K.; Brown, E. N.; Ramaswamy, S. Horse Liver Alcohol Dehydrogenase: Zinc Coordination and Catalysis. *Biochemistry* **2017**, *56* (28), 3632–3646.

(31) Ramaswamy, S.; Plapp, B.; Eklund, H. Structures of Horse Liver Alcohol Dehydrogenase Complexed with NAD+ and Substituted Benzyl Alcohols. *Biochemistry* **1994**, *33* (17), 5230–5237.

(32) Pietrusko, R. Human Liver Alcohol Dehydrogenase—inhibition of Methanol Activity by Pyrazole, 4-Methylpyrazole, 4-Hydroxymethylpyrazole and 4-Carboxypyrazol. *Biochem. Pharmacol.* **1975**, *24* (17), 1603–1607.

(33) Morris, G.; Lindstrom, W.; Sanner, M.; Belew, R.; Goodsell, D.; Olsen, A.; Huey, R. AutoDock4 and AutoDockTools4: Automated Docking with Selective Receptor Flexibility. *J. Comput. Chem.* **2009**, *30* (16), 2785–2791.

(34) Andrasi, F.; Botka, P.; Farkas, S.; Goldschmidt, K.; Hamori, T.; Korosi, J.; Moravcsik, I.; Tarnawa, I.; Berzenyi, P. N-Acyl-2,3-Benzoidazepine Derivatives, Pharmaceutical Compositions Containing Them and Process for Preparing Same, 1996.

(35) Jacobson, R. M. N-Aryl-3-Aryl-4-Substituted-4,5-Dihydro-1H-Pyrazole-1-Carboxamides and Methods of Their Production, 1995.

(36) Perlman, R. L.; Wolff, J. Dimethyl Sulfoxide: An Inhibitor of Liver Alcohol Dehydrogenase. *Science*. pp 317–319.

(37) Parajuli, B.; Kimble-Hill, A. C.; Khanna, M.; Ivanova, Y.; Meroueh, S.; Hurley, T. D. Discovery of Novel Regulators of Aldehyde Dehydrogenase Isoenzymes. *Chem. Biol. Interact.* **2011**, *191* (1–3), 153–158.

(38) Sharkawi, M. Inhibition of Alcohol Dehydrogenase by Dimethyl Formamide and Dimethyl Sulfoxide. *Toxicol. Lett.* **1979**, *4*, 493–497.

(39) Perlman, R.; Wolff, J. Dimethyl Sulfoxide: An Inhibitor of Liver Alcohol Dehydrogenase. *Science (80-.).* **1968**, *160* (3825), 317–319.

(40) Agneta Tjernberg William J. Griffiths and Dan Hallen, N. M. DMSO-Related Effects in Protein Characterization. *J. Biomol. Screen.* **2006**, *11* (2), 131–137.

(41) Meijers, R.; Dauter, Z.; Wilson, K. S.; Lamzin, V. S.; Cedergren-Zeppezauer, E. S. Structural Evidence for a Ligand Coordination Switch in Liver Alcohol Dehydrogenase. *Biochemistry* **2007**, *46*, 5446–5454.

(42) Fibla, J.; Gonzalez-Duarte, R. Colorimetric Assay to Determine Alcohol Dehydrogenase Activity. *J. Biochem. Biophys. Methods* **1993**, *26* (1), 87–93.

Supplemental Information A

Compound 5

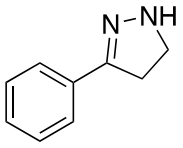

Synthesis of 3-phenyl-4,5-dihydro-1*H*-pyrazole:

Acetophenone, (9.90 mL, 83.2 mmol, 1.00 equiv.), dimethylamine hydrochloride (8.89 g, 108 mmol, 1.30 equiv.), and paraformaldehyde (3.30 g, 108 mmol, 1.30 equiv.) and four drops of 0.40 M hydrochloric acid was refluxed in a stirred solution of 13.5 mL of ethanol. After two hours, the solution was cooled and 100 mL of acetone was added. The white crystalline solid was washed and dried. A warm solution of 26.4 mL methanol and 37.0 mmol of this product was added to a solution of 5.00 mL hydrazine hydrate, and 2.70 mL 50% sodium hydroxide in 6.70 mL methanol over 10 minutes and refluxed for 45 minutes. The methanol was evaporated under reduced pressure to yield 3-phenyl-4,5-dihydro-1*H*-pyrazole as an oil, in 50.7% yield.

Compound 7

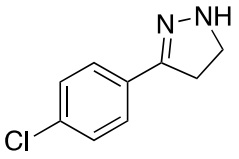

Synthesis of 3-(4-chlorophenyl)-4,5-1*H*-pyrazole:

4-chloroacetophenone (2.50 g, 32.5 mmol, 1 equiv.), dimethylamine hydrochloride (2.62 g, 32.1 mmol, 1 equiv.), paraformaldehyde (1.27 g, 42.4 mmol, 1.30 equiv.) and four drops of 0.40 M hydrochloric acid was refluxed in a stirring solution of 5.20 mL ethanol. After

two hours, the solution was cooled and 26.0 mL of acetone was added. The white crystalline solid was washed and dried. A warm solution of 11.0 mL methanol and 22.2 mmol of this product was added to a solution of 2.25 mL hydrazine hydrate, and 1.11 mL 50% sodium hydroxide in 2.70 mL methanol over 10 minutes and refluxed for 45 minutes. The methanol was evaporated under reduced pressure to yield 3-(4-chlorophenyl)-4,5-dihydro-1*H*-pyrazole as a white solid, in 47.5% yield.

Compound 27

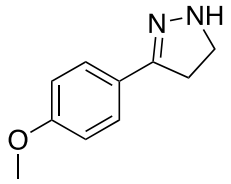

Synthesis of 3-(4-methoxyphenyl)-4,5-1*H*-pyrazole:

4-chloroacetophenone (2.03 g, 13.3 mmol, 1.00 equiv.), dimethylamine hydrochloride (1.51 g, 17.3 mmol, 1.30 equiv.), paraformaldehyde (0.56 g, 17.3 mmol, 1.30 equiv.), and four drops of 0.40 M hydrochloric acid was refluxed in a stirring solution of 2.25 mL ethanol. After two hours, the solution was cooled and 10.0 mL of acetone was added. The white crystalline solid was washed and dried. A warm solution of 6.00 mL methanol and this dried product (1.37 g, 7.80 mmol, 1 equiv.) was added to a solution of 1.50 mL hydrazine hydrate, and 1 mL 50% sodium hydroxide in 2.00 mL methanol over 10 minutes and refluxed for 45 minutes. The methanol was evaporated under reduced pressure to yield 3-(4-methoxyphenyl)-4,5-dihydro-1*H*-pyrazole as a white solid, in 58.7% yield.

Compound 28

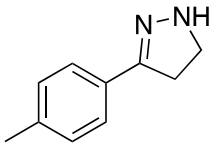

Synthesis of 3-(4-methylphenyl)-4,5-dihydro-1*H*-pyrazole:

4-methylacetophenone (2.09 g, 14.9 mmol, 1.00 equiv.), dimethylamine hydrochloride (1.64 g, 19.4 mmol, 1.3 equiv.), paraformaldehyde (0.62 g, 19.4 mmol, 1.30 equiv.), and four drops of 0.40 M hydrochloric acid was refluxed as a stirring solution of 2.50 mL ethanol. After 1.5 hours, the solution was cooled and 10.0 mL of acetone was added. The white crystalline solid was washed and dried. A warm solution of 4.00 mL methanol and this dried product (0.92 g, 5.77 mmol, 1 equiv.) was added to a solution of 0.78 mL hydrazine hydrate and 0.40 mL 50% sodium hydroxide in 1.00 mL methanol over 10 minutes and refluxed for 45 minutes. The methanol was evaporated under reduced pressure to yield 3-(4-methylphenyl)-4,5-dihydro-1*H*-pyrazole as a yellow solid, in 18.5% yield.

Compound 29

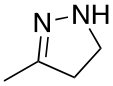

Synthesis of 3-methyl-4,5-dihydro-1H-pyrazole:

Methyl vinyl ketone (10.0 mL 176 mmol, , 1.00 equiv.) was added gradually to an ice-cold solution of hydrazine hydrate (10.0 mL, 176 mmol, 1.0 equiv.) in 10.0 mL of methanol. Upon addition, significant heat was generated, and the solution was maintained at 50°C for two hours. The methanol was evaporated under reduced pressure to yield white solid residue that was directed to the synthesis of compound **17** immediately.

Compound 30

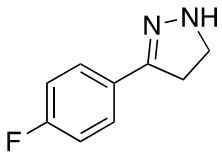

Synthesis of 3-(4-fluorophenyl)-4,5-dihydro-1*H*-pyrazole:

4-fluoroacetophenone (2.85 g, 20.6 mmol, 1.00 equiv.), dimethylamine hydrochloride (2.26 g, 26.8 mmol, 1.33 equiv.), paraformaldehyde (0.80 g, 26.8 mmol, 1.33 equiv.) and four drops 0.40 M hydrochloric acid was added to a stirring solution of 3.5 mL ethanol. This solution was cooled after 1.5 hours and 10.0 mL acetone was added. White crystalline solid was washed and dried. A warm solution of 10.0 mL methanol and this product (3.07 g, 18.7 mmol, 1.00 equiv.) was added to a solution of 2.00 mL hydrazine hydrate and 1.00 mL 50% sodium hydroxide in 3.00 mL methanol over 10 minutes and refluxed for 45 minutes. The methanol was evaporated under reduced pressure to yield 3-(4-fluorophenyl)-4,5-dihydro-1*H*-pyrazole as a white solid residue, in 42.8% yield.

Screened Inhibitor Compounds

Compound 1

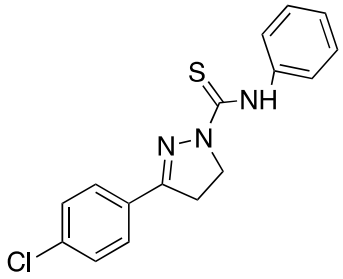

Synthesis of 3-(4-chlorophenyl)-*N*-phenyl-4,5-dihydro-1*H*-pyrazole-1-carbothioamide:

3-(4-chlorophenyl)-4,5-dihydro-1*H*-pyrazole (1.91 g, 10.5 mmol, 1.00 equiv.) was dissolved in 55.0 mL anhydrous ether with two drops of triethylamine and phenyl isocyanate (2.51 mL, 18.5 mmol, 1.00 equiv.) phenyl isothiocyanate. This solution stirred 1.5 hours at room temperature and the solid yellow product was filtered and dried, in 39.4% yield.

^{1}H NMR (300 MHz, $CDCl_3$) δ (ppm): 9.05 (bs,1H) 7.66 (dd, *J*= 8.6 Hz, 10.9 Hz 5H), 7.41 (t, *J*= 8.3Hz, 5H), 4.47 (t, *J*= 9.2 Hz, 2H), 3.32 (t, *J*= 8.5 Hz, 2H).

^{13}C NMR (75.6 MHz, CD_2Cl_2) δ (ppm): 173.9, 156.0, 139.0, 136.7, 129.7, 129.1, 128.6, 128.2, 125.4, 124.4, 48.6, 32.0.

DEPT-135 (75.6 MHz, CD_2Cl_2) δ (ppm): (+) 129.1, 128.6, 128.2, 125.4, 124.4; (-) 48.7, 32.1.

IR (neat, cm^{-1}): 3285.4, 1595.3, 1513.6, 1449.7, 1412.8, 1349.8, 1226.1, 1086.2, 993.3, 834.7, 761.5, 667.5.

Melting Point Range: 145- 147°C

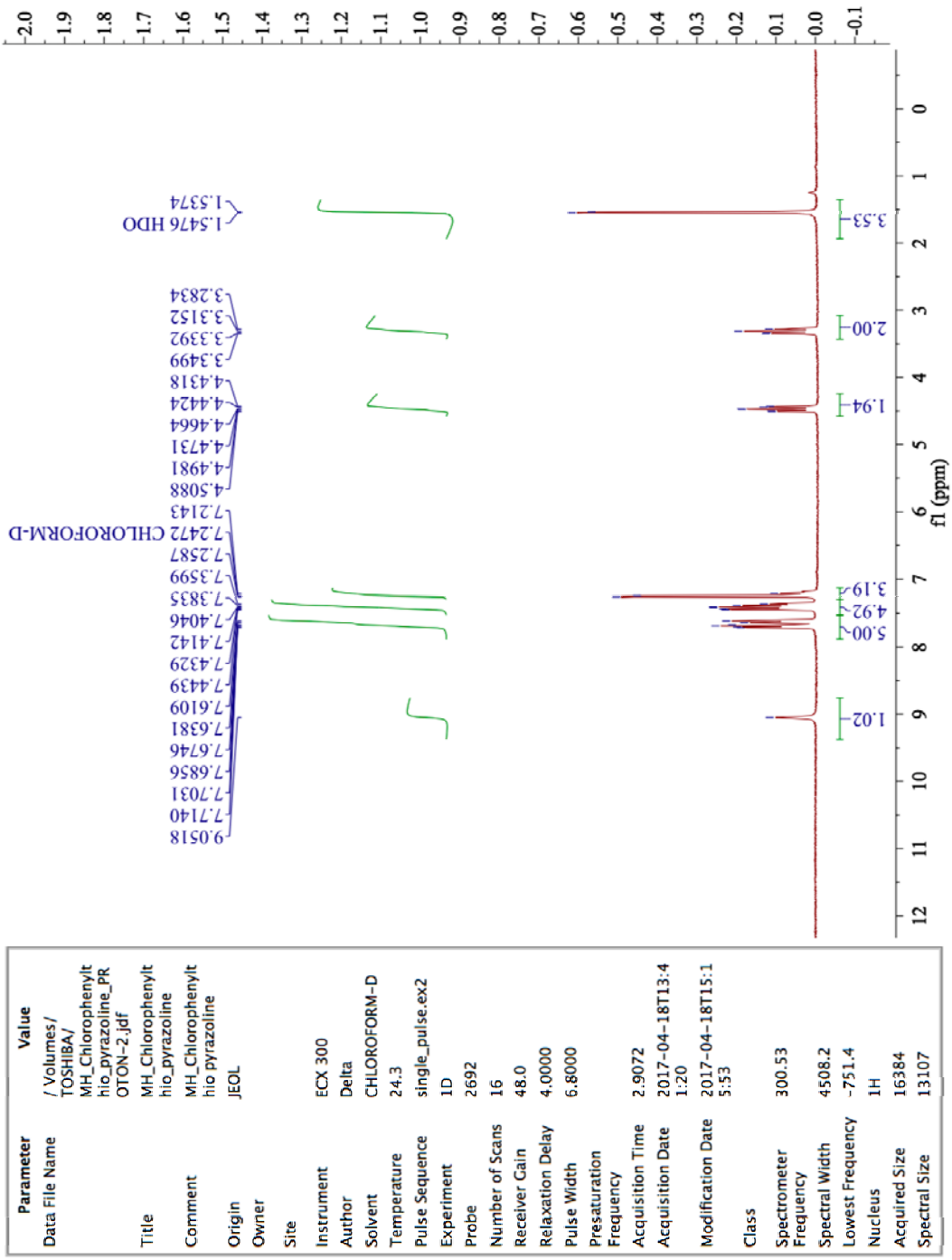
Parameter
Value
Data File Name
/ Volumes/ TOSHIBA/ MH_Chlorophenylt hio_Pyrazoline_PR OTON-2.jdf
Title
MH_Chlorophenylt hio_pyrazoline
Comment
MH_Chlorophenylt hio pyrazoline
Origin
JEOL
Owner
Site
Instrument
ECX 300
Author
Delta
Solvent
CHLOROFORM-D
Temperature
24.3
Pulse Sequence
single_pulse.ex2
Experiment
1D
Probe
2692
Number of Scans
16
Receiver Gain
48.0
Relaxation Delay
4.0000
Pulse Width
6.8000
Presaturation Frequency
Acquisition Time
2.9072
Acquisition Date
2017-04-18T13:4 1:20
Modification Date
2017-04-18T15:1 5:53
Class
Spectrometer Frequency
300.53
Spectral Width
4508.2
Lowest Frequency
-751.4
Nucleus
1H
Acquired Size
16384
Spectral Size
13107
9.0518
7.7140
7.7031
7.6856
7.6746
7.6381
7.6109
7.4439
7.4329
7.4142
7.4046
7.3835
7.3599
7.2587
7.2472 CHLOROFORM-D
7.2143
4.5088
4.4981
4.4731
4.4664
4.4424
4.4318
3.3499
3.3392
3.3152
3.2834
1.5476 HDO
1.5374
1.02
5.00
4.92
3.19
1.94
2.00
3.53
f1 (ppm)

Parameter	Value
Data File Name	/ Volumes/ Lexar/ MHchlorothio_DEPT_DEPT135-3.jdf
Title	MHchlorothio_DEPT
Comment	
Origin	JEOL
Owner	
Site	
Instrument	ECX 300
Author	Delta
Solvent	METHYLENE-CHLORI
Temperature	22.3
Pulse Sequence	dept.ex2
Experiment	1D
Probe	2692
Number of Scans	29
Receiver Gain	58.0
Relaxation Delay	2.0000
Pulse Width	9.2082
Presaturation Frequency	
Acquisition Time	1.3841
Acquisition Date	2018-04-15T22:50:18
Modification Date	2018-04-15T23:24:43
Class	
Spectrometer Frequency	75.57
Spectral Width	18938.4
Lowest Frequency	-1912.4
Nucleus	13C
Acquired Size	32768
Spectral Size	26214

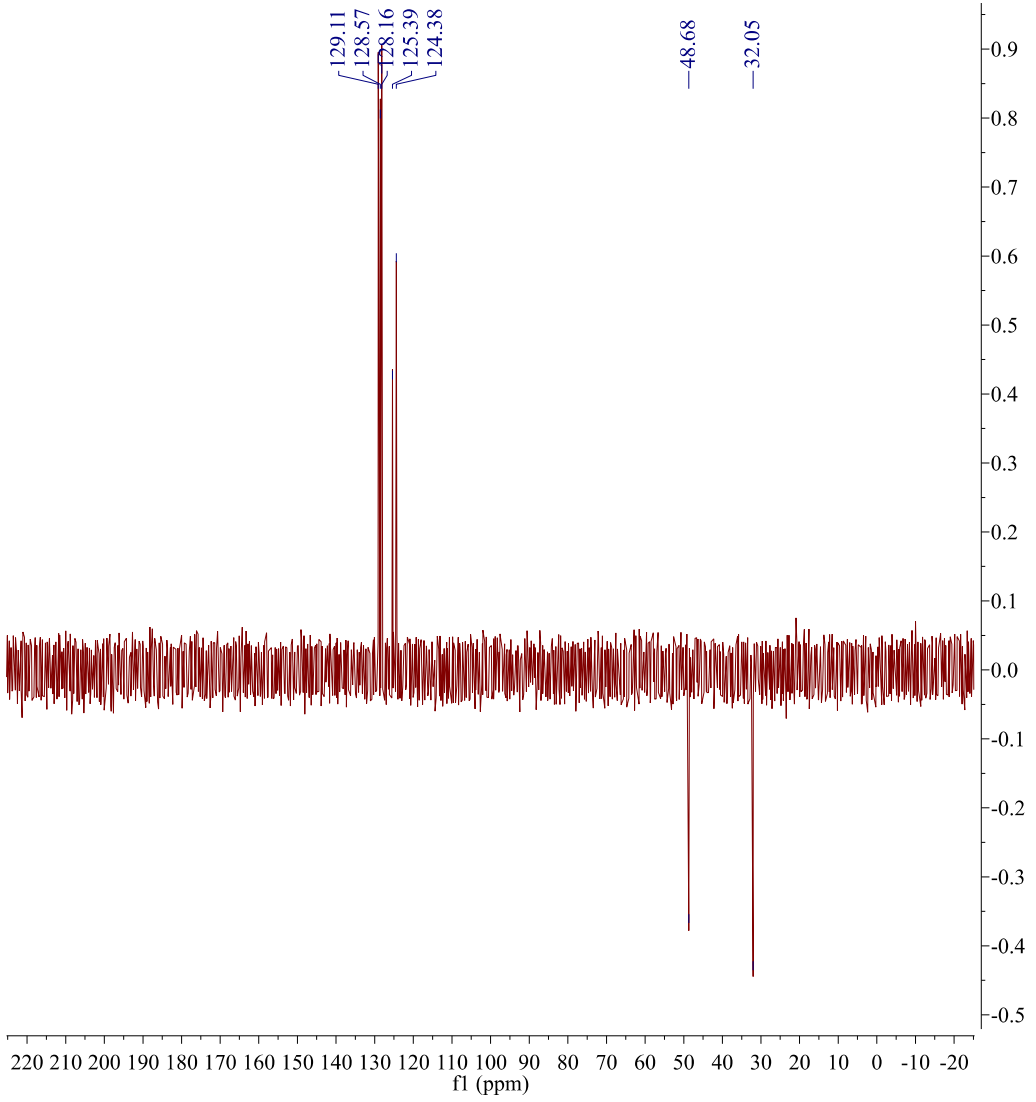

Parameter	Value
Data File Name	/ Volumes/ Lexar/ MHchlorothio_DEPT_CARBON-3.jdf
Title	MHchlorothio_DEPT
Comment	
Origin	JEOL
Owner	
Site	
Instrument	ECX 300
Author	Delta
Solvent	METHYLENE-CHLORI
Temperature	22.3
Pulse Sequence	single_pulse_dec
Experiment	1D
Probe	2692
Number of Scans	196
Receiver Gain	60.0
Relaxation Delay	2.0000
Pulse Width	3.0694
Presaturation Frequency	
Acquisition Time	1.3841
Acquisition Date	2018-04-15T22:47:52
Modification Date	2018-04-15T23:24:41
Class	
Spectrometer Frequency	75.57
Spectral Width	18938.4
Lowest Frequency	-1912.4
Nucleus	13C
Acquired Size	32768
Spectral Size	26214

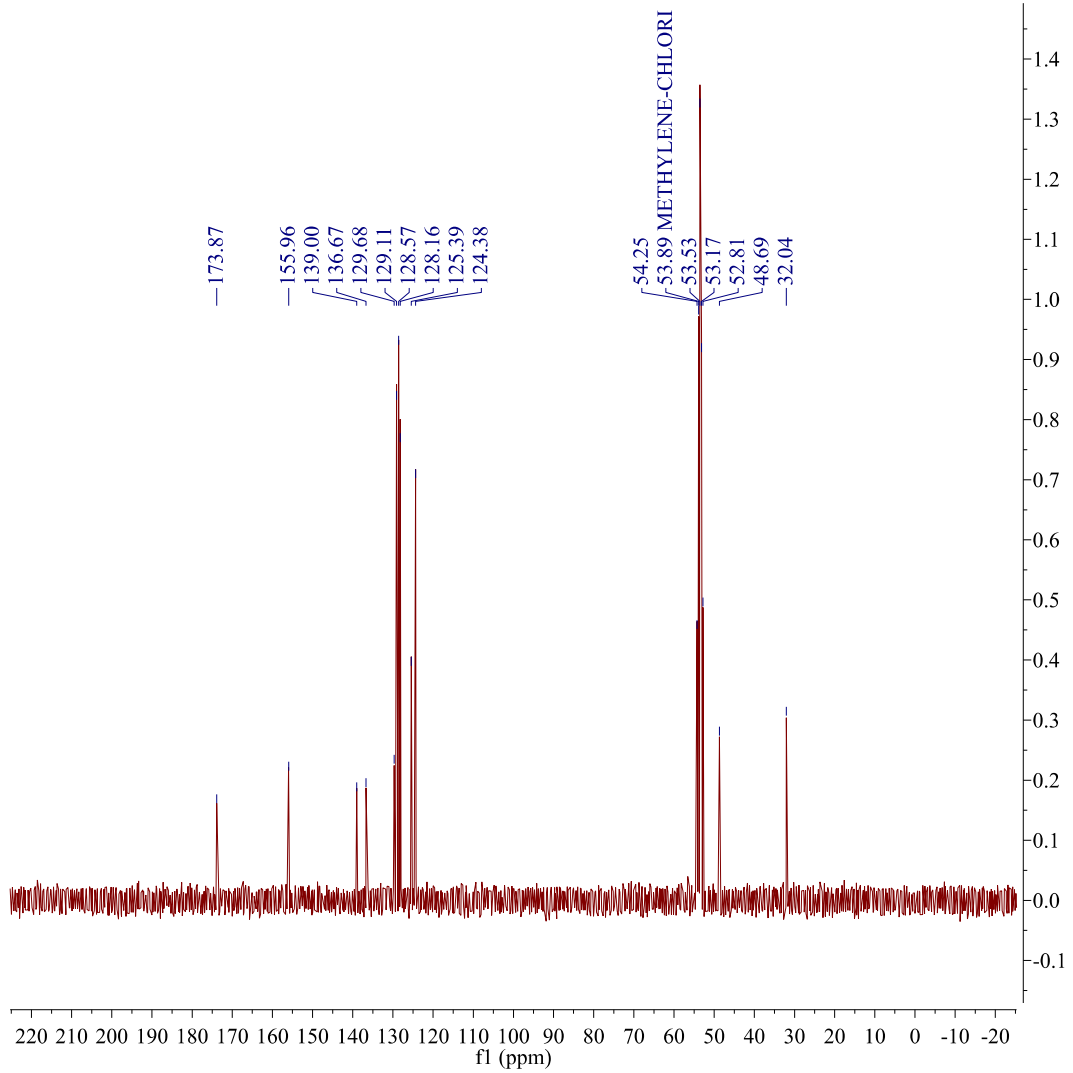

Who	What	When	Parameters	Comment
Organic Chem	Created as New Dataset	4/18/2017 10:10:48 AM		Sample 000 By organic lab Date Tuesday, April 18 2017
Organic Chem	Atmospheric Correction	4/18/2017 10:10:48 AM		

Spectrum Graph

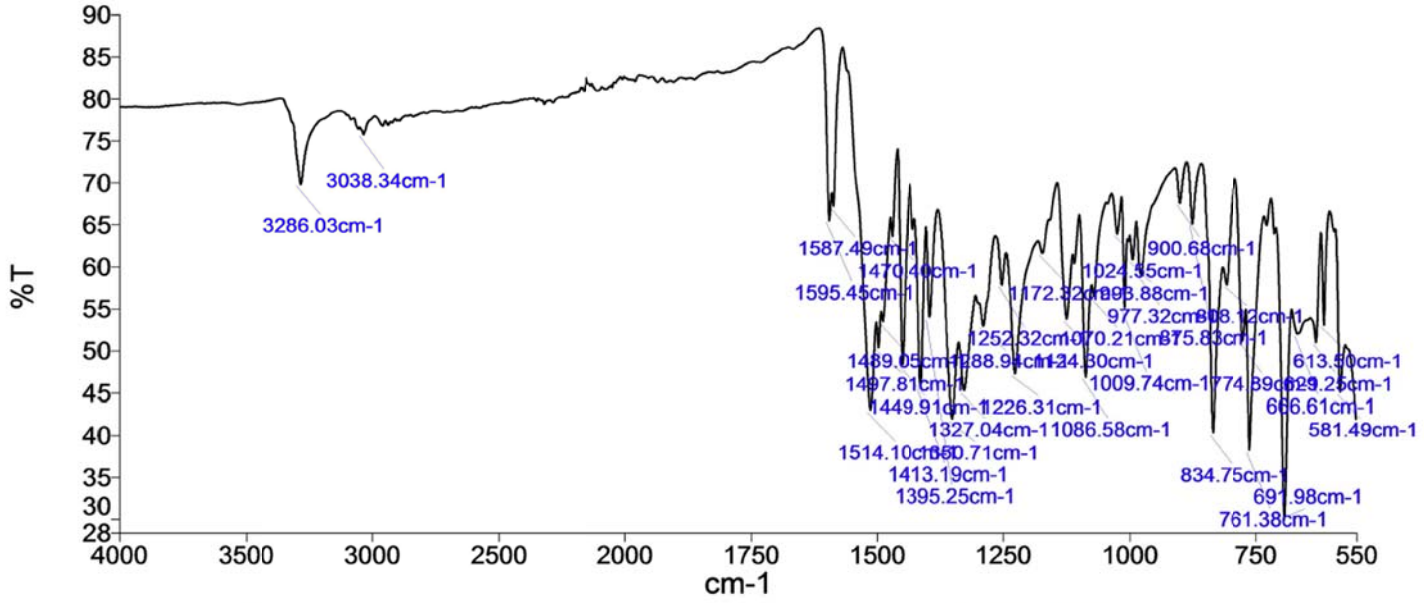

Name	Description
Chlorothio Pyrazoline	Sample 000 By organic lab Date Tuesday, April 18 2017

Compound 2

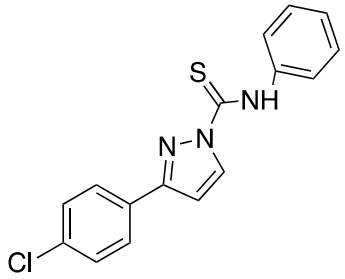

Synthesis of 3-(4-chlorophenyl)-*N*-phenyl-1*H*-pyrazole-1-carbothiamide:

3-(4-chlorophenyl)-4,5-dihydro-1*H*-pyrazole (0.025 g, 0.079 mmol, 1 equiv.) and an iodine crystal (0.0373 g, 0.147 mmol) was dissolved in 0.50 mL of DMSO.[18] This solution was refluxed for 2 hours before cooling to ambient temperature. A thick paste resulted on the glass with an orange-brown liquid supernatant. The liquid resulting was decanted and the solid was washed twice with aqueous 10% sodium thiosulfate. The washes were combined with the decanted liquid. Ethanol (2 mL) was added with two drops of 0.60 M acetic acid resulting in the precipitation of black solid. The supernatant was decanted, and a small quantity of ice was added to the supernatant which induced immediate precipitation.

This compound was not fully characterized and has not been screened for ADH inhibition.

IR (neat, cm^{-1}): 3286.0, 3038.3, 1595.5, 1514.1, 1327.0, 834.8, 761.4, 692.0.

Compound 3

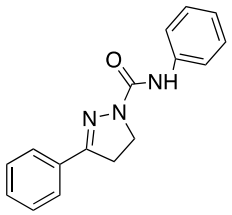

Synthesis of *N*,3-diphenyl-4,5-dihydro-1*H*-pyrazole-1-carboxamide:

3-phenyl-4,5-dihydro-1*H*-pyrazole (1.43 g, 9.82 mmol, 1.00 equiv.) was dissolved in 25.0 mL anhydrous ether with three drops of triethylamine and phenyl isocyanate (1.00 mL, 9.82 mmol, 1.00 equiv.) phenyl isocyanate. This solution stirred for three days at room temperature and the solid orange product was filtered and dried, in 39.0% yield.

^{1}H NMR (300 MHz, dmso-*d*$_6$) δ (ppm): 8.91 (s, 1H), 8.61 (s, 6H), 7.86 (dd, *J*= 2.9 Hz, 8.6 Hz, 2H), 7.62 (dd, *J*= 1.2Hz, 7.3 Hz, 2H), 7.44 (dd, *J*= 1.4 Hz, 8.8 Hz, 16H), 7.24 (t, *J*= 8.5 Hz, 15H), 6.93 (tt, *J*= 1.2 Hz, 7.3 Hz, 8H), 3.91(t, *J*= 10.0 Hz, 2H), 3.28 (t, *J*= 10.1 Hz, 4H, overlap with H_2O impurity at 3.33 ppm). Aromatic impurity observed in spectrum.

^{13}C NMR (75.6 MHz, CD_2Cl_2) δ (ppm): 153.7, 152.1, 139.0, 131.6, 130.1, 129.3, 128.9, 128.7, 128.7, 128.5, 126.7, 126.5, 126.2, 122.7, 119.3, 118.9, 44.5, 32.5.

DEPT-135 (75.6 MHz, CD_2Cl_2) δ (ppm): (+) 120.1, 128.9, 128.7, 126.7, 126.5, 126.2, 122.7, 118.9; (-) 44.5, 32.5.

IR (neat, cm^{-1}): 3390.8, 3348.4, 2949.0, 1671.8, 1591.4, 1532.6, 1444.1, 1309.0, 746.7, 687.0.

Melting Point Range: 142.4- 153.6°C

Parameter	Value
Data File Name	/ Volumes/ TOSHIBA/ MH03_06_recrys DMSO_PROTON-1.jdf
Title	MH03_06_recrys DMSO
Comment	
Origin	JEOL
Owner	
Site	
Instrument	ECX 300
Author	Delta
Solvent	DMSO-D6
Temperature	26.4
Pulse Sequence	single_pulse.ex2
Experiment	1D
Probe	2692
Number of Scans	16
Receiver Gain	46.0
Relaxation Delay	4.0000
Pulse Width	6.4750
Presaturation Frequency	
Acquisition Time	2.9072
Acquisition Date	2018-01-12T14: 40:20
Modification Date	2018-01-12T15: 13:50
Class	
Spectrometer Frequency	300.53
Spectral Width	4508.6
Lowest Frequency	-751.6
Nucleus	1H
Acquired Size	16384
Spectral Size	52430

Parameter	Value
Data File Name	/ Volumes/ Lexar/ MHoxyphenyl_DEPT_CARBON-3.jdf
Title	MHoxyphenyl_DEPT
Comment	
Origin	JEOL
Owner	
Site	
Instrument	ECX 300
Author	Delta
Solvent	METHYLENE-CHLORI
Temperature	22.4
Pulse Sequence	single_pulse_dec
Experiment	1D
Probe	2692
Number of Scans	102
Receiver Gain	60.0
Relaxation Delay	2.0000
Pulse Width	3.0694
Presaturation Frequency	
Acquisition Time	1.3841
Acquisition Date	2018-04-15T19:59:53
Modification Date	2018-04-15T20:36:03
Class	
Spectrometer Frequency	75.57
Spectral Width	18938.4
Lowest Frequency	-1912.4
Nucleus	13C
Acquired Size	32768
Spectral Size	26214

Parameter	Value
Data File Name	/ Volumes/ Lexar/ MHoxyphenyl_DEPT_DEPT135-3.jdf
Title	MHoxyphenyl_DEPT
Comment	
Origin	JEOL
Owner	
Site	
Instrument	ECX 300
Author	Delta
Solvent	METHYLENE-CHLORI
Temperature	22.3
Pulse Sequence	dept.ex2
Experiment	1D
Probe	2692
Number of Scans	19
Receiver Gain	60.0
Relaxation Delay	2.0000
Pulse Width	9.2082
Presaturation Frequency	
Acquisition Time	1.3841
Acquisition Date	2018-04-15T20:01:40
Modification Date	2018-04-15T20:36:03
Class	
Spectrometer Frequency	75.57
Spectral Width	18938.4
Lowest Frequency	-1912.4
Nucleus	13C
Acquired Size	32768
Spectral Size	26214

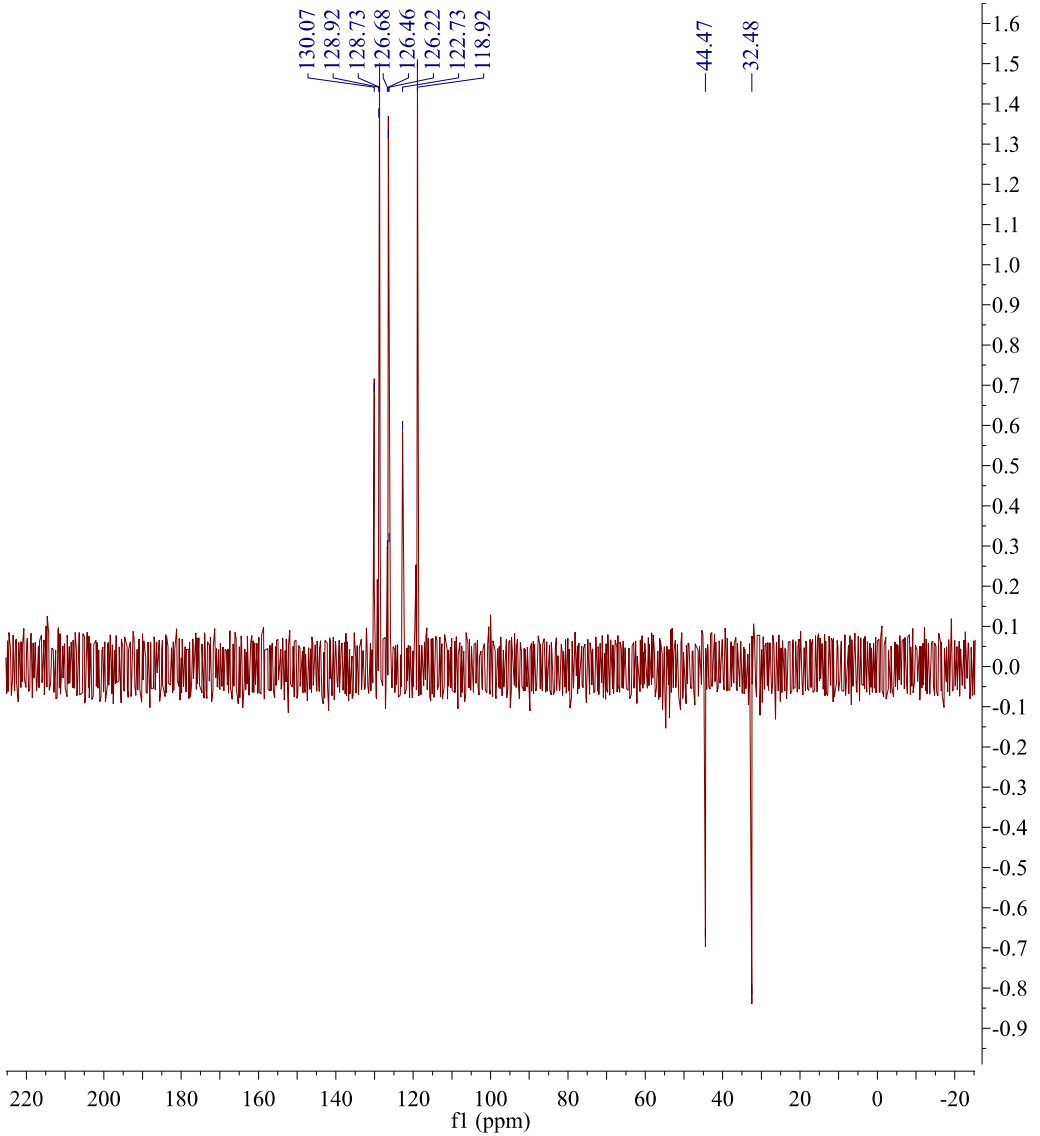

Who	What	When	Parameters	Comment
Organic Chem	Created as New Dataset	4/18/2017 10:17:44 AM		Sample 002 By organic lab Date Tuesday, April 18 2017
Organic Chem	Atmospheric Correction	4/18/2017 10:17:44 AM		

Spectrum Graph

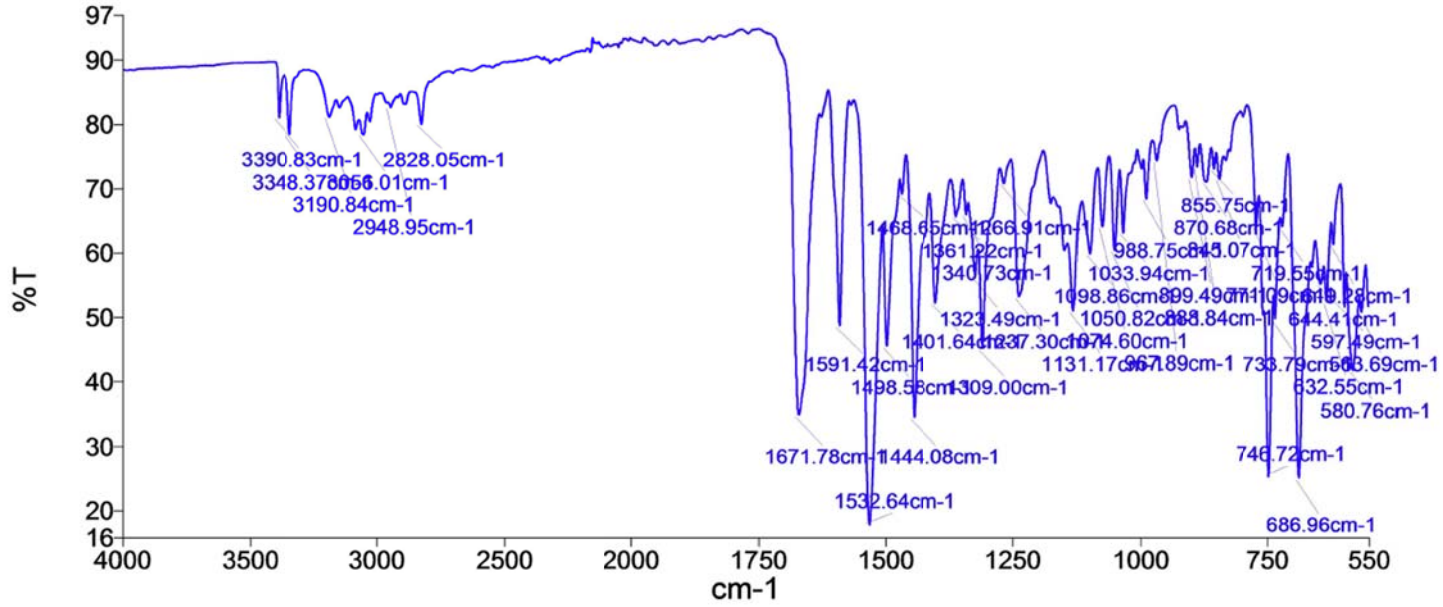

Name	Description
Phenyloxy Pyrazoline	Sample 002 By organic lab Date Tuesday, April 18 2017

Compound 6

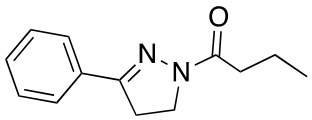

Synthesis of 1-(3-phenyl-4,5-dihydro-1*H*-pyrazol-1-yl)butan-1-one:

A solution of 3-phenyl-4,5-dihydro-1*H*-pyrazole (1.58 g, 12.5 mmol, 1 equiv.) in 50.0 mL chloroform was chilled on ice before the addition of triethylamine (1.26 mL, 12.5 mmol, 1.00 equiv.) followed by butyric anhydride (2.00 mL, 12.5 mmol, 1.00 equiv.). This solution was warmed to room temperature and stirred for three hours. White solid precipitate was washed and dried, in 76.3% yield.

^{1}H NMR (300 MHz, $CDCl_3$) δ (ppm): 7.72 (m, *J*= 2.6Hz, 2H), 7.43 (m, *J*= 2.2Hz, 3H), 2.61 (t, *J*= 7.5Hz, 2H), 1.57 (m, *J*= 7.4Hz, 2H), 0.90 (t, *J*= 7.4Hz, 3H)

^{13}C NMR (75.6 MHz, dmso-d_6) δ (ppm): 170.7, 156.5, 130.9, 130.7, 129.3, 127.0, 44.5, 35.7, 31.8, 18.5, 14.4.

IR (neat, cm^{-1}): 3055.3, 2957.2, 1625.5, 1412.1, 1319.5, 1152.8, 1040.6, 848.4, 756.5, 690.5, 582.8.

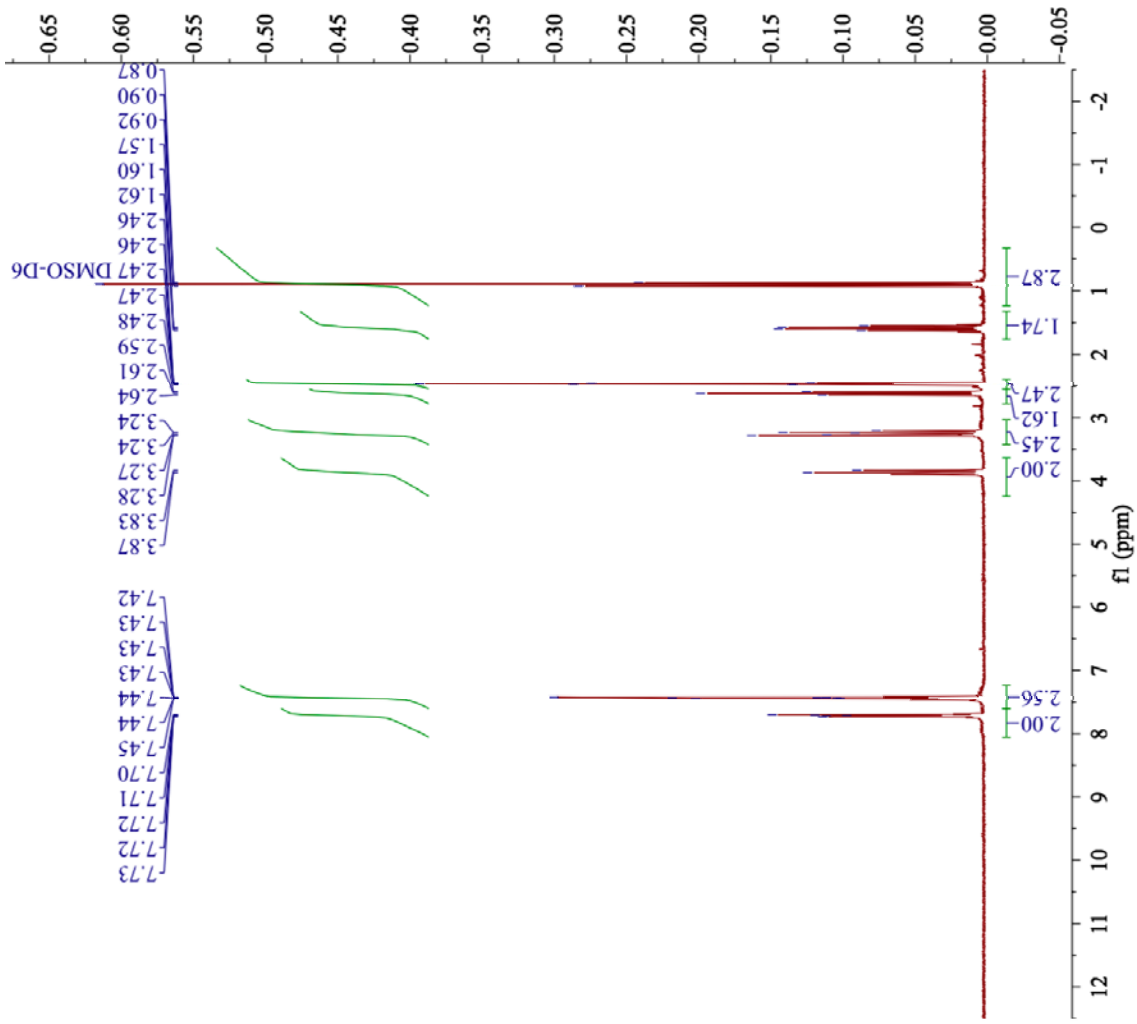

Parameter	Value
Data File Name	/ Volumes/ TOSHIBA/ MH03_68_DMSOrecrys_PROTON-1.jdf
Title	MH03_68_DMSOrecrys
Comment	
Origin	JEOL
Owner	
Site	
Instrument	ECX 300
Author	Delta
Solvent	DMSO-D6
Temperature	26.4
Pulse Sequence	single_pulse.ex2
Experiment	1D
Probe	2692
Number of Scans	16
Receiver Gain	46.0
Relaxation Delay	4.0000
Pulse Width	6.4750
Presaturation Frequency	2.9072
Acquisition Time	2018-01-12T14:28:26
Acquisition Date	2018-01-12T15:01:58
Modification Date	
Class	300.53
Spectrometer Frequency	4508.6
Spectral Width	-751.6
Lowest Frequency	1H
Nucleus	16384
Acquired Size	52430
Spectral Size	

Parameter	Value
Data File Name	/ Volumes/ Lexar/ single_pulse_dec-59.jdf
Title	MH03_68_DMSO
Comment	single pulse decoupled gated NOE_carbon
Origin	JEOL
Owner	
Site	
Instrument	ECX 300
Author	Delta
Solvent	DMSO-D6
Temperature	23.0
Pulse Sequence	single_pulse_dec
Experiment	1D
Probe	2692
Number of Scans	23625
Receiver Gain	60.0
Relaxation Delay	2.0000
Pulse Width	3.0694
Presaturation Frequency	
Acquisition Time	1.3841
Acquisition Date	2018-01-26T14:45:40
Modification Date	2018-01-26T15:19:29
Class	
Spectrometer Frequency	75.57
Spectral Width	18938.4
Lowest Frequency	-1912.4
Nucleus	13C
Acquired Size	32768
Spectral Size	26214

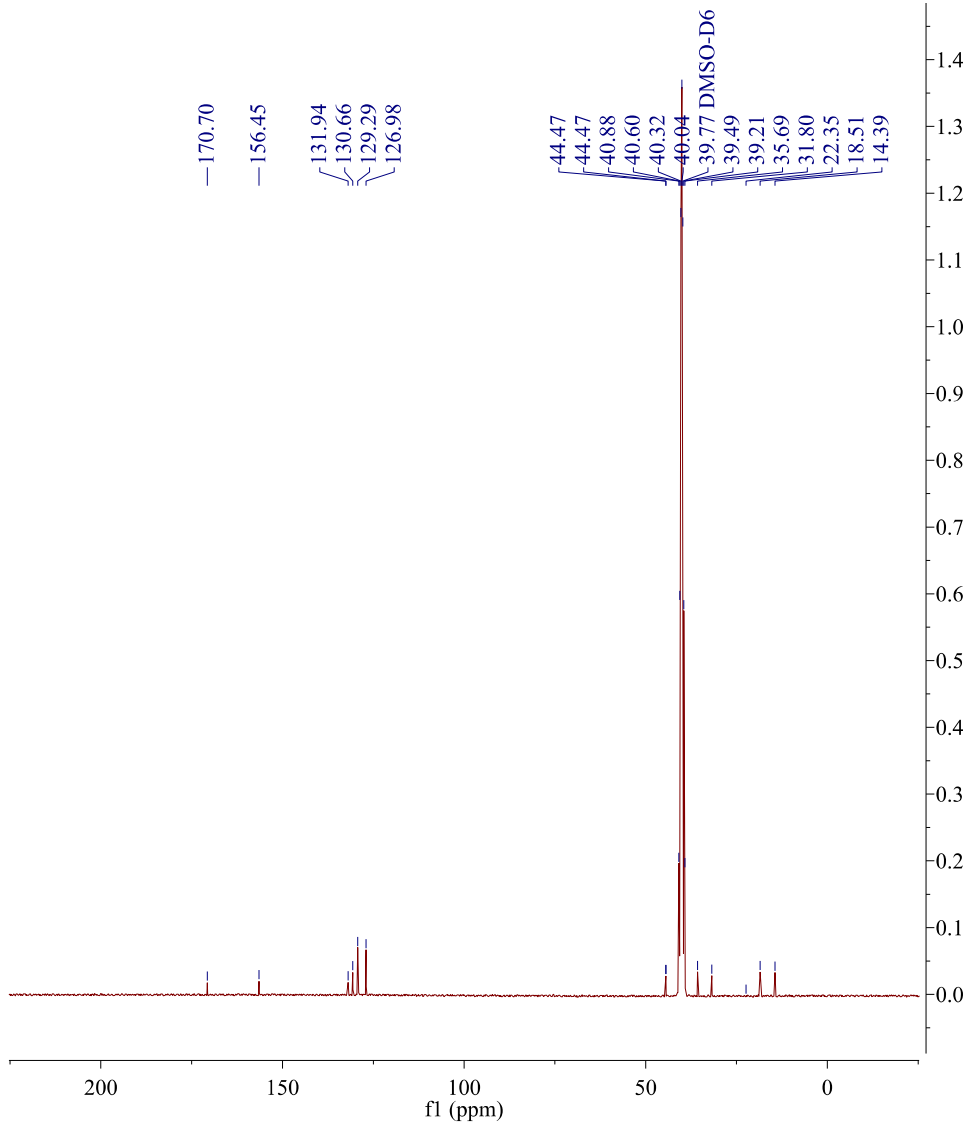

Who	What	When	Parameters	Comment
Organic Chem	Created as New Dataset	4/15/2018 12:41:21 PM		Sample 006 By organic lab Date Sunday, April 15 2018
Organic Chem	Atmospheric Correction	4/15/2018 12:41:21 PM		

Spectrum Graph

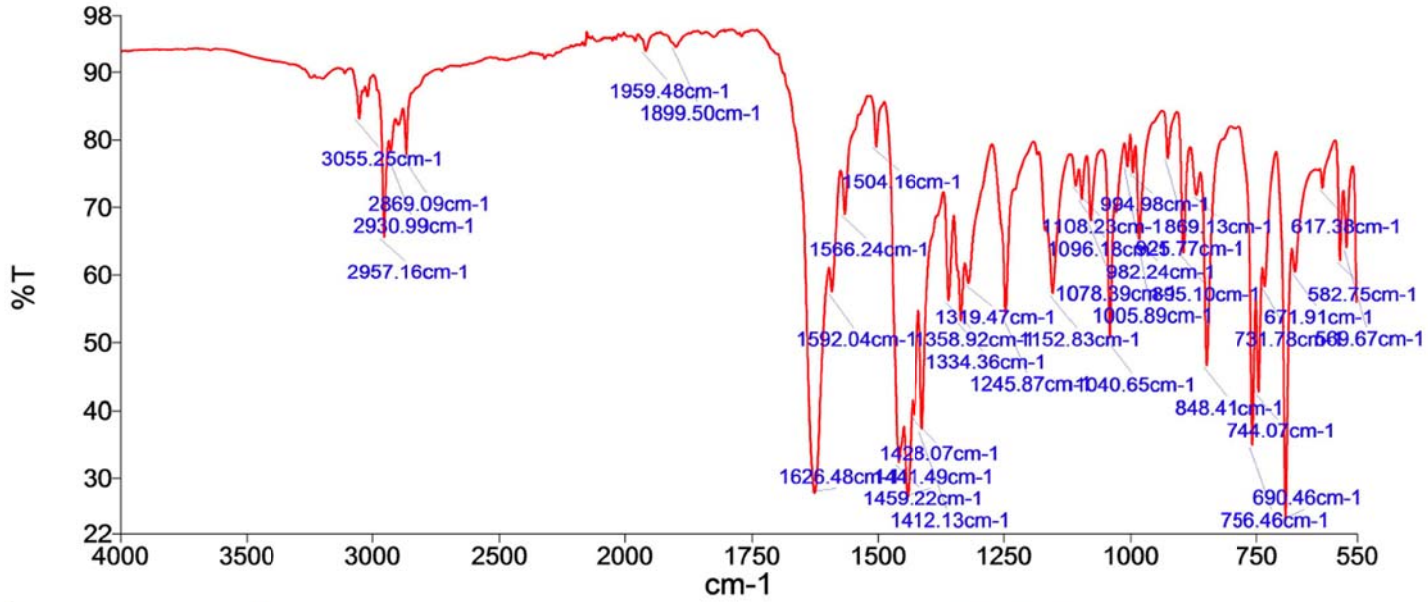

Name	Description
MH03-68	Sample 006 By organic lab Date Sunday, April 15 2018

Compound 9

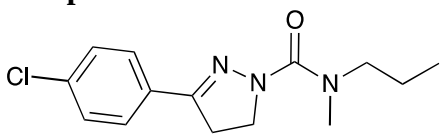

Synthesis of 3-(4-chlorophenyl)-*N*-methyl-*N*-propyl-4,5-dihydro-1*H*-pyrazole-1-carboxamide:

3-(4-chlorophenyl)-*N*-propyl-4,5-dihydro-1*H*-pyrazole-carboxamide **8** (0.020 g, 0.08 mmol, 1.00 equiv.) was dissolved in 0.40 mL THF, anhydrous under nitrogen. Sodium hydride (60%) (0.010 g, 0.23 mmol, 3.00 equiv.) was added to the solution and stirred one hour on ice. Methyl iodide (10.0 μL, 0.080 mmol, 1.00 equiv.) was added to the stirring solution dropwise and stirred. The reaction was monitored by TLC with a 50.% ethyl acetate: hexanes mobile phase. After two hours the solution was cooled on ice and an additional equivalent of NaH was added followed by an additional 1.50 equivalents (15.0 μL) of methyl iodide. After another four hours an additional equivalent of methyl iodide (10.0 μL) was added. After another 24 hours stirring at room temperature under nitrogen, ice was added to the solution and the resulting precipitate was filtered. The resulting yellow oil and solid white precipitate was isolated as an off-white solid (6.3 mg, 29% yield) following purification (12-52% ethyl acetate: hexanes, silica gel column chromatography). Recovered 15.6 mg of 3-(4-chlorophenyl)-*N*-propyl-4,5-dihydro-1*H*-pyrazole-carboxamide **8**.

^{1}H NMR (300 MHz, $CDCl_3$) δ (ppm): 7.58 (d, *J*= 8.3Hz, 2H), 7.37 (d, *J*= 8.5Hz, 2H), 3.96 (t, *J*= 9.7Hz, 2H), 3.39 (t, *J*= 7.7Hz, 2H), 3.02 (t, *J*= 10.1Hz, 4H), 1.69 (m, *J*= 7.5Hz, 3H), 0.92 (t, *J*= 7.5Hz, 3H).

^{13}C NMR (75.6 MHz, $CDCl_3$) δ (ppm): 151.2, 135.3, 131.0, 128.9, 127.4, 21.2. (Missing signals are observed in DEPT-135 spectra).

DEPT-135 (75.6 MHz, $CDCl_3$) δ (ppm): (+) 128.9, 127.4, 56.3, 36.6, 11.3; (-) 52.6, 47.3, 30.6, 21.2.

Parameter	Value
Data File Name	/ Volumes/ Lexar/ LRpg76f23_PROTON~10.jdf
Title	LRpg76f23
Comment	f223-29, NCH3
Origin	JEOL
Owner	
Site	
Instrument	ECX 300
Author	Delta
Solvent	CHLOROFORM-D
Temperature	23.8
Pulse Sequence	single_pulse.ex2
Experiment	1D
Probe	2692
Number of Scans	16
Receiver Gain	46.0
Relaxation Delay	4.0000
Pulse Width	6.4750
Presaturation Frequency	
Acquisition Time	2.9072
Acquisition Date	2017-07-10T10:51:34
Modification Date	2017-07-10T11:18:21
Class	
Spectrometer Frequency	300.53
Spectral Width	4508.6
Lowest Frequency	-751.6
Nucleus	1H
Acquired Size	16384
Spectral Size	52430

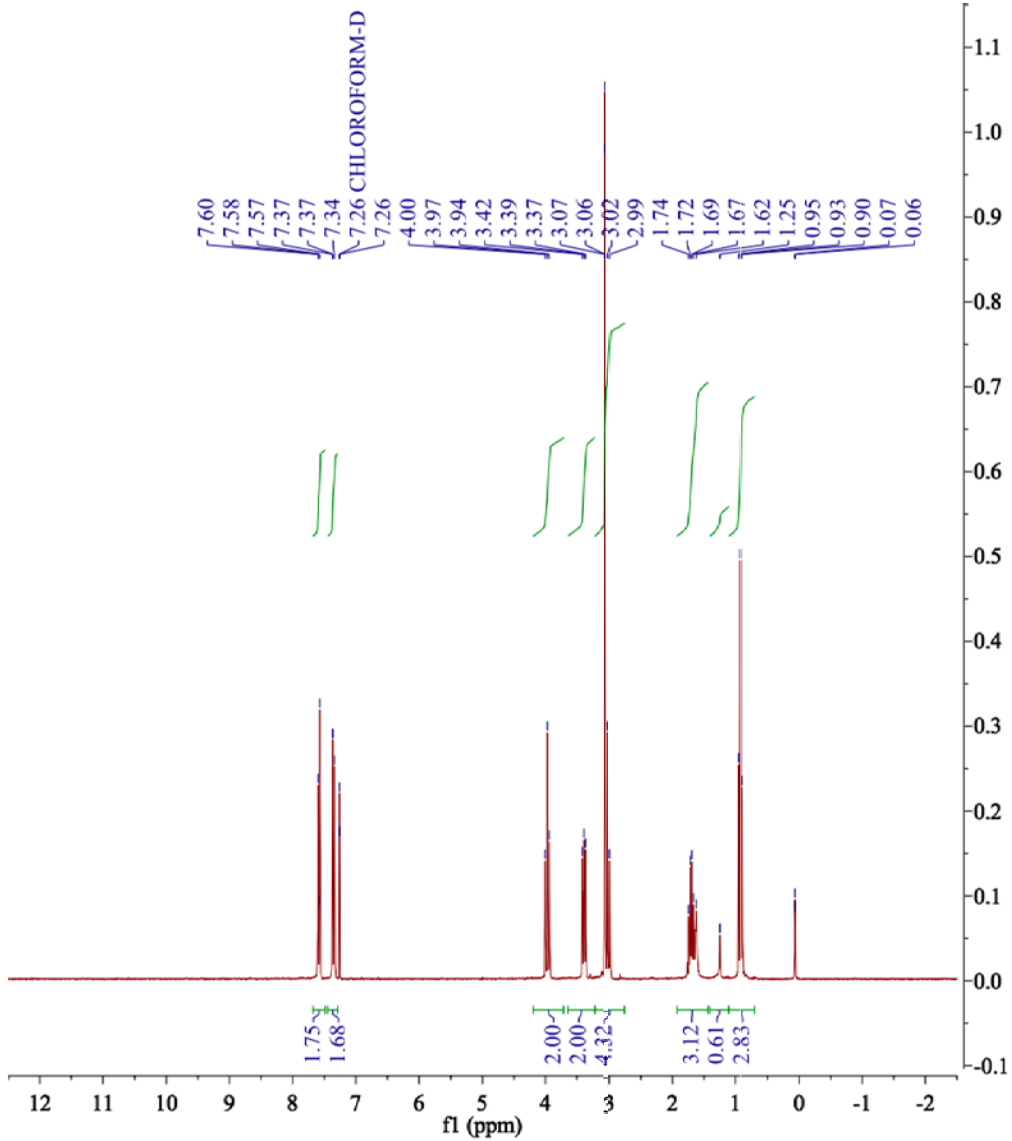

Parameter	Value
Data File Name	/ Volumes/ Lexar/ LRpg76f23_CARBON-6.jdf
Title	LRpg76f23
Comment	f223-29, NCH3
Origin	JEOL
Owner	
Site	
Instrument	ECX 300
Author	Delta
Solvent	CHLOROFORM-D
Temperature	23.9
Pulse Sequence	single_pulse_dec
Experiment	1D
Probe	2692
Number of Scans	319
Receiver Gain	58.0
Relaxation Delay	2.0000
Pulse Width	2.9867
Presaturation Frequency	
Acquisition Time	1.3841
Acquisition Date	2017-07-10T11:10:15
Modification Date	2017-07-10T11:37:04
Class	
Spectrometer Frequency	75.57
Spectral Width	18939.4
Lowest Frequency	-1912.9
Nucleus	13C
Acquired Size	32768
Spectral Size	52430

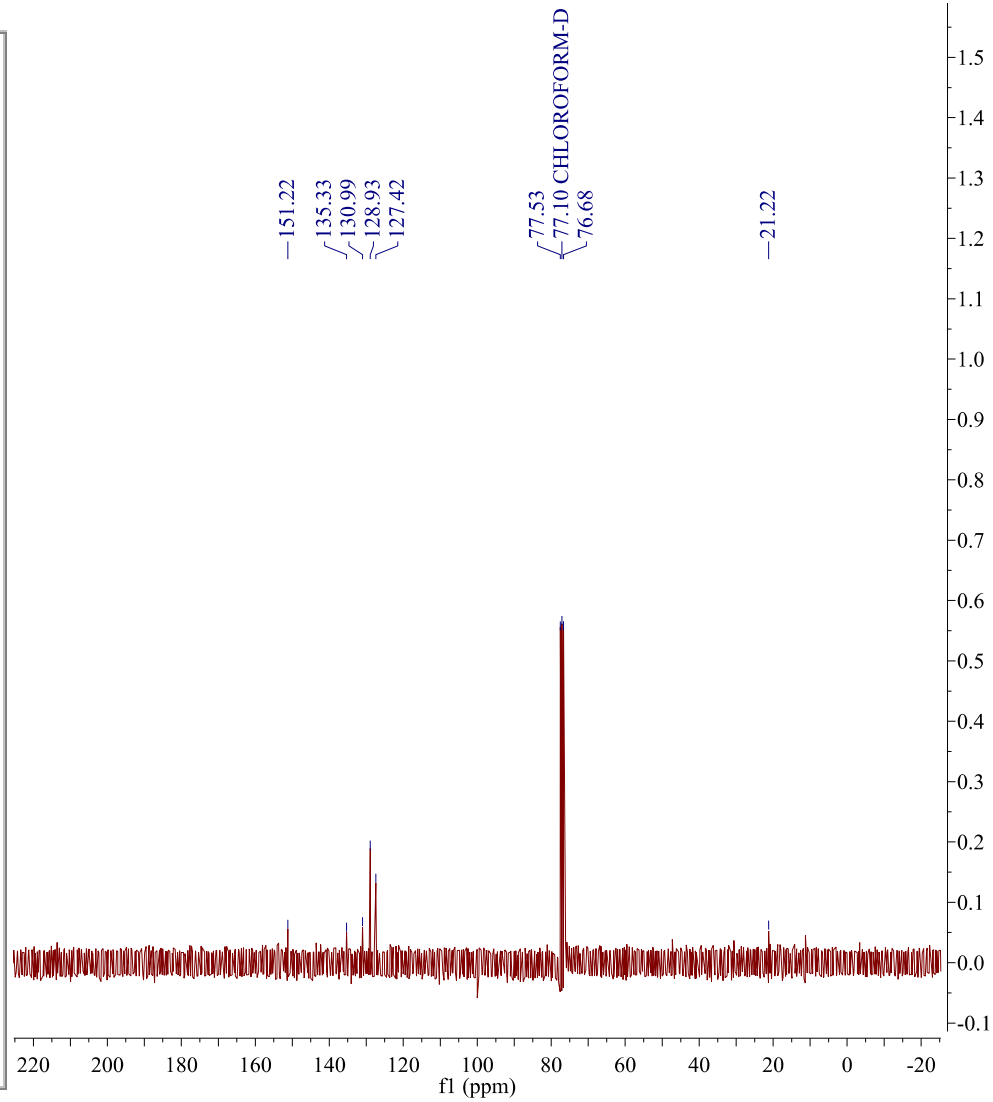

Parameter	Value
Data File Name	/ Volumes/ Lexar/ LRpg76_DEPT135-3.jdf
Title	LRpg76
Comment	F23-29, prep
Origin	JEOL
Owner	
Site	
Instrument	ECX 300
Author	Delta
Solvent	CHLOROFORM-D
Temperature	23.6
Pulse Sequence	dept.ex2
Experiment	1D
Probe	2692
Number of Scans	976
Receiver Gain	60.0
Relaxation Delay	2.0000
Pulse Width	8.9600
Presaturation Frequency	
Acquisition Time	1.3841
Acquisition Date	2017-06-30T11:17:02
Modification Date	2017-06-30T11:44:00
Class	
Spectrometer Frequency	75.57
Spectral Width	18938.4
Lowest Frequency	-1912.4
Nucleus	13C
Acquired Size	32768
Spectral Size	26214

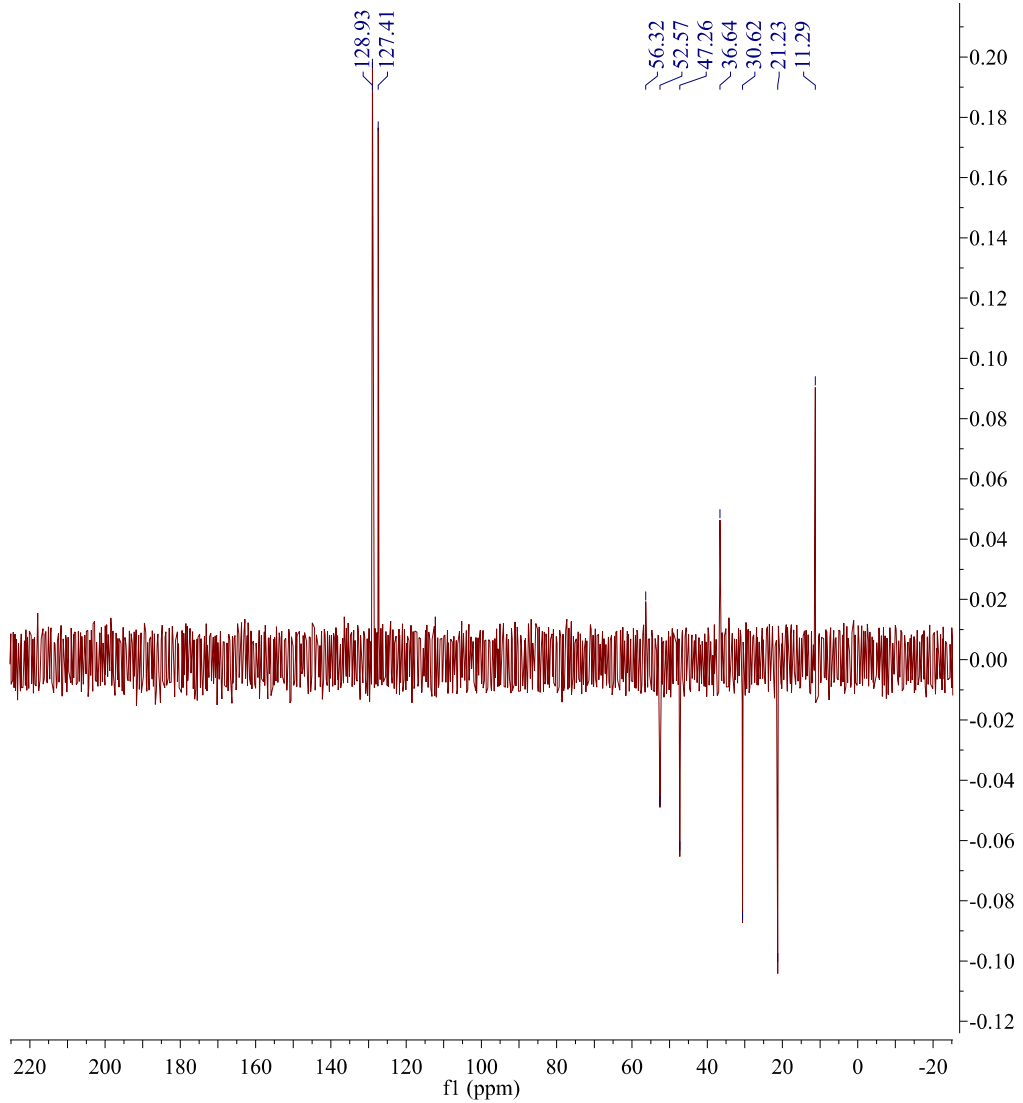

Compound 11

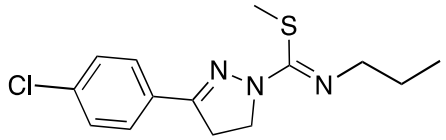

Synthesis of (1Z)-1-(methylsulfanyl)-*N*-propy1-(3-phenyl-4,5-dihydro-1*H*-pyrazol-1-yl) methanimine:

3-(4-chlorophenyl)-*N*-propyl-4,5-dihydro-1*H*-pyrazole carbothiamide **10** (0.030 g, 0.09 mmol, 1.00 equiv.) was dissolved in 1 mL CH_2Cl_2. This solution was chilled on ice before the gradual addition of methyl iodide (0.32 g, 2.3 mmol, 25 equiv.). This stirring solution was warmed to room temperature and stirred at ambient temperature for 68 hours. The reaction was monitored by TLC with a 4:1 hexanes: ethyl acetate mobile phase. This solution was concentrated under reduced pressure, reconstituted in CH_2Cl_2, and washed with 10% NaOH. The organic layer was dried over $MgSO_4$, filtered, and concentrated to yield a yellow viscous oil. This oil was purified to yield **11** as a white solid (21.6 mg, 81%).

^{1}H NMR (300 MHz, $CDCl_3$) δ (ppm): 7.63 (d, *J*= 6.6Hz, 2H), 7.33 (d, *J*= 6.8Hz, 2H), 3.96 (t, *J*= 10.2, 2H), 3.48 (t, *J*= 7.1, 2H), 3.08 (t, *J*= 10.0Hz, 2H), 2.53 (s, 3H), 1.58 (m, *J*= 7.2Hz, 3H), 0.94 (t, *J*= 7.4Hz, 3H)

^{13}C NMR (75.6 MHz, $CDCl_3$) δ (ppm): 150.9, 135.0, 128.9, 127.2, 53.6, 48.4, 31.2, 25.0, 16.9, 12.0.

DEPT-135 (75.6 MHz, $CDCl_3$) δ (ppm): (+) 128.9, 127.2, 29.5, 16.9, 12.0; (-) 53.6, 48.4, 31.2, 25.0.

Parameter	Value
Data File Name	/ Volumes/ Lexar/ LRpg72_PROTON-13.jdf
Title	LRpg72
Comment	crude
Origin	JEOL
Owner	
Site	
Instrument	ECX 300
Author	Delta
Solvent	CHLOROFORM-D
Temperature	24.2
Pulse Sequence	single_pulse.ex2
Experiment	1D
Probe	2692
Number of Scans	16
Receiver Gain	40.0
Relaxation Delay	4.0000
Pulse Width	6.4750
Presaturation Frequency	
Acquisition Time	2.9072
Acquisition Date	2017-06-19T14:06:23
Modification Date	2017-06-19T14:55:20
Class	
Spectrometer Frequency	300.53
Spectral Width	4508.2
Lowest Frequency	-751.4
Nucleus	1H
Acquired Size	16384
Spectral Size	13107

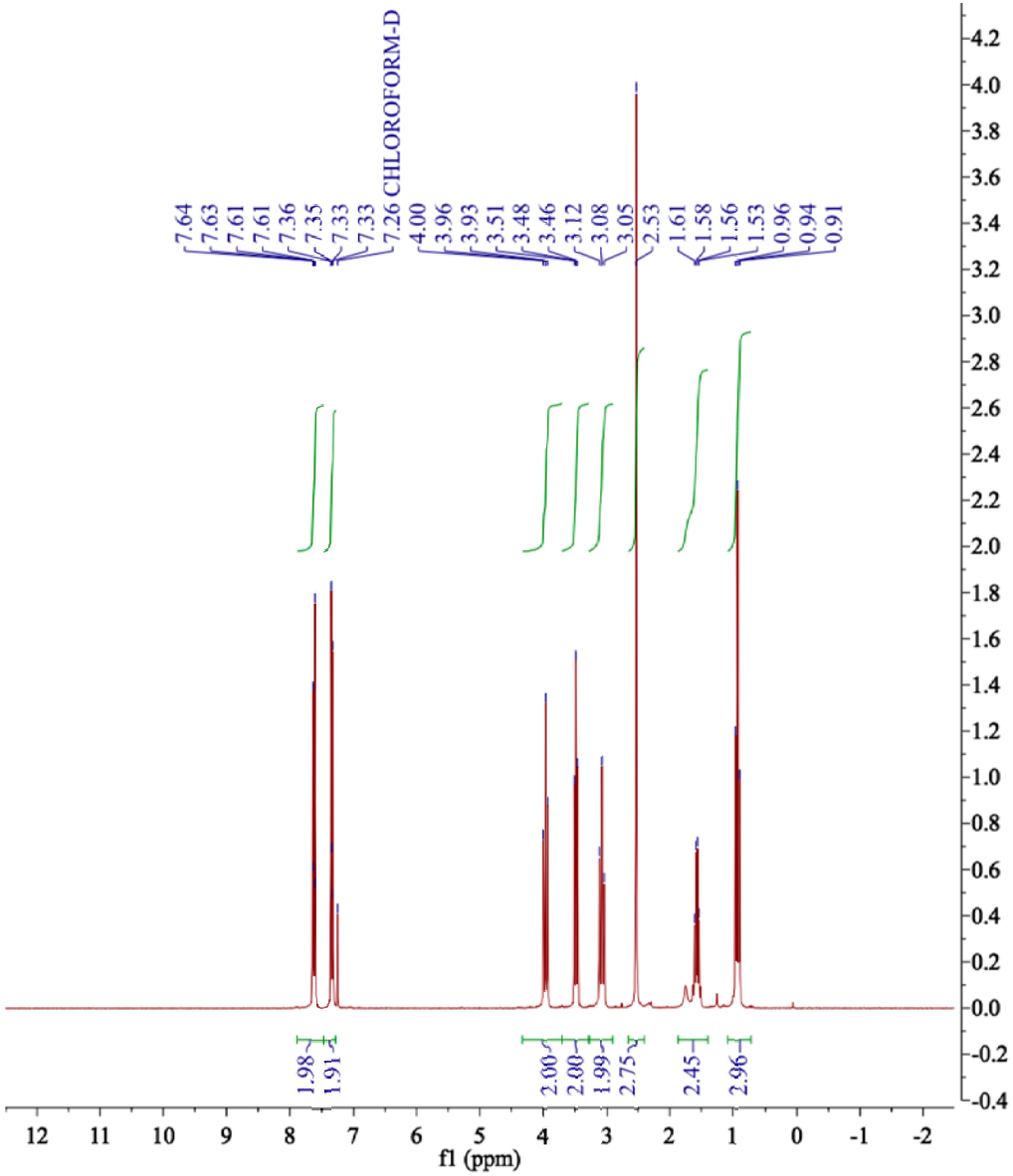

Parameter
Value
Data File Name
/ Volumes/ Lexar/ LRpg72_CARBON-12.jdf
Title
LRpg72
Comment
crude
Origin
JEOL
Owner
Site
Instrument
ECX 300
Author
Delta
Solvent
CHLOROFORM-D
Temperature
24.3
Pulse Sequence
single_pulse_dec
Experiment
1D
Probe
2692
Number of Scans
65
Receiver Gain
58.0
Relaxation Delay
2.0000
Pulse Width
2.9867
Presaturation Frequency
Acquisition Time
1.3841
Acquisition Date
2017-06-19T13:43:55
Modification Date
2017-06-19T14:30:22
Class
Spectrometer Frequency
75.57
Spectral Width
18938.4
Lowest Frequency
-1912.4
Nucleus
13C
Acquired Size
32768
Spectral Size
26214
150.80
134.99
128.87
127.22
77.54
77.12 CHLOROFORM-D
76.70
53.64
48.43
31.17
24.98
16.87
12.01
f1 (ppm)

Parameter	Value
Data File Name	/ Volumes/ Lexar/ LRpg72_DEPT135-3.jdf
Title	LRpg72
Comment	crude
Origin	JEOL
Owner	
Site	
Instrument	ECX 300
Author	Delta
Solvent	CHLOROFORM-D
Temperature	24.2
Pulse Sequence	dept.ex2
Experiment	1D
Probe	2692
Number of Scans	81
Receiver Gain	60.0
Relaxation Delay	2.0000
Pulse Width	8.9600
Presaturation Frequency	
Acquisition Time	1.3841
Acquisition Date	2017-06-19T13:36:36
Modification Date	2017-06-19T14:03:46
Class	
Spectrometer Frequency	75.57
Spectral Width	18938.4
Lowest Frequency	-1912.4
Nucleus	13C
Acquired Size	32768
Spectral Size	26214

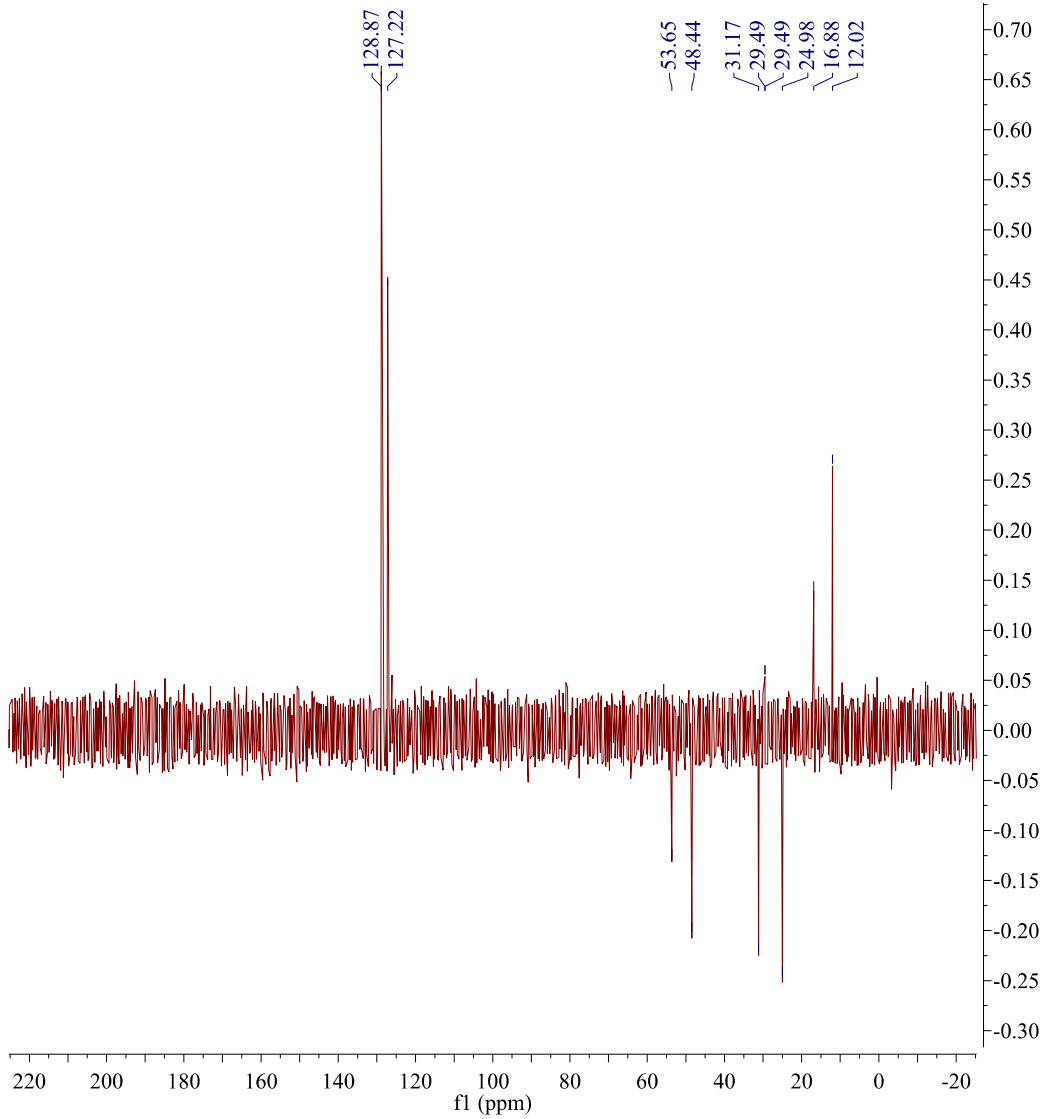

Compound 12

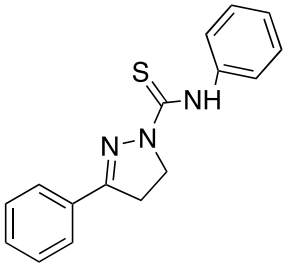

Synthesis of *N*,3-diphenyl-4,5-dihydro-1*H*-pyrazole-1-carbothioamide:

3-phenyl-4,5-dihydro-1*H*-pyrazole (2.58 g, 17.6 mmol, 1.00 equiv.) was dissolved in 47 mL anhydrous ether with three drops of triethylamine and phenyl isothiocyanate (1.00 mL, 16.9 mmol, 1.00 equiv.) phenyl isothiocyanate. This solution stirred for 1.5 hours at room temperature and the solid yellow product was filtered and dried, 54.5% yield.

^{1}H NMR (300 MHz, $CDCl_3$) δ (ppm): 9.13 (bs, 1H), 7.76 (dd, *J*= 2.1 Hz, 6.2 Hz, 2H), 7.65 (d, *J*= 7.9 Hz, 2H), 7.46 (t, *J*= 1.9 Hz, 3H), 7.38 (t, *J*= 7.6 Hz, 2H), 7.21 (t, *J*= 7.9 Hz, 1H), 4.46 (t, *J*= 10.3 Hz, 2H), 3.34 (t, *J*= 10.2 Hz, 2H).

^{13}C NMR (75.6 MHz, dmso-d_6) δ (ppm): 157.0, 138.8, 131.0, 129.0, 128.8, 126.9, 125.7, 124.6, 48.5, 32.2.

IR (neat, cm^{-1}): 3335.0, 3050.9, 1588.1, 1516.2, 1343.6, 760.6, 688.5.

Melting Point Range: 158.4- 159.4°C

Parameter	Value
Data File Name	/ Volumes/ TOSHIBA/ MH_Phenylthio_pyrazoline_PROTON-1.jdf
Title	MH_Phenylthio_pyrazoline
Comment	MH Phenylthiopyrazoline
Origin	JEOL
Owner	
Site	
Instrument	ECX 300
Author	Delta
Solvent	CHLOROFORM-D
Temperature	23.2
Pulse Sequence	single_pulse.ex2
Experiment	1D
Probe	2692
Number of Scans	16
Receiver Gain	46.0
Relaxation Delay	4.0000
Pulse Width	6.8000
Presaturation Frequency	
Acquisition Time	2.9072
Acquisition Date	2017-04-18T10:22:43
Modification Date	2017-04-18T10:48:36
Class	
Spectrometer Frequency	300.53
Spectral Width	4508.6
Lowest Frequency	-751.6
Nucleus	1H
Acquired Size	16384
Spectral Size	52430

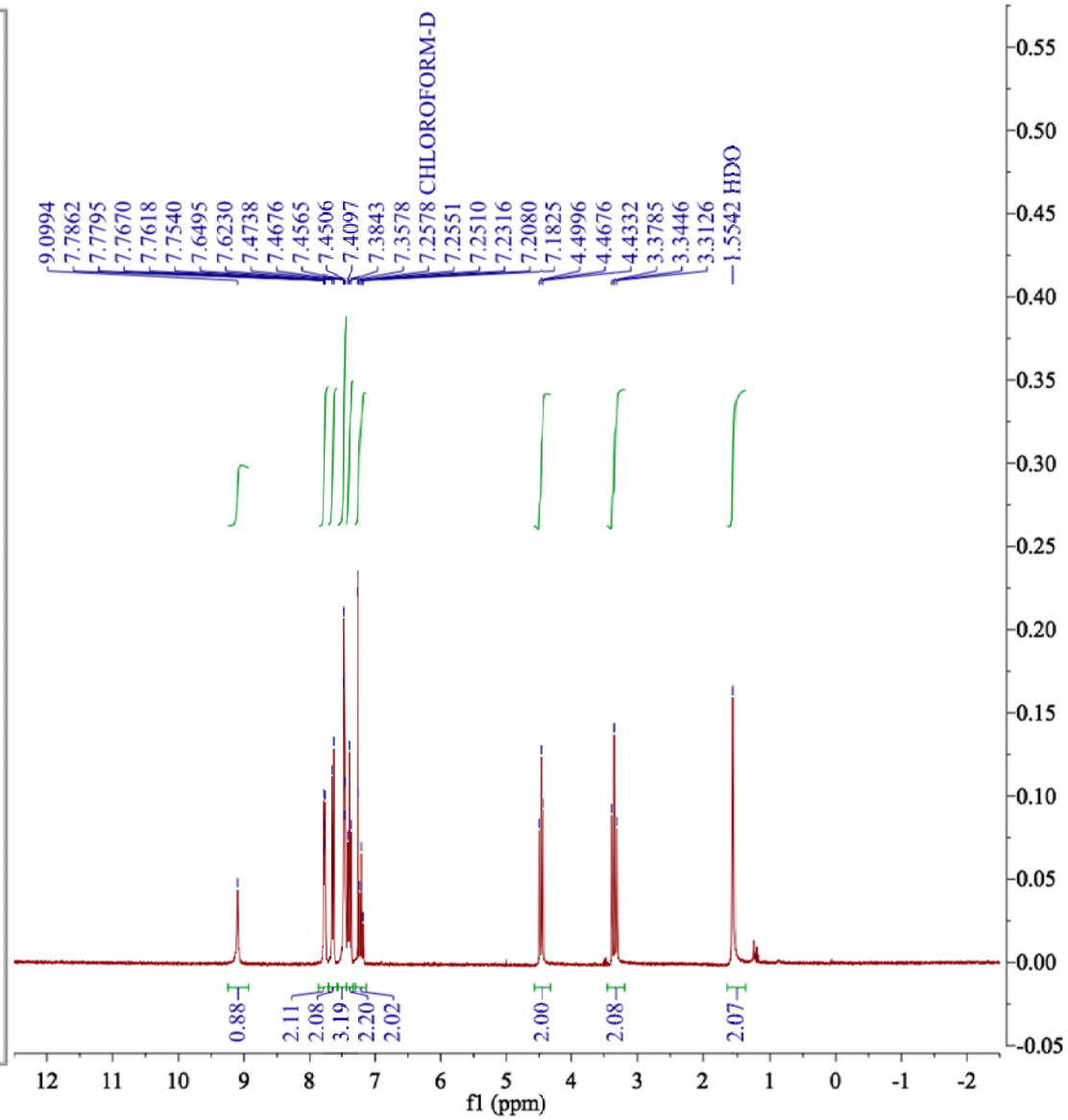

Parameter	Value
Data File Name	/ Volumes/ Lexar/ MH_Phenylthio_pyrazoline_CARBON-4.jdf
Title	MH_Phenylthio_pyrazoline
Comment	MH Phenylthiopyrazoline
Origin	JEOL
Owner	
Site	
Instrument	ECX 300
Author	Delta
Solvent	CHLOROFORM-D
Temperature	23.8
Pulse Sequence	single_pulse_dec
Experiment	1D
Probe	2692
Number of Scans	1024
Receiver Gain	60.0
Relaxation Delay	2.0000
Pulse Width	3.0600
Presaturation Frequency	
Acquisition Time	1.3841
Acquisition Date	2017-04-18T11:21:16
Modification Date	2017-04-18T11:47:15
Class	
Spectrometer Frequency	75.57
Spectral Width	18938.4
Lowest Frequency	-1912.4
Nucleus	13C
Acquired Size	32768
Spectral Size	26214

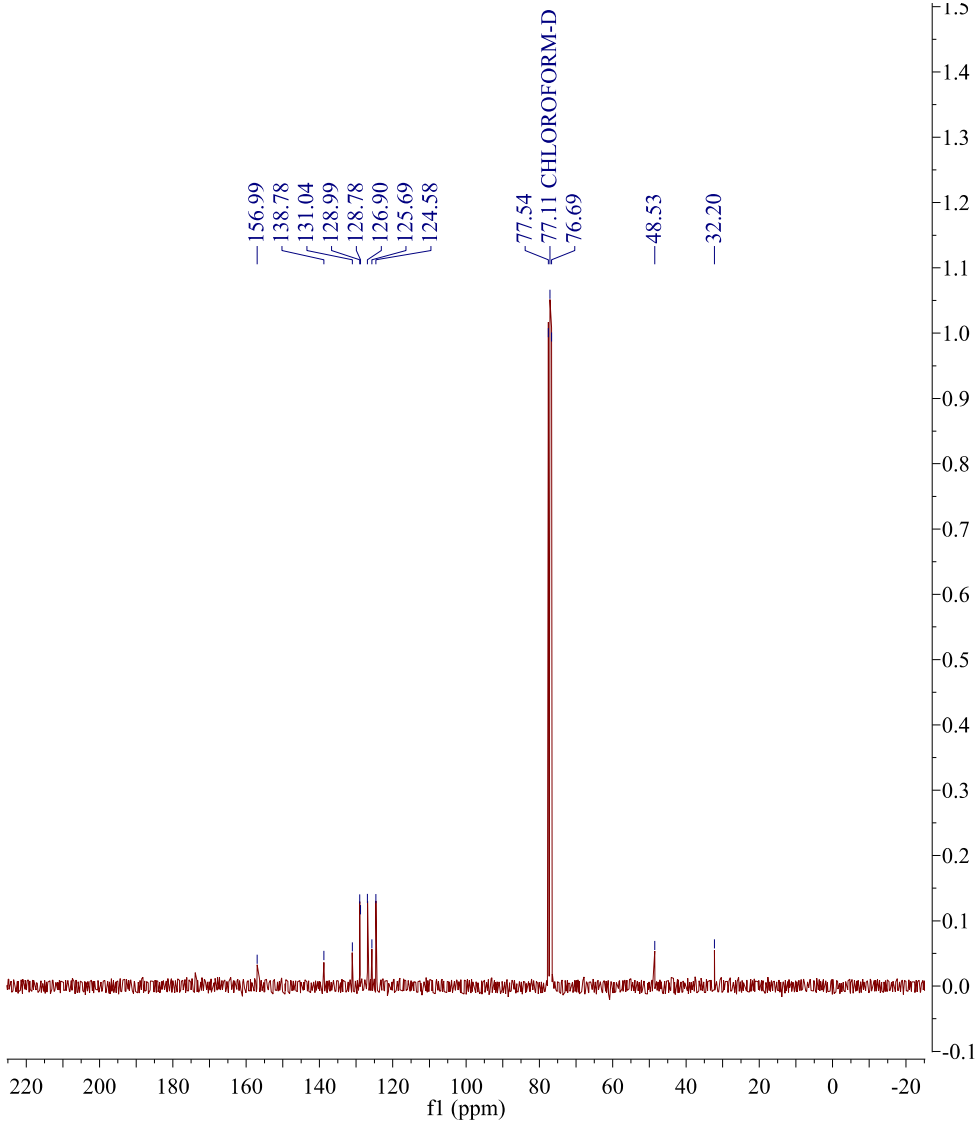

Who	What	When	Parameters	Comment
Organic Chem	Created as New Dataset	4/18/2017 10:14:40 AM		Sample 001 By organic lab Date Tuesday, April 18 2017
Organic Chem	Atmospheric Correction	4/18/2017 10:14:40 AM		

Spectrum Graph

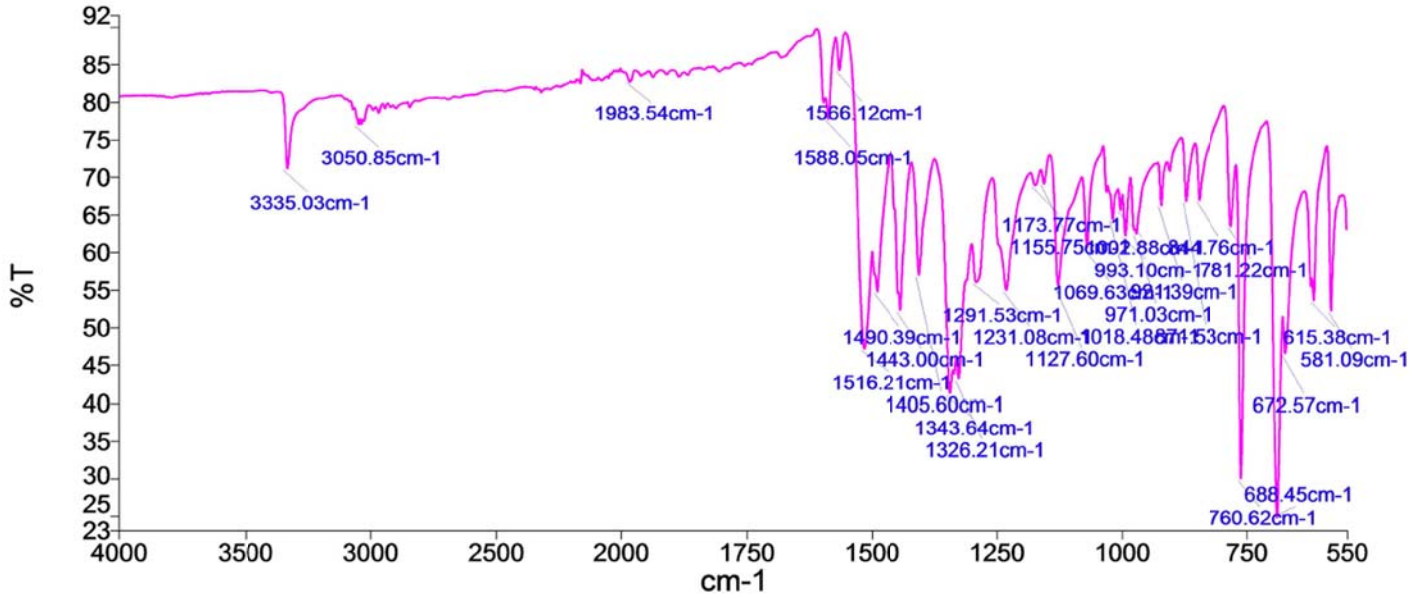

Name	Description
Phenylthio Pyrazoline	Sample 001 By organic lab Date Tuesday, April 18 2017

Compound 13

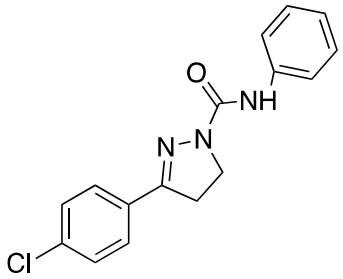

Synthesis of 3-(4-chlorophenyl)-*N*-phenyl-4,5-dihydro-1*H*-pyrazole-1-carboxamide:

3-(4-chlorophenyl)-4,5-dihydro-1*H*-pyrazole (1.58 g, 9.66 mmol, 1.00 equiv.) was dissolved in 50.0 mL anhydrous ether with three drops triethylamine and phenyl isocyanate (2.11 g, 9.66 mmol, 1.00 equiv.). The solution stirred for 1.5 hours at room temperature and yellow crystalline solid was filtered and dried, in 40.0% yield.

^{1}H NMR (300 MHz, $CDCl_3$) δ (ppm):7.98 (bs, 1H), 7.66 (dd, *J*= 4.7 Hz, 2.9Hz, 2H), 7.54 (d, *J*= 7.5Hz, 2H), 7.41 (dt, *J*= 4.7Hz, 2.0Hz, 2H), 7.32 (td, *J*= 6.1Hz, 2.1, 2H), 7.05 (t, *J*= 7.4Hz, 1H), 4.11 (t, *J*= 9Hz, 2H), 3.27 (t, *J*= 9Hz, 2H).

^{13}C NMR (75.6 MHz, $CDCl_3$) δ (ppm): 152.5, 152.1, 138.5, 136.2, 129.9, 129.3, 129.1, 127.7, 123.2, 120.7, 119.2, 44.6, 32.5.

IR (neat, cm^{-1}): 3284.0, 3036.0, 1647.10, 1592.6, 1532.8, 1496.7, 1314.3, 1231.2, 741.4, 684.6.

Melting Point Range: 143- 148°C

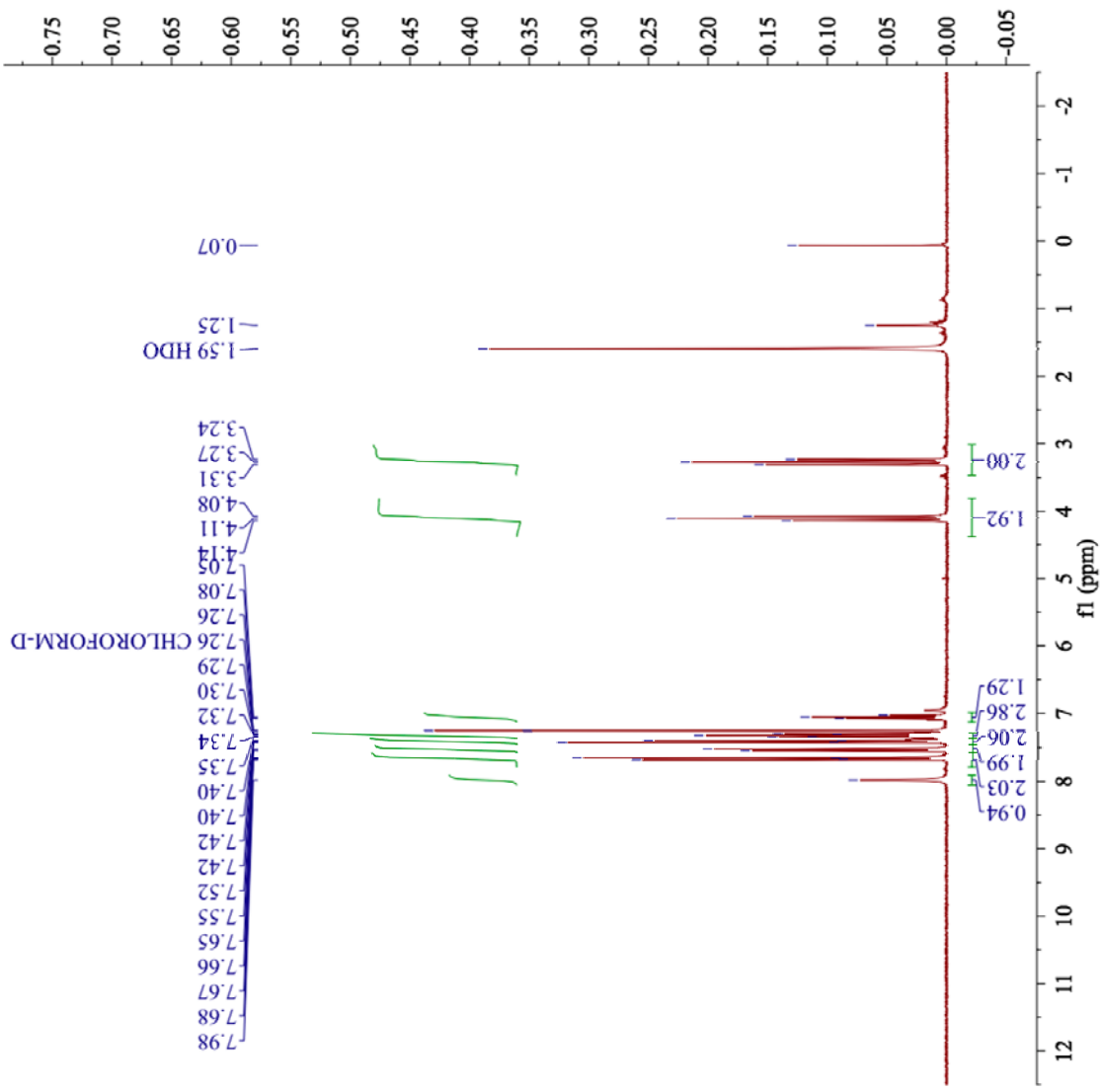

Parameter	Value
Data File Name	/ Volumes/TOSHIBA/Oxychloro_pyrazoline_MH_4.28.17_PROTON-1.jdf
Title	Oxychloro_pyrazoline_MH_4.28.17
Comment	Oxychloropyrazoline MH 4.28.17
Origin	JEOL
Owner	
Site	
Instrument	ECX 300
Author	Delta
Solvent	CHLOROFORM-D
Temperature	24.2
Pulse Sequence	single_pulse.ex2
Experiment	1D
Probe	2692
Number of Scans	16
Receiver Gain	48.0
Relaxation Delay	4.0000
Pulse Width	6.4750
Presaturation Frequency	
Acquisition Time	2.9072
Acquisition Date	2017-04-28T12:50:17
Modification Date	2017-04-28T13:18:14
Class	
Spectrometer Frequency	300.53
Spectral Width	4508.6
Lowest Frequency	-751.6
Nucleus	1H
Acquired Size	16384
Spectral Size	52430

Parameter	Value
Data File Name	/ Volumes/ Lexar/ Oxychloro_pyrazoline_MH_4.28.17_CARBON-3.jdf
Title	Oxychloro_pyrazoline_MH_4.28.17
Comment	Oxychloropyrazoline MH 4.28.17
Origin	JEOL
Owner	
Site	
Instrument	ECX 300
Author	Delta
Solvent	CHLOROFORM-D
Temperature	25.0
Pulse Sequence	single_pulse_dec
Experiment	1D
Probe	2692
Number of Scans	1024
Receiver Gain	60.0
Relaxation Delay	2.0000
Pulse Width	2.9867
Presaturation Frequency	
Acquisition Time	1.3841
Acquisition Date	2017-04-28T13:48:51
Modification Date	2017-04-28T14:16:49
Class	
Spectrometer Frequency	75.57
Spectral Width	18938.4
Lowest Frequency	-1912.4
Nucleus	13C
Acquired Size	32768
Spectral Size	26214

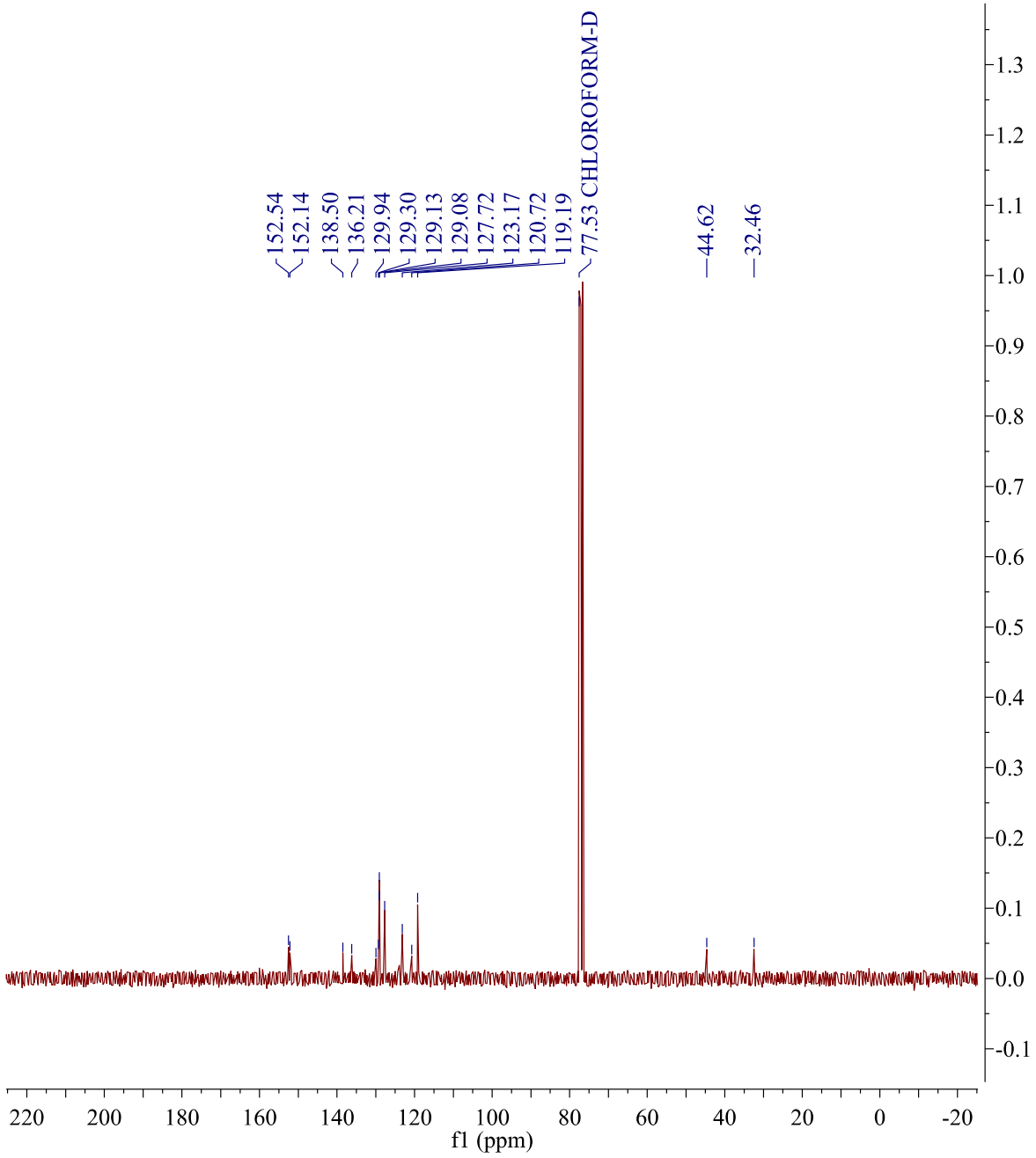

Who	What	When	Parameters	Comment
Organic Chem	Created as New Dataset	4/28/2017 1:20:07 PM		Sample 000 By organic lab Date Friday, April 28 2017
Organic Chem	Atmospheric Correction	4/28/2017 1:20:07 PM		

Spectrum Graph

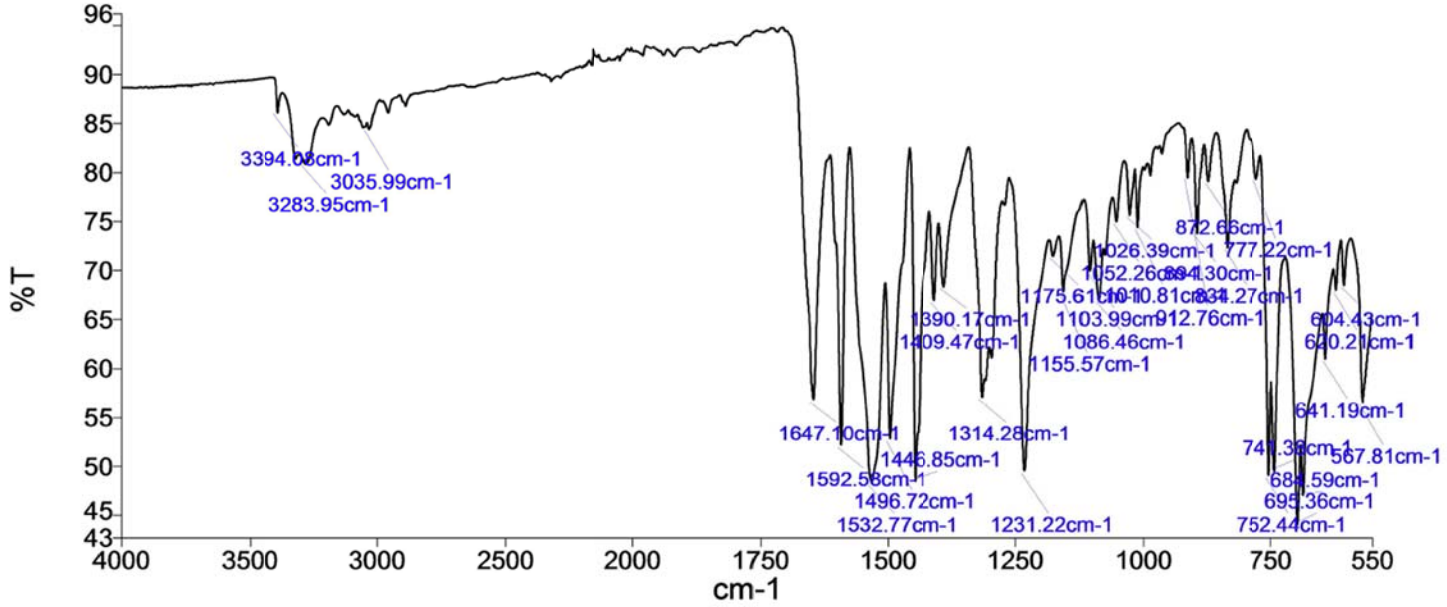

Name	Description
Chlorooxy Pyrazoline MH	Sample 000 By organic lab Date Friday, April 28 2017

Compound 14

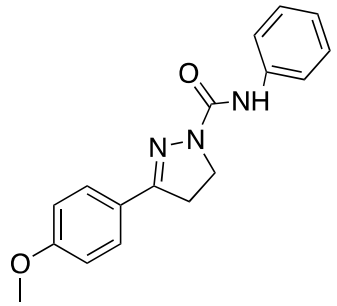

Synthesis of 3-(4-methoxyphenyl)-*N*-phenyl-4,5-dihydro-1*H*-pyrazole-1-carboxamide:

3-(4-methoxyphenyl)-4,5-dihydro-1*H*-pyrazole (1.37 g, 7.80 mmol, 1.00 equiv.) was dissolved in 50.0 mL dry ether with three drops of triethylamine and phenyl isocyanate (0.85 mL, 7.80 mmol, 1.00 equiv.). This solution stirred for two hours at room temperature and yellow solid product was filtered and dried, in 32.0% yield.

^{1}H NMR (300 MHz, $CDCl_3$) δ (ppm): 8.01 (bs, 1H), 7.68 (d, *J*= 9.0 Hz, 2H), 7.54 (dd, *J*= 1.2 Hz, 8.7 Hz, 2H), 7.32 (tt, *J*= 1.2 Hz, 7.3 Hz, 2H), 7.04 (t, *J*= 9 Hz, 2H), 6.95 (d, *J*= 8.9 Hz, 2H), 4.07 (t, *J*=9.9 Hz, 2H), 3.87 (s, 3H), 3.27 (t, *J*= 9.9 Hz, 2H).

^{13}C NMR (75.6 MHz, dmso-d_6) δ (ppm): 161.2, 154.1, 152.1, 140.0, 129.0, 128.9, 124.6, 122.6, 119.8, 114.5, 55.9, 45.0, 32.3.

DEPT-135 (75.6 MHz, CD_2Cl_2) δ (ppm): (+) 128.9, 122.6, 119.8, 114.5, 55.9; (-) 45.0, 32.3

IR (neat, cm^{-1}): 3348.6, 2961.4, 1658.7, 1591.9, 1418.1, 1169.6, 878.8, 687.3, 583.7.

Parameter	Value
Data File Name	/ Volumes/ TOSHIBA/ MH03_13_PROTON-2.jdf
Title	MH03_13
Comment	
Origin	JEOL
Owner	
Site	
Instrument	ECX 300
Author	Delta
Solvent	CHLOROFORM-D
Temperature	21.0
Pulse Sequence	single_pulse.ex2
Experiment	1D
Probe	2692
Number of Scans	16
Receiver Gain	48.0
Relaxation Delay	4.0000
Pulse Width	6.4750
Presaturation Frequency	
Acquisition Time	2.9072
Acquisition Date	2017-10-02T12:35:58
Modification Date	2017-10-02T13:07:32
Class	
Spectrometer Frequency	300.53
Spectral Width	4508.6
Lowest Frequency	-751.6
Nucleus	1H
Acquired Size	16384
Spectral Size	52430

Parameter	Value
Data File Name	/ Volumes/ Lexar/ MH03_13_DEPT_ CARBON-3.jdf
Title	MH03_13_DEPT
Comment	
Origin	JEOL
Owner	
Site	
Instrument	ECX 300
Author	Delta
Solvent	DMSO-D6
Temperature	22.3
Pulse Sequence	single_pulse_dec
Experiment	1D
Probe	2692
Number of Scans	1024
Receiver Gain	58.0
Relaxation Delay	2.0000
Pulse Width	3.0694
Presaturation Frequency	
Acquisition Time	1.3841
Acquisition Date	2018-04-15T14: 56:03
Modification Date	2018-04-15T15: 50:50
Class	
Spectrometer Frequency	75.57
Spectral Width	18938.4
Lowest Frequency	-1912.4
Nucleus	13C
Acquired Size	32768
Spectral Size	26214

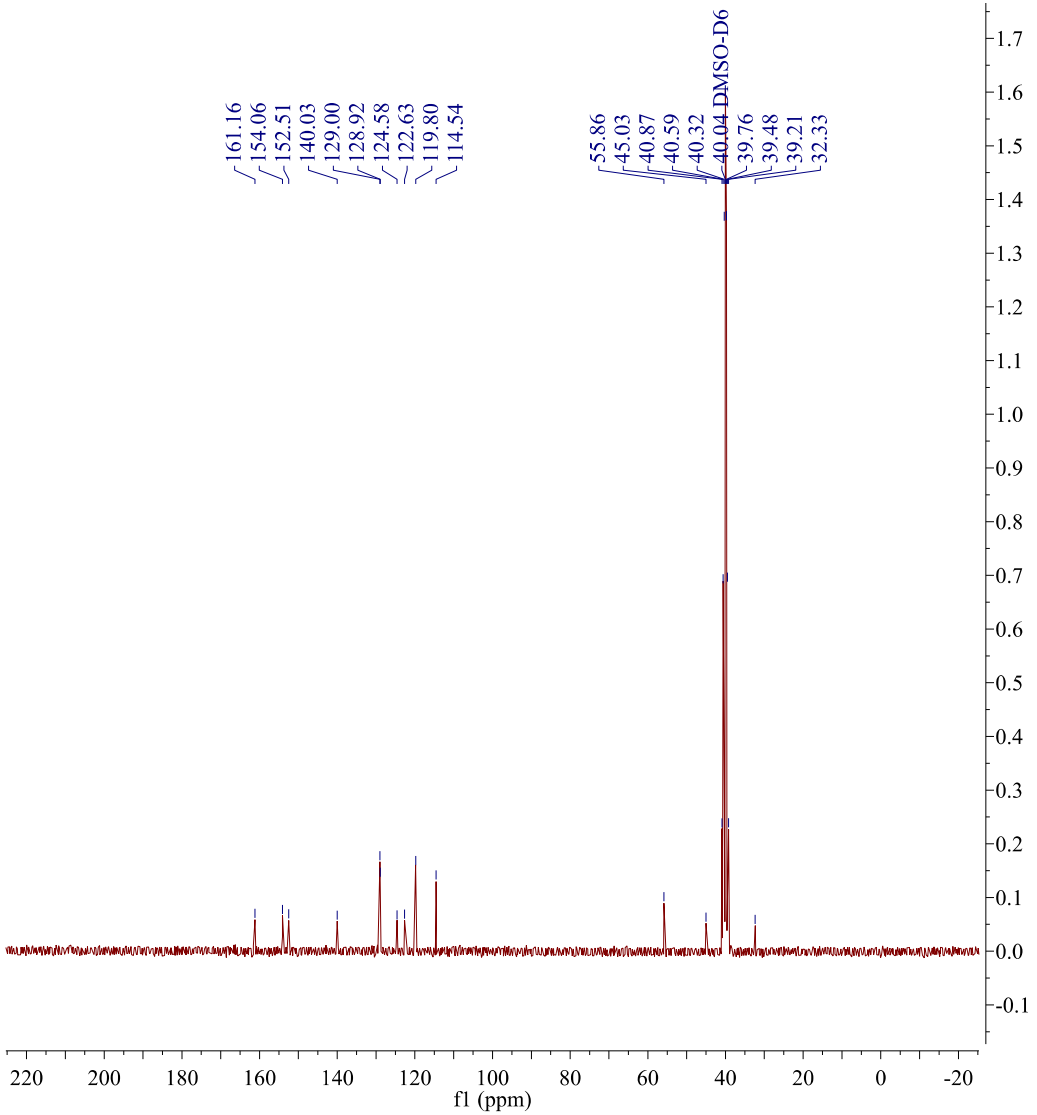

Parameter	Value
Data File Name	/ Volumes/ Lexar/ MH03_13_DEPT _DEPT135-3.jdf
Title	MH03_13_DEPT
Comment	
Origin	JEOL
Owner	
Site	
Instrument	ECX 300
Author	Delta
Solvent	DMSO-D6
Temperature	22.2
Pulse Sequence	dept.ex2
Experiment	1D
Probe	2692
Number of Scans	348
Receiver Gain	58.0
Relaxation Delay	2.0000
Pulse Width	9.2082
Presaturation Frequency	
Acquisition Time	1.3841
Acquisition Date	2018-04-15T15:16:27
Modification Date	2018-04-15T15:50:50
Class	
Spectrometer Frequency	75.57
Spectral Width	18938.4
Lowest Frequency	-1912.4
Nucleus	13C
Acquired Size	32768
Spectral Size	26214

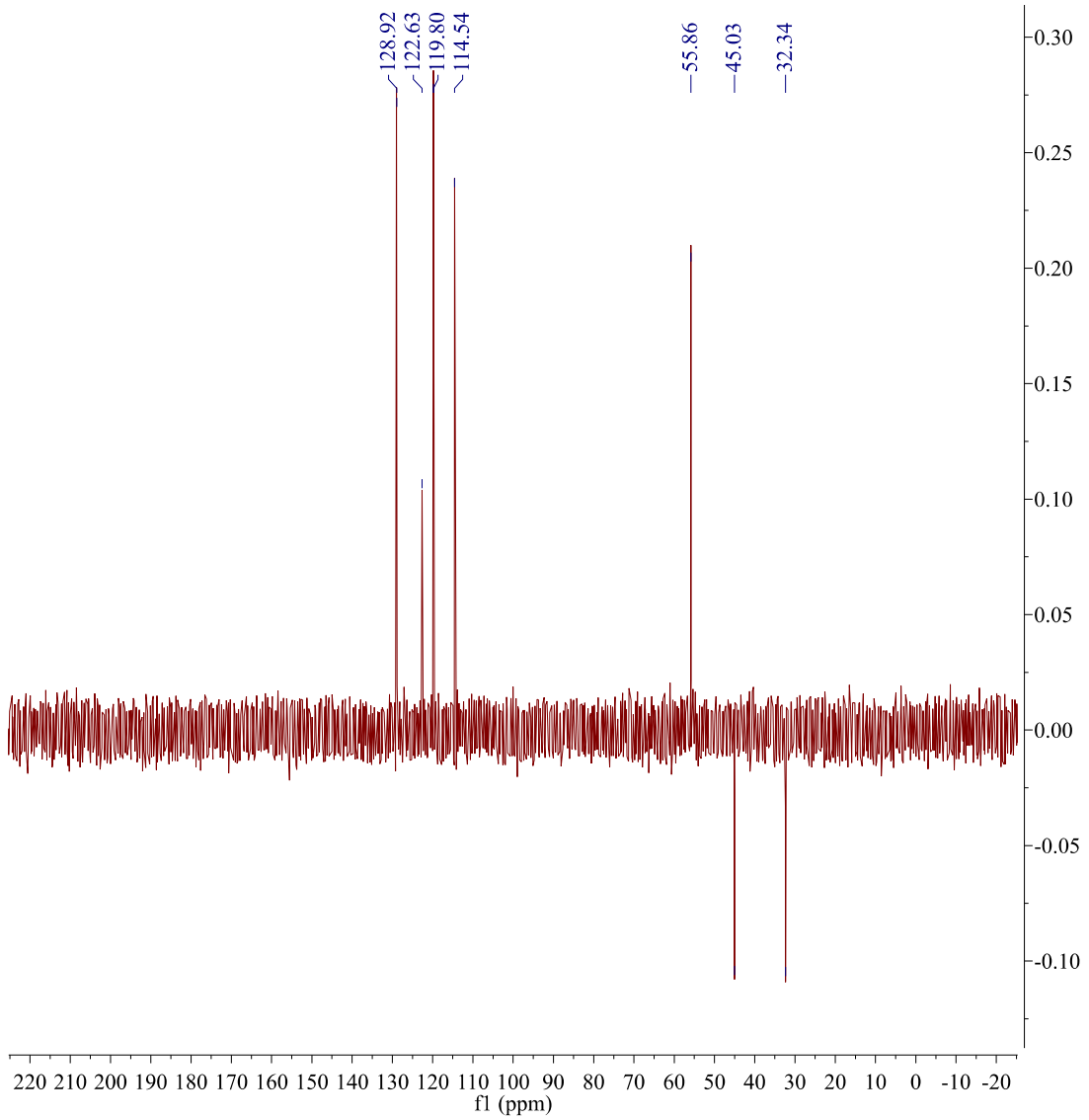

Who	What	When	Parameters	Comment
Organic Chem	Created as New Dataset	10/15/2017 3:10:43 PM		Sample 019 By organic lab Date Sunday, October 15 2017
Organic Chem	Atmospheric Correction	10/15/2017 3:10:43 PM		

Spectrum Graph

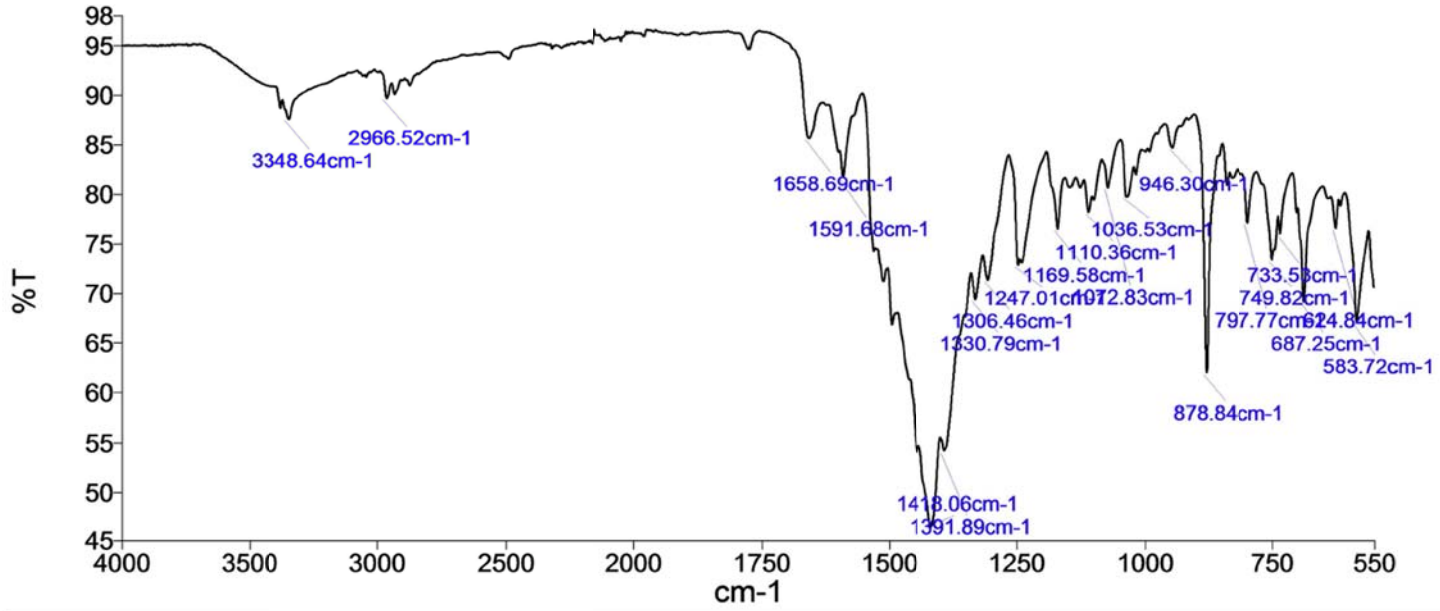

Name	Description
MH03_13_finesolid	Sample 019 By organic lab Date Sunday, October 15 2017

Compound 15

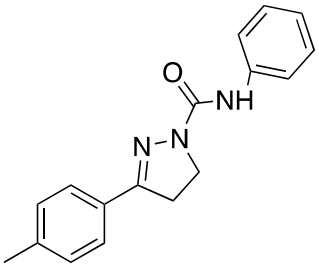

Synthesis of *N*-phenyl-3-(*p*-tolyl)-4,5-dihydro-1*H*-pyrazole-1-carboxamide:

3-(4-methylphenyl-4,5-dihydro-1*H*-pyrazole (0.92 g, 5.77 mmol, 1.00 equiv.) was dissolved in 40.0 mL anhydrous ether with three drops triethylamine and phenyl isocyanate (0.70 mL, 5.77 mmol, 1.00 equiv.). The solution stirred for two hours at room temperature and sand colored solid/paste was filtered and dried, in 58.0% yield.

^{1}H NMR (300 MHz, $CDCl_3$) δ (ppm): 8.03 (bs, 1H), 7.62 (d, *J*=8.1 Hz, 2H), 7.54 (dd, *J*= 1.8 Hz, *J*= 7.6 Hz, 2H), 7.31 (t, *J*=7.5 Hz, 5H, overlap with $CHCl_3$ solvent impurity peak), 7.05 (t, *J*= 8.7 Hz, 1H), 4.08 (t, *J*=10.5 Hz, 2H), 3.28 (t, *J*=10.2 Hz, 2H), 2.41 (s, 3H).

^{13}C NMR (75.6 MHz, dmso-d_6) δ (ppm): 154.3, 152.5, 140.2, 140.0, 129.6, 129.3, 129.0, 127.3, 122.7, 119.8, 114.4, 45.1, 32.2, 21.6.

DEPT-135 (75.6 MHz, dmso-d_6) δ (ppm): (+) 129.7, 129.0, 127.3, 122.7, 119.8, 21.6; (-) 45.1, 32.2.

IR (neat, cm^{-1}): 3426.2, 1665.1, 1591.0, 1497.8, 1427.1, 1237.1, 742.8, 687.0, 563.3.

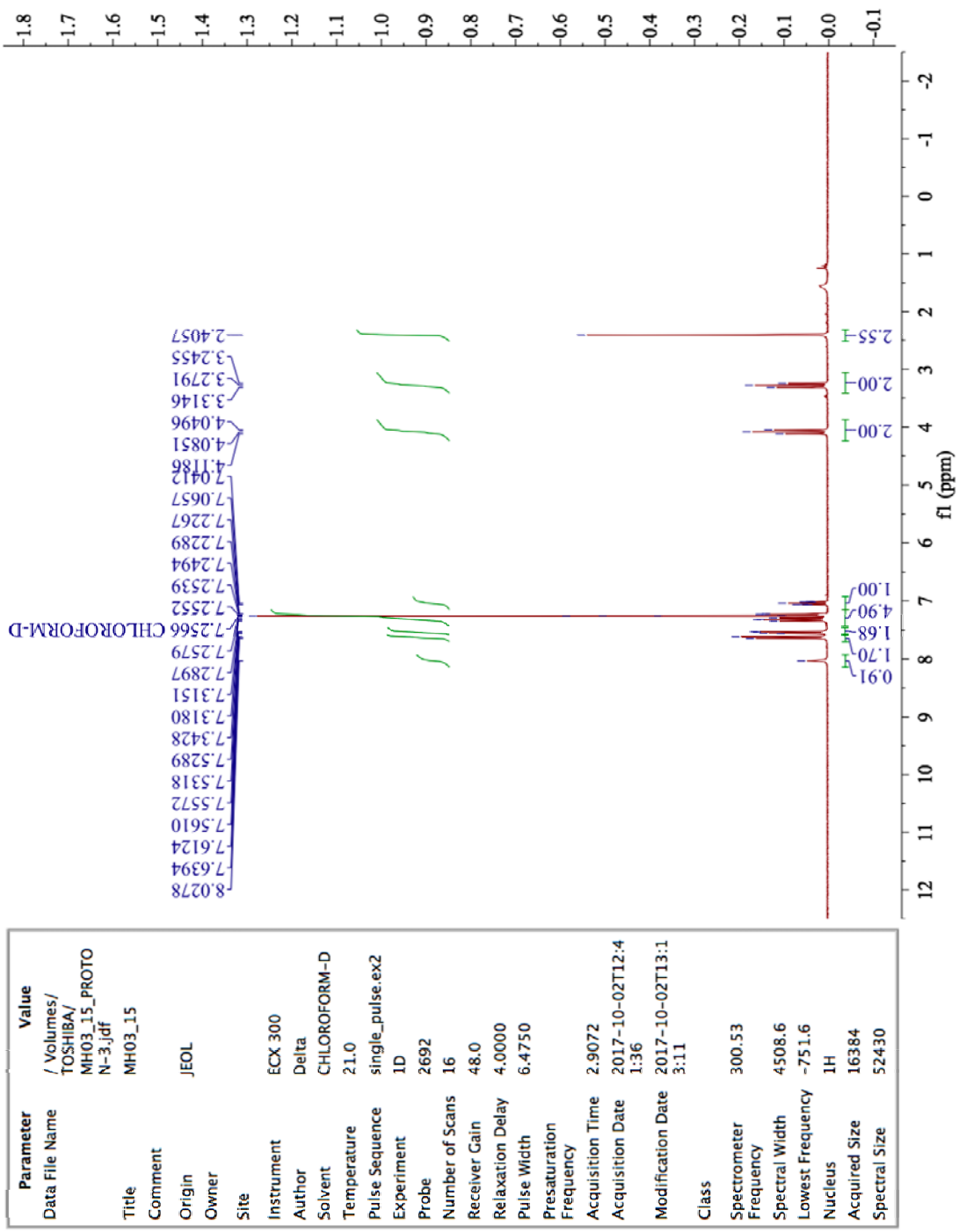
Parameter
Value
Data File Name
/ Volumes/TOSHIBA/MH03_15_PROTON-3.jdf
Title
MH03_15
Comment
Origin
JEOL
Owner
Site
Instrument
ECX 300
Author
Delta
Solvent
CHLOROFORM-D
Temperature
21.0
Pulse Sequence
single_pulse.ex2
Experiment
1D
Probe
2692
Number of Scans
16
Receiver Gain
48.0
Relaxation Delay
4.0000
Pulse Width
6.4750
Presaturation Frequency
Acquisition Time
2.9072
Acquisition Date
2017-10-02T12:41:36
Modification Date
2017-10-02T13:13:11
Class
Spectrometer Frequency
300.53
Spectral Width
4508.6
Lowest Frequency
-751.6
Nucleus
1H
Acquired Size
16384
Spectral Size
52430
8.0278
7.6394
7.6124
7.5610
7.5572
7.5318
7.5289
7.3428
7.3180
7.3151
7.2897
7.2579
7.2566
CHLOROFORM-D
7.2552
7.2539
7.2494
7.2289
7.2267
7.0657
7.0412
4.1186
4.0851
4.0496
3.3146
3.2791
3.2455
2.4057
2.55
2.00
2.00
1.00
4.90
1.68
1.70
0.91
f1 (ppm)

Parameter	Value
Data File Name	/ Volumes/ Lexar/ MH03_15_DEPT_ CARBON-1.jdf
Title	MH03_15_DEPT
Comment	
Origin	JEOL
Owner	
Site	
Instrument	ECX 300
Author	Delta
Solvent	DMSO-D6
Temperature	22.3
Pulse Sequence	single_pulse_dec
Experiment	1D
Probe	2692
Number of Scans	1024
Receiver Gain	58.0
Relaxation Delay	2.0000
Pulse Width	3.0694
Presaturation Frequency	
Acquisition Time	1.3841
Acquisition Date	2018-04-15T13: 45:31
Modification Date	2018-04-15T14: 19:55
Class	
Spectrometer Frequency	75.57
Spectral Width	18939.4
Lowest Frequency	-1912.9
Nucleus	13C
Acquired Size	32768
Spectral Size	52430

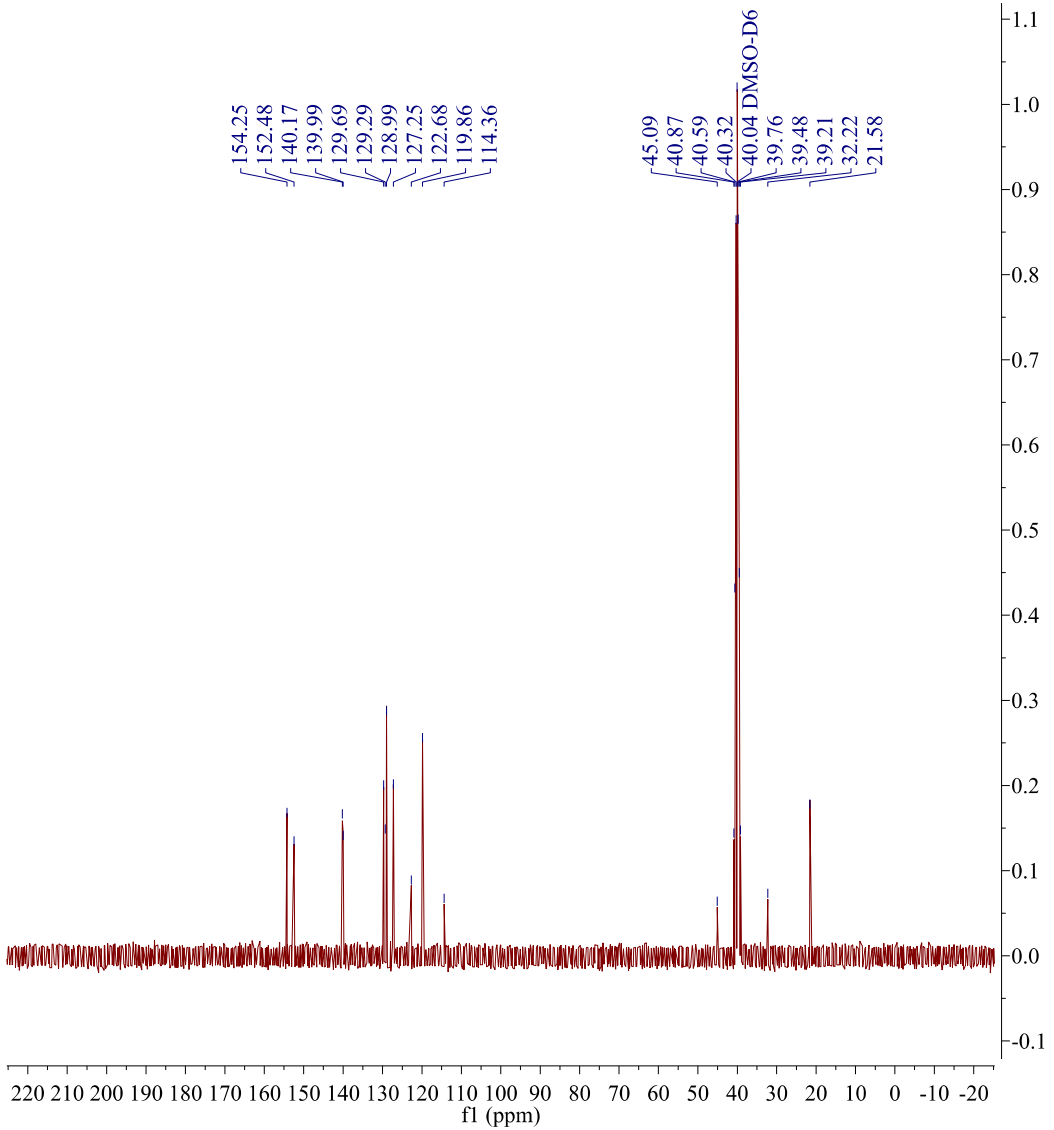

Parameter	Value
Data File Name	/ Volumes/ Lexar/ MH03_15_DEPT_ DEPT135-3.jdf
Title	MH03_15_DEPT
Comment	
Origin	JEOL
Owner	
Site	
Instrument	ECX 300
Author	Delta
Solvent	DMSO-D6
Temperature	22.2
Pulse Sequence	dept.ex2
Experiment	1D
Probe	2692
Number of Scans	148
Receiver Gain	60.0
Relaxation Delay	2.0000
Pulse Width	9.2082
Presaturation Frequency	
Acquisition Time	1.3841
Acquisition Date	2018-04-15T13 :54:29
Modification Date	2018-04-15T14 :28:55
Class	
Spectrometer Frequency	75.57
Spectral Width	18938.4
Lowest Frequency	-1912.4
Nucleus	13C
Acquired Size	32768
Spectral Size	26214

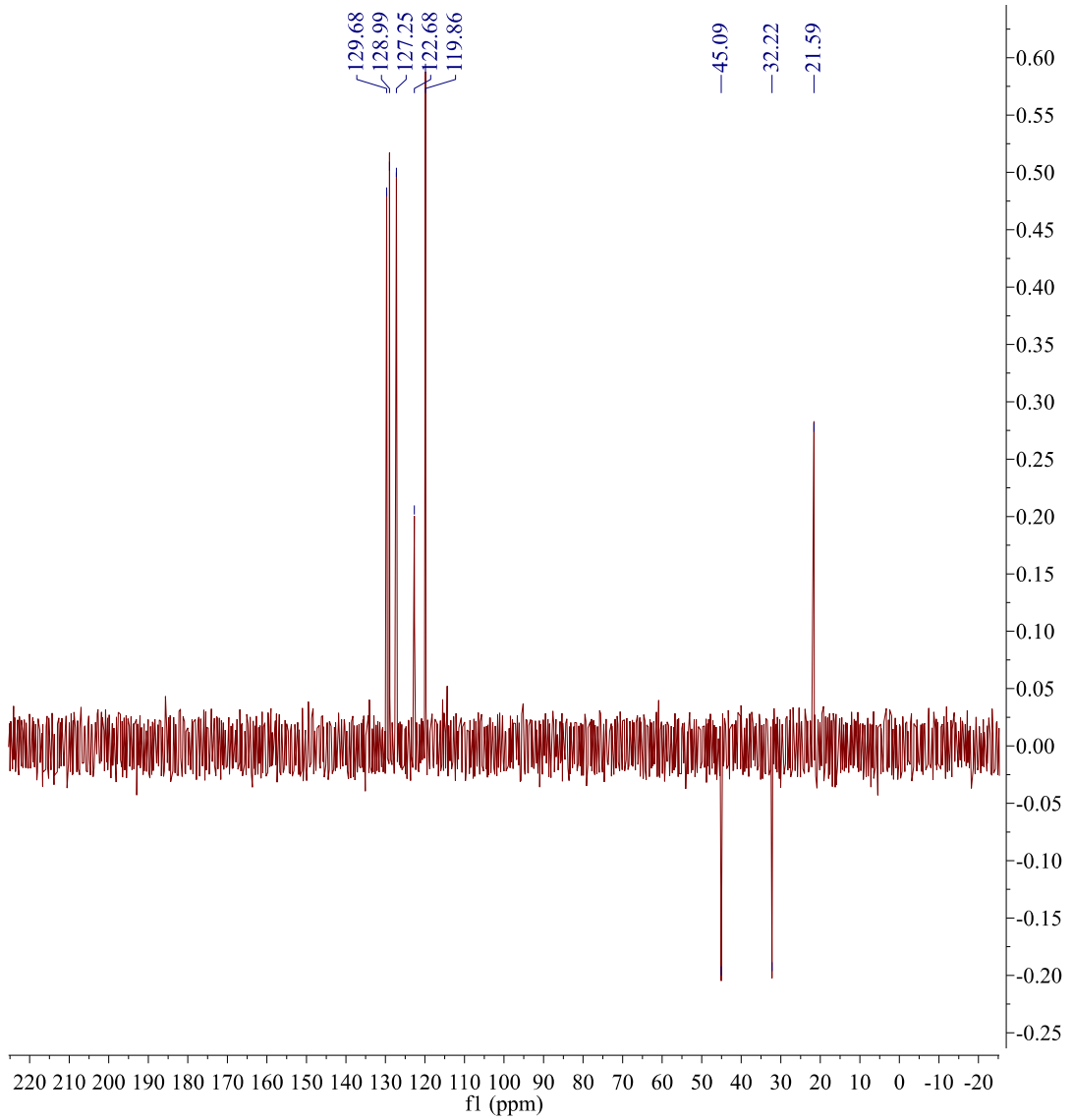

Who	What	When	Parameters	Comment
Organic Chem	Created as New Dataset	10/15/2017 3:01:38 PM		Sample 015 By organic lab Date Sunday, October 15 2017
Organic Chem	Atmospheric Correction	10/15/2017 3:01:38 PM		

Spectrum Graph

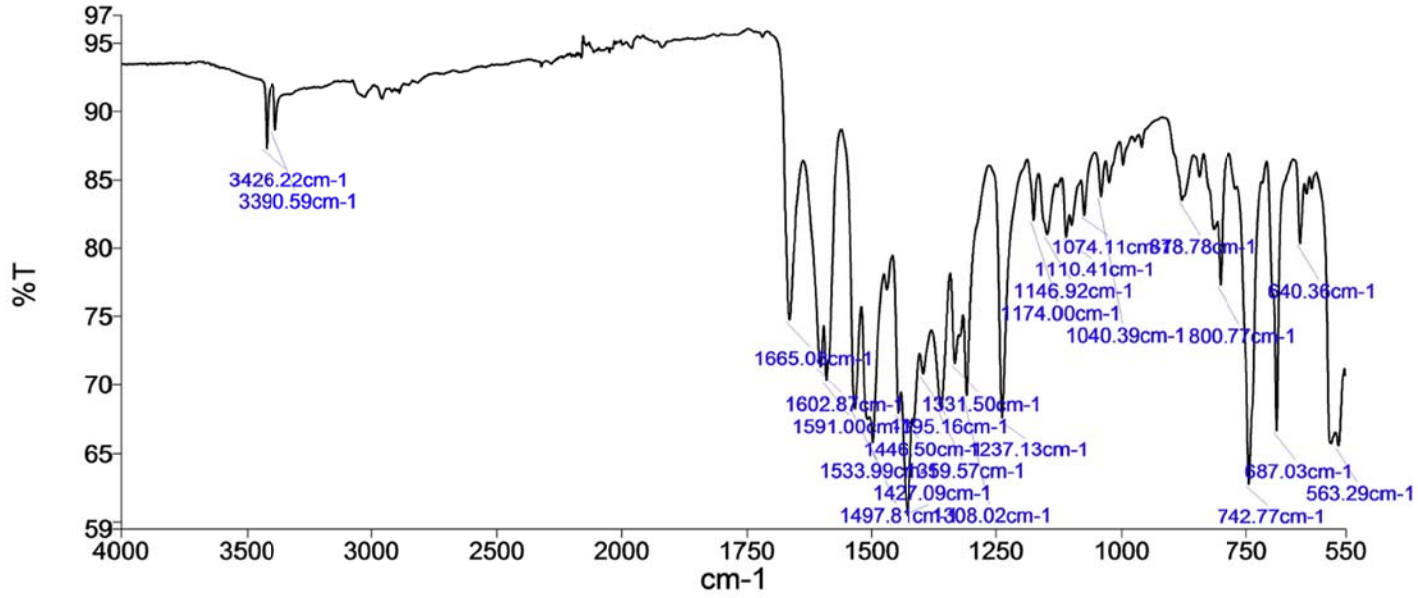

Name	Description
MH03_15	Sample 015 By organic lab Date Sunday, October 15 2017

Compound 16

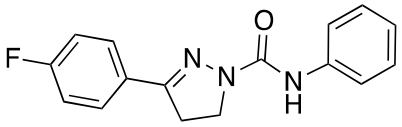

Synthesis of 3-(4-fluorophenyl)-*N*-phenyl-4,5-dihydro-1*H*-pyrazole-1-carboxamide:

3-(4-fluorophenyl)-4,5-dihydro-1*H*-pyrazole (2.35 g, 14.3 mmol, 1.00 equiv.) was dissolved in 45.0 mL anhydrous ether with three drops triethylamine and phenyl isocyanate (1.80 mL, 14.3 mmol, 1.00 equiv.). This solution stirred for one hour at room temperature and the pale-yellow solid was filtered and dried, in 97.0% yield.

^{1}H NMR (300 MHz, $CDCl_3$) δ (ppm): 7.98 (bs, 1H), 7.72 (td, *J*= 5.3, 2.2Hz, 2H), 7.54 (dd, *J*= 7.6, 1.0Hz, 2H), 7.32 (t, *J*= 8.4Hz, 2H), 7.13 (t, *J*= 8.4Hz, 1H), 7.05 (t, *J*= 7.3Hz, 1H), 4.11 (t, *J*= 9.6Hz, 2H), 3.28 (t, *J*= 10.0Hz, 2H).

^{13}C NMR (75.6 MHz, CD_2Cl_2) δ (ppm): 165.5, 162.2, 152.7, 152.0, 138.9, 128.9, 128.4, 128.0, 127.9, 122.8, 118.9, 115.9, 115.6, 44.6, 32.6.

DEPT-135 (75.6 MHz, CD_2Cl_2)) δ (ppm): (+) 128.9, 128.5, 128.4, 122.8, 118.9, 115.9, 115.6; (-) 44.6, 32.6.

IR (neat, cm^{-1}): 3393.9, 1664.5, 1593.8, 1534.9, 1446.6, 1223.1, 838.3, 814.2, 742.6, 685.8, 581.5.

Parameter	Value
Data File Name	/ Volumes/ TOSHIBA/ MH03_62_recrys_PROTON-1.jdf
Title	MH03_62_recrys
Comment	
Origin	JEOL
Owner	
Site	
Instrument	ECX 300
Author	Delta
Solvent	CHLOROFORM-D
Temperature	24.0
Pulse Sequence	single_pulse.ex2
Experiment	1D
Probe	2692
Number of Scans	16
Receiver Gain	46.0
Relaxation Delay	4.0000
Pulse Width	6.4750
Presaturation Frequency	
Acquisition Time	2.9072
Acquisition Date	2018-01-09T11:21:08
Modification Date	2018-01-09T11:54:44
Class	
Spectrometer Frequency	300.53
Spectral Width	4508.6
Lowest Frequency	-751.6
Nucleus	1H
Acquired Size	16384
Spectral Size	52430

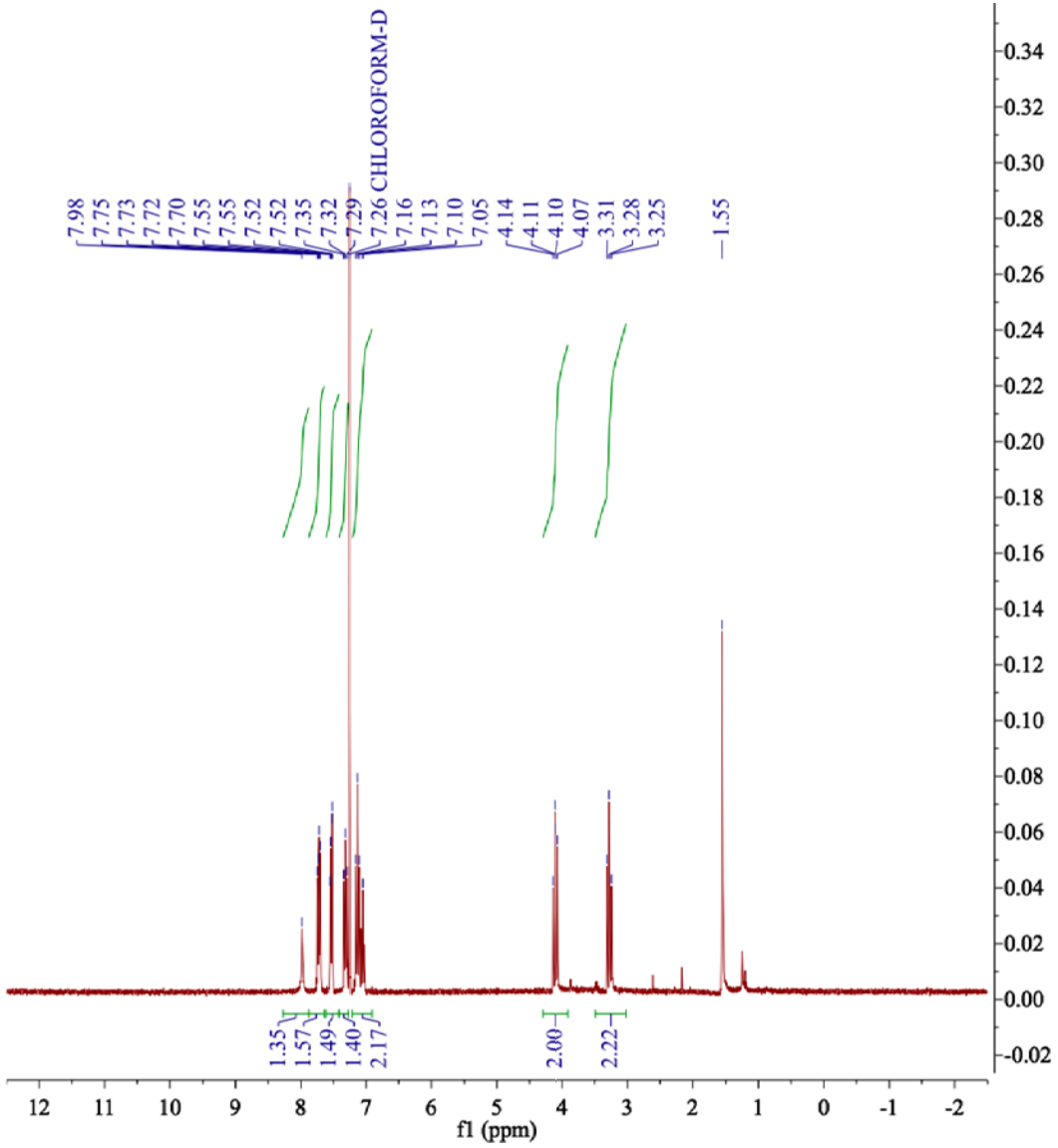

Parameter	Value
Data File Name	/ Volumes/ Lexar/ MH03_62_DEPT_CARBON-1.jdf
Title	MH03_62_DEPT
Comment	
Origin	JEOL
Owner	
Site	
Instrument	ECX 300
Author	Delta
Solvent	METHYLENE-CHLORI
Temperature	22.3
Pulse Sequence	single_pulse_dec
Experiment	1D
Probe	2692
Number of Scans	1024
Receiver Gain	60.0
Relaxation Delay	2.0000
Pulse Width	3.0694
Presaturation Frequency	
Acquisition Time	1.3841
Acquisition Date	2018-04-15T21:03:11
Modification Date	2018-04-15T21:37:33
Class	
Spectrometer Frequency	75.57
Spectral Width	18939.4
Lowest Frequency	-1912.9
Nucleus	13C
Acquired Size	32768
Spectral Size	52430

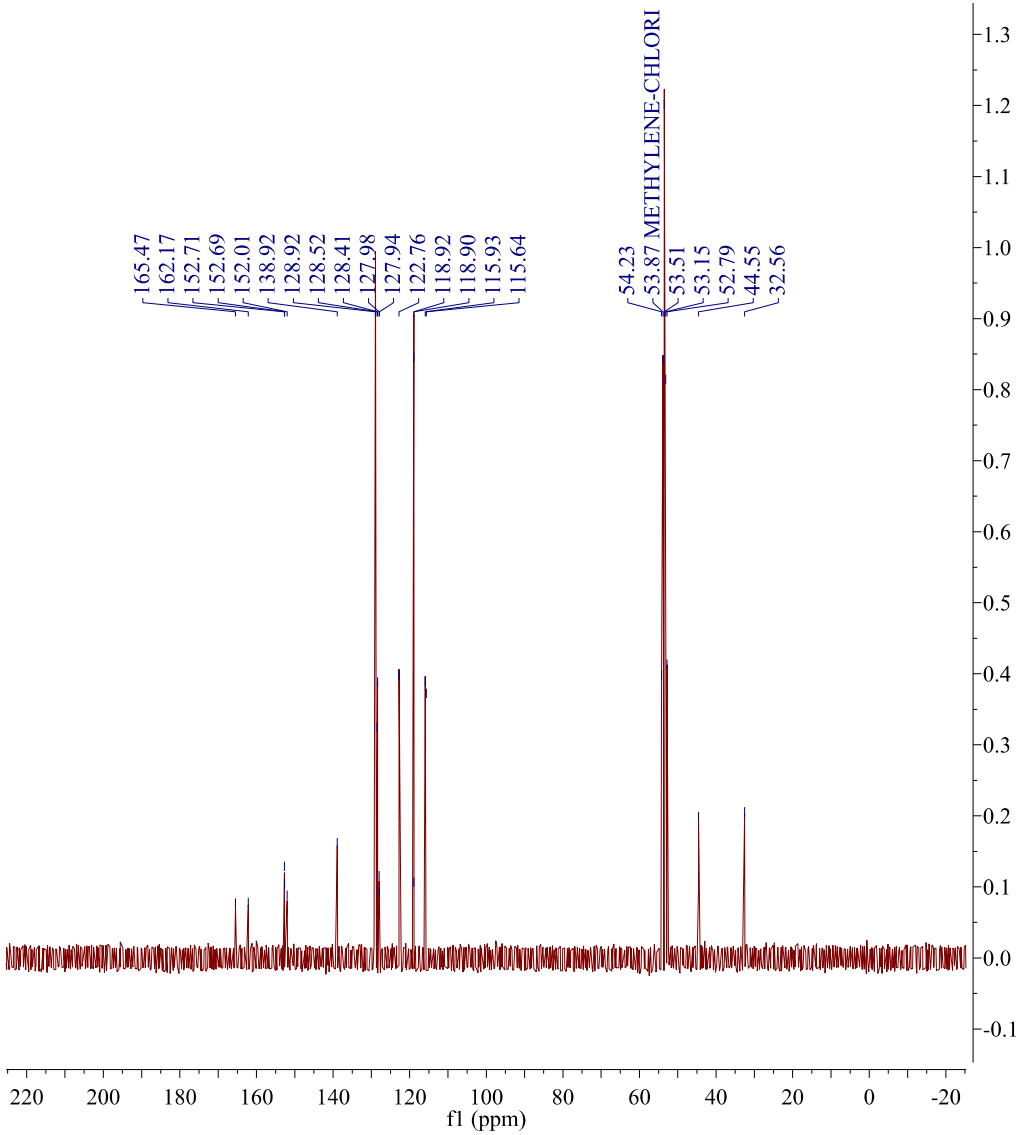

Parameter	Value
Data File Name	/ Volumes/ Lexar/ MH03_62_DEPT_DEPT135-3.jdf
Title	MH03_62_DEPT
Comment	
Origin	JEOL
Owner	
Site	
Instrument	ECX 300
Author	Delta
Solvent	METHYLENE-CHLORI
Temperature	22.3
Pulse Sequence	dept.ex2
Experiment	1D
Probe	2692
Number of Scans	61
Receiver Gain	54.0
Relaxation Delay	2.0000
Pulse Width	9.2082
Presaturation Frequency	
Acquisition Time	1.3841
Acquisition Date	2018-04-15T21:07:20
Modification Date	2018-04-15T21:41:43
Class	
Spectrometer Frequency	75.57
Spectral Width	18938.4
Lowest Frequency	-1912.4
Nucleus	13C
Acquired Size	32768
Spectral Size	26214

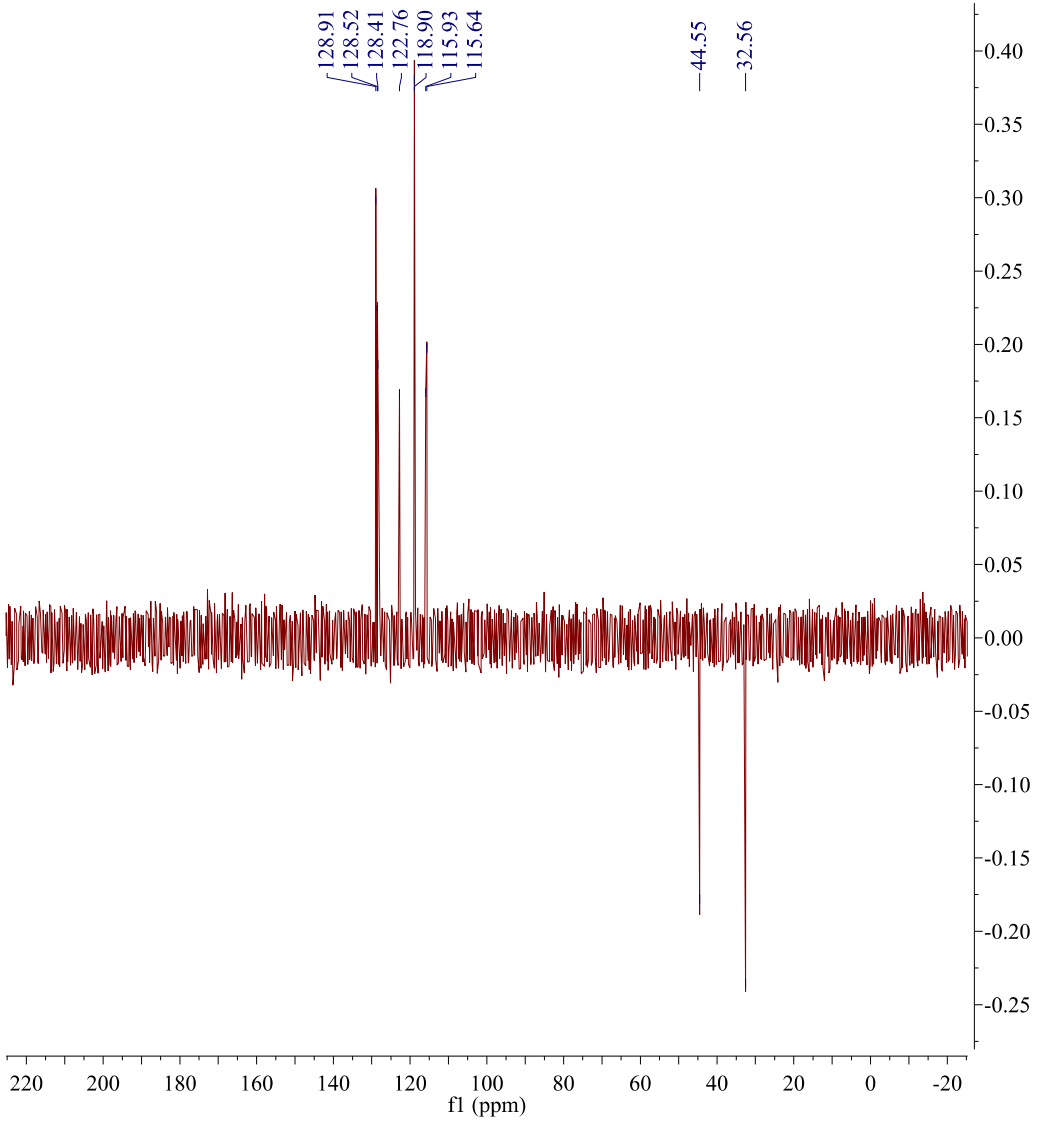

Who	What	When	Parameters	Comment
Organic Chem	Created as New Dataset	4/15/2018 12:46:27 PM		Sample 007 By organic lab Date Sunday, April 15 2018
Organic Chem	Atmospheric Correction	4/15/2018 12:46:27 PM		

Spectrum Graph

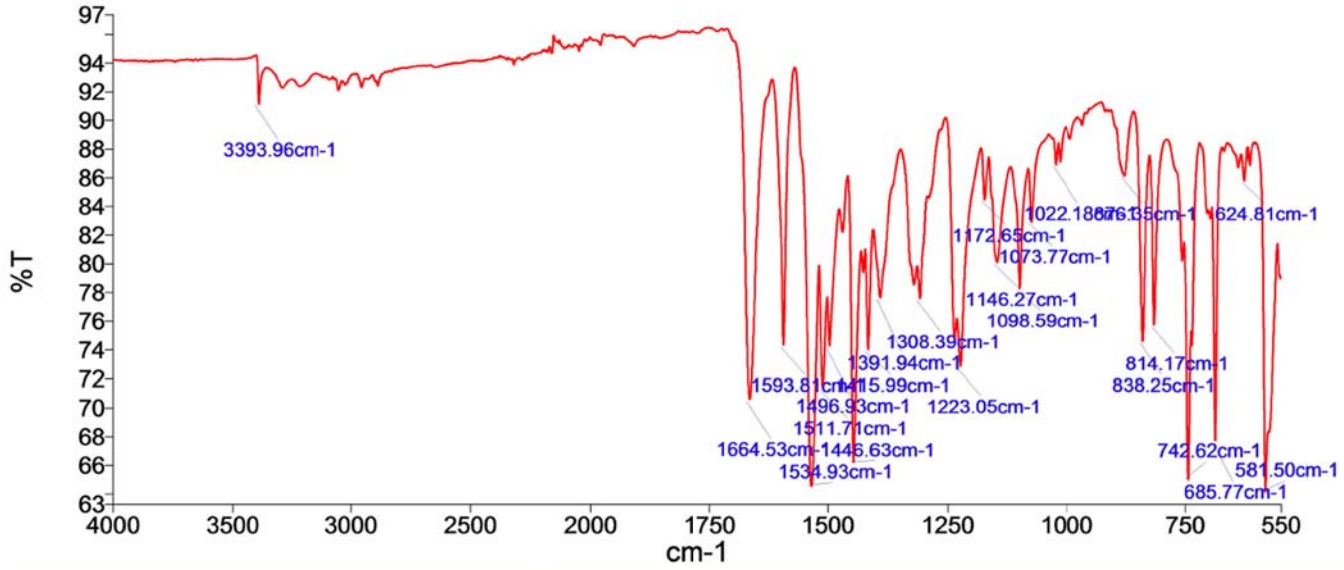

Name	Description
MH03_62	Sample 007 By organic lab Date Sunday, April 15 2018

Compound 17

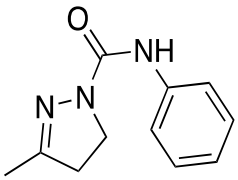

Synthesis of 3-methyl-*N*-phenyl-4,5-dihydro-1*H*-pyrazole-1-carboxamide:

3-methyl-4,5-dihydro-1*H*-pyrazole (176 mmol, 14.8g, 2.80 equiv.) was re-dissolved in 50.0 mL anhydrous ether. Five drops triethylamine was added with phenyl isocyanate (61.2 mmol, 8.00 mL, 1.00 equiv.) and stirred at room temperature for 1.5 hours. The resulting taupe-colored solid was filtered and dried, in 69% yield.

^{1}H NMR (300 MHz, $CDCl_3$) δ (ppm): 9.12 (bs, 1H), 7.77 (dd, *J*= 4.5, 1.7Hz, 2H), 7.64 (d, *J*= 7.9Hz, 2H), 7.46 (dd, *J*= 1.9, 4.1Hz, 2H), 7.39 (t, *J*= 8.3Hz, 2H), 7.21 (t, *J*= 7.3Hz, 1H), 4.47 (t, *J*= 10.3Hz, 2H), 3.35 (t, *J*= 9.7Hz, 2H)

IR (neat, cm^{-1}): 3276.7, 3050.8, 1645.6, 1592.8, 1546.0, 1439.6, 1293.2, 1230.1, 751.9, 694.9.

Parameter	Value
Data File Name	/ Volumes/ Lexar/ MH03_63_PROTON-2.jdf
Title	MH03_63
Comment	
Origin	JEOL
Owner	
Site	
Instrument	ECX 300
Author	Delta
Solvent	CHLOROFORM-D
Temperature	23.2
Pulse Sequence	single_pulse.ex2
Experiment	1D
Probe	2692
Number of Scans	16
Receiver Gain	48.0
Relaxation Delay	4.0000
Pulse Width	6.4750
Presaturation Frequency	
Acquisition Time	2.9072
Acquisition Date	2017-12-01T16:11:47
Modification Date	2017-12-01T16:44:44
Class	
Spectrometer Frequency	300.53
Spectral Width	4508.6
Lowest Frequency	-751.6
Nucleus	1H
Acquired Size	16384
Spectral Size	52430

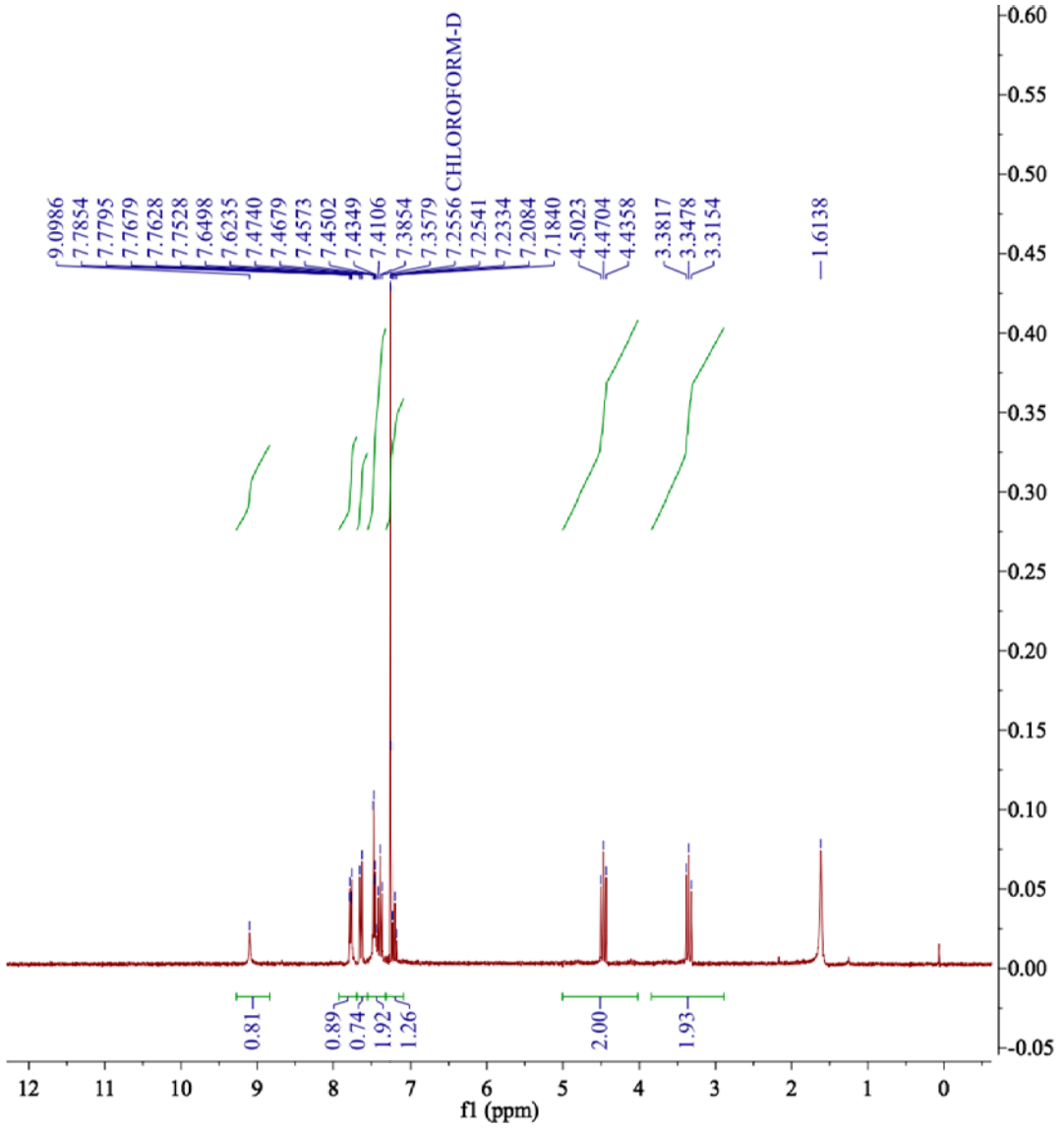

Who	What	When	Parameters	Comment
Organic Chem	Created as New Dataset	12/7/2017 3:18:18 PM		Sample 003 By organic lab Date Thursday, December 07 2017
Organic Chem	Atmospheric Correction	12/7/2017 3:18:18 PM		

Spectrum Graph

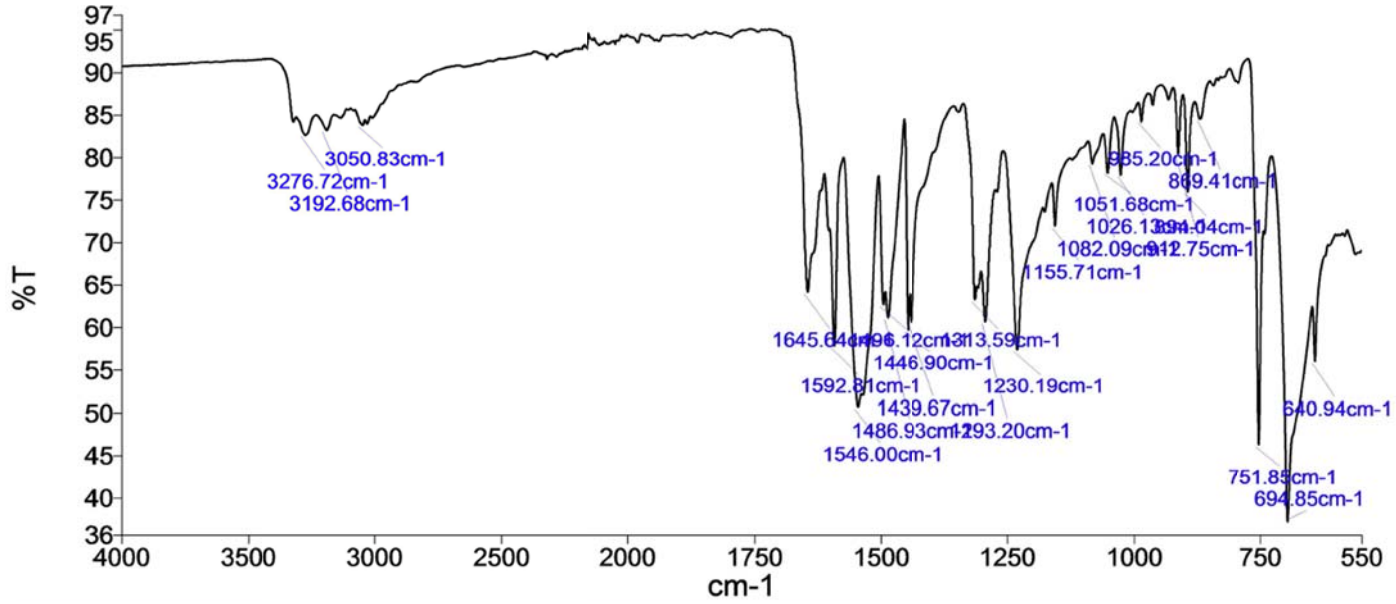

Name	Description
MH03_63	Sample 003 By organic lab Date Thursday, December 07 2017

Compound 18

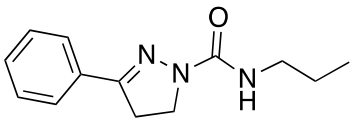

Synthesis of 3-phenyl-*N*-propyl-4,5-dihydro-1*H*-pyrazole-1-carboxamide:

3-phenyl-4,5-dihydro-1*H*-pyrazole (2.00 g, 13.7 mmol, 1.00 equiv.) was dissolved in 50.0 mL anhydrous ether with three drops of triethylamine and propyl isocyanate (1.28 mL, 13.7 mmol, 1.00 equiv.). This solution stirred for three days at room temperature and the orange prude product was purified via silica flash column with a 30- 100% ethyl acetate: hexanes gradient, in 39.2% yield.

^{1}H NMR (300 MHz, dmso-d_6) δ (ppm): 7.68 (dd, *J*= 5.6, 2.4Hz, 2H), 7.40 (m, *J*= 6Hz, 3H), 6.9120 (t, *J*= 5.9 Hz, 1 H), 4.01 (t, *J*= 10.6Hz, 2H), 3.17 (t, *J*= 10.6Hz, 2H), 3.04 (q, *J*= 6.1, 2H) 1.43 (m, *J*= 7.2Hz, 2H), 0.84 (t, *J*= 7.5Hz, 3H).

^{13}C NMR (75.6 MHz, dmso-d_6) δ (ppm): 155.4, 152.9, 130.3, 130.0, 129.1, 126.8, 45.4, 41.8, 32.0, 23.8, 11.8.

IR (neat, cm^{-1}): 3353.4, 2871.6, 1637.6, 1517.6, 1256.8, 1130.1, 858.2, 757.1, 694.5.

Parameter	Value
Data File Name	/ Volumes/ TOSHIBA/ MH03_05_recrysDMSO_PROTON-1.jdf
Title	MH03_05_recrysDMSO
Comment	
Origin	JEOL
Owner	
Site	
Instrument	ECX 300
Author	Delta
Solvent	DMSO-D6
Temperature	26.4
Pulse Sequence	single_pulse.ex2
Experiment	1D
Probe	2692
Number of Scans	16
Receiver Gain	44.0
Relaxation Delay	4.0000
Pulse Width	6.4750
Presaturation Frequency	
Acquisition Time	2.9072
Acquisition Date	2018-01-12T14:46:10
Modification Date	2018-01-12T15:19:42
Class	
Spectrometer Frequency	300.53
Spectral Width	4508.6
Lowest Frequency	-751.6
Nucleus	1H
Acquired Size	16384
Spectral Size	52430

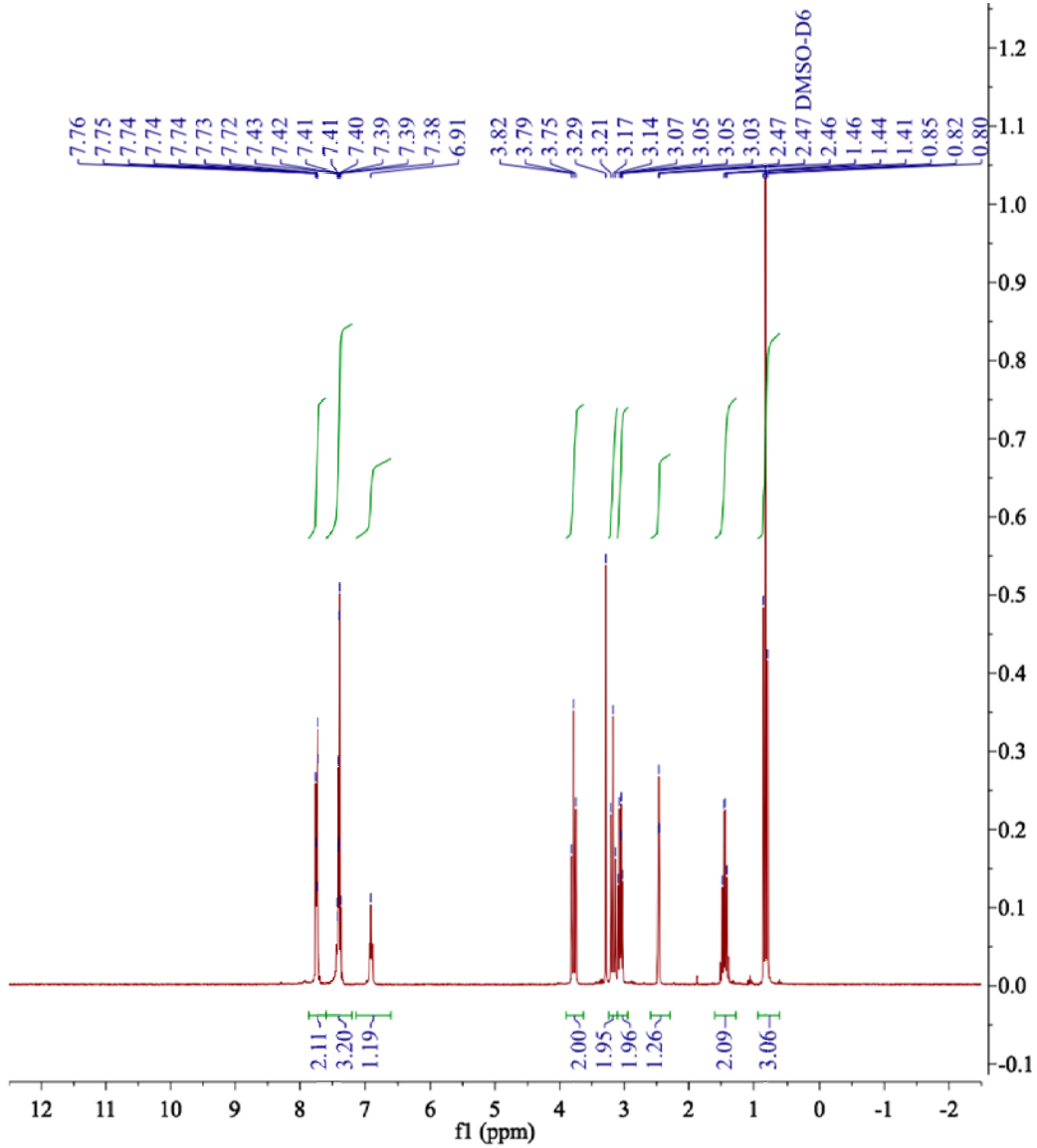

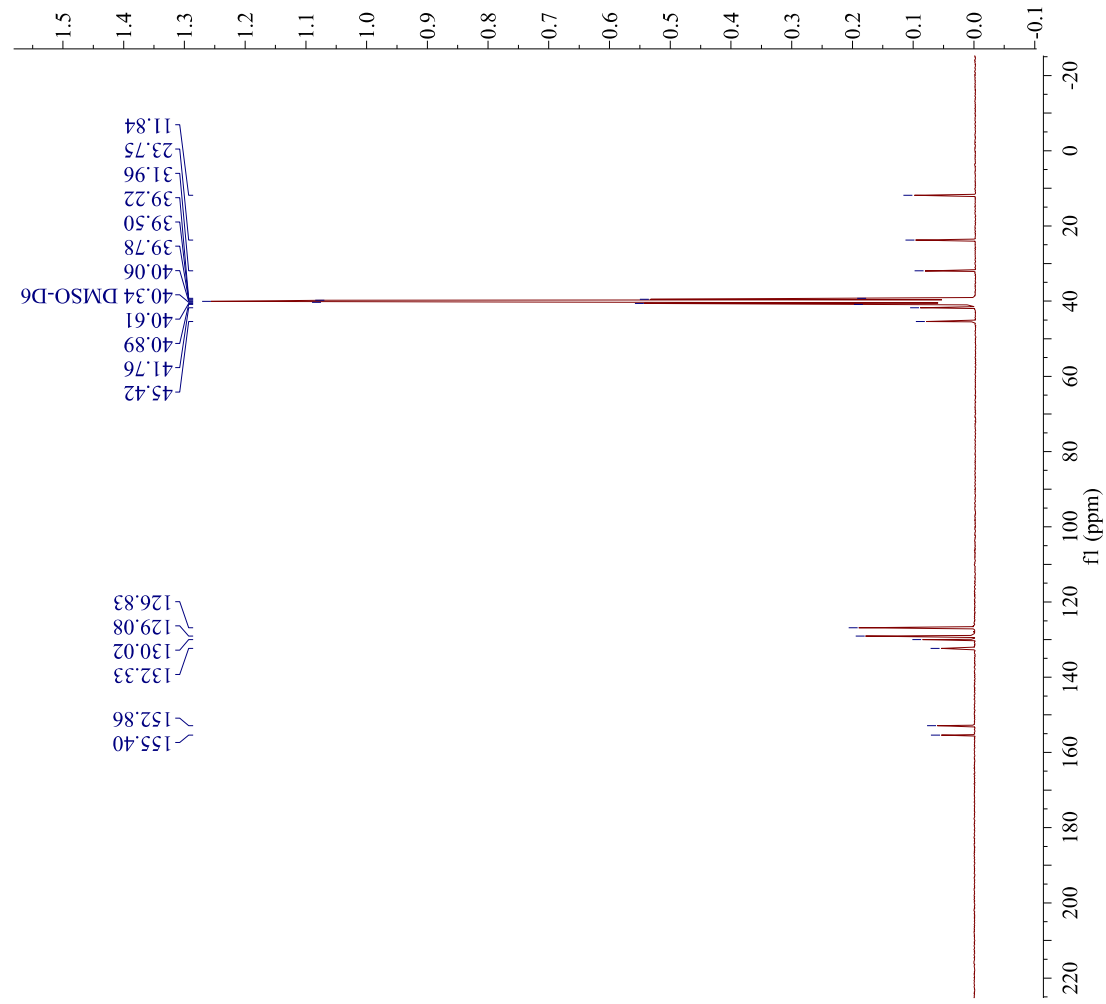

Parameter	Value
Data File Name	/ Volumes/ Lexar/ single_pulse_dec-54.jdf
Title	MH03_05_DMSO
Comment	single pulse decoupled gated NOE
Origin	JEOL
Owner	
Site	
Instrument	ECX 300
Author	Delta
Solvent	DMSO-D6
Temperature	25.1
Pulse Sequence	single_pulse_dec
Experiment	1D
Probe	2692
Number of Scans	97792
Receiver Gain	60.0
Relaxation Delay	2.0000
Pulse Width	3.0694
Presaturation Frequency	
Acquisition Time	1.3841
Acquisition Date	2018-01-23T12:30:08
Modification Date	2018-01-23T13:06:50
Class	
Spectrometer Frequency	75.57
Spectral Width	18938.4
Lowest Frequency	-1912.4
Nucleus	13C
Acquired Size	32768
Spectral Size	26214

Spectrum Graph

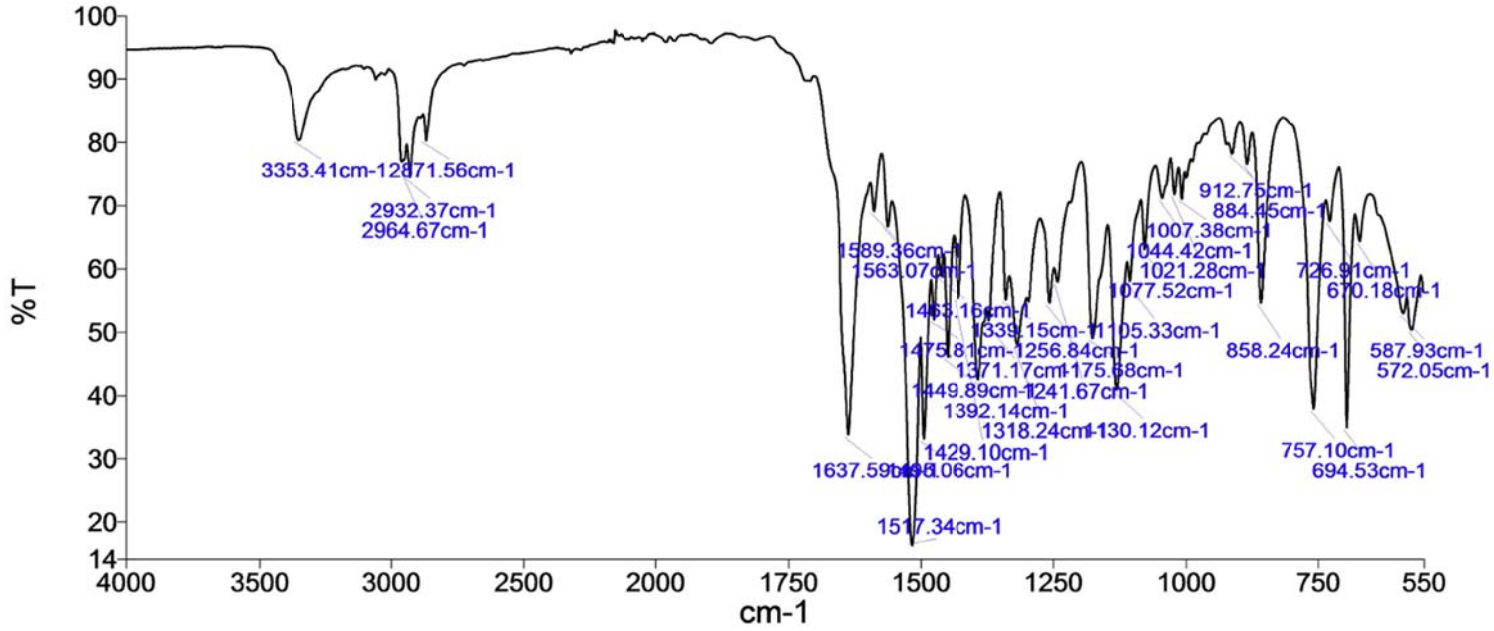

Name	Description
MH03_05	Sample 001 By organic lab Date Thursday, December 07 2017

Summary

Sample Name	Description	Quality
MH03_05	Sample 001 By organic lab Date Thursday, December 07 2017	The Quality Checks do not report any warnings for the sample.

Compound 19

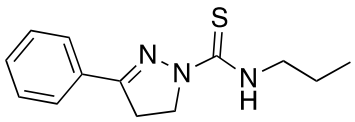

Synthesis of 3-phenyl-*N*-propyl-4,5-dihydro-1*H*-pyrazole-1-carbothioamide:

3-phenyl-4,5-dihydro-1*H*-pyrazole (2.17 g, 14.8 mmol, 1.00 equiv.) was dissolved in 50.0 mL anhydrous ether with 3 drops of triethylamine and propyl isocyanate (1.50 mL, 14.8 mmol, 1.00 equiv.). This solution stirred for three days at room temperature and ice was added to the red liquid product. Crystals formed along the phase boundary were isolated and dried via vacuum filtration. Compound **19** was isolated as a crystalline solid (0.25 g, 6.9% yield) following purification via gradient silica flash column chromatography (30-100% ethyl acetate: hexanes).

^{1}H NMR (300 MHz, $CDCl_3$) δ (ppm): 7.72 (dd, *J*= 3.9, 2.1Hz, 2H), 7.43 (dd, *J*= 2.1, 2.3Hz, 3H), 4.38 (t, *J*= 9.8Hz, 2H), 3.64 (q, *J*= 5.9, 2H), 3.26 (t, *J*= 9.8Hz, 2H), 1.71 (m, *J*= 7.3Hz, 2H), 1.0 (t, *J*= 7.4Hz, 3H).

^{13}C NMR (75.6 MHz, dmso-d_6) δ (ppm): 175.6, 156.8, 131.8, 130.8, 129.2, 127.4, 49.3, 46.2, 31.6, 22.7, 11.8.

DEPT-135 (75.6 MHz, dmso-d_6) δ (ppm): (+) 130.8, 129.2, 127.4, 11.8; (-) 49.3, 46.2, 31.7, 22.7.

IR (neat, cm^{-1}): 3349.1, 2966.0, 1689.5, 1589.3, 1520.0, 1385.3, 1175.1, 752.0, 687.9, 626.9.

Parameter	Value
Data File Name	/ Volumes/ TOSHIBA/ MH03_04_solid_PROTON-1.jdf
Title	MH03_04_solid
Comment	
Origin	JEOL
Owner	
Site	
Instrument	ECX 300
Author	Delta
Solvent	CHLOROFORM-D
Temperature	20.4
Pulse Sequence	single_pulse.ex2
Experiment	1D
Probe	2692
Number of Scans	16
Receiver Gain	48.0
Relaxation Delay	4.0000
Pulse Width	6.4750
Presaturation Frequency	
Acquisition Time	2.9072
Acquisition Date	2017-10-02T10:31:17
Modification Date	2017-10-02T11:02:49
Class	
Spectrometer Frequency	300.53
Spectral Width	4508.6
Lowest Frequency	-751.6
Nucleus	1H
Acquired Size	16384
Spectral Size	52430

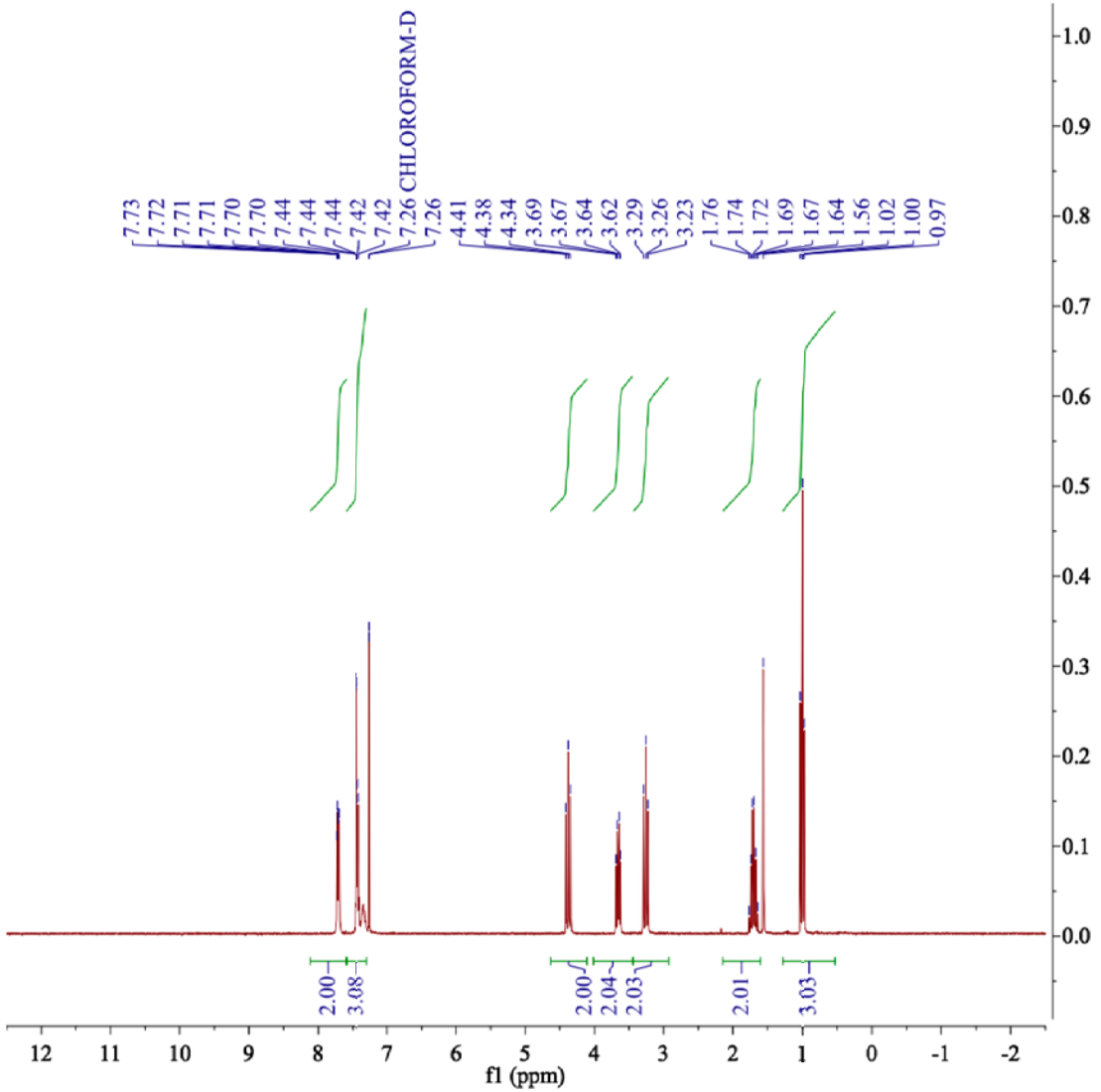

Parameter	Value
Data File Name	/ Volumes/ Lexar/ MH03_04_DEPT_ CARBON-3.jdf
Title	MH03_04_DEPT
Comment	
Origin	JEOL
Owner	
Site	
Instrument	ECX 300
Author	Delta
Solvent	DMSO-D6
Temperature	22.4
Pulse Sequence	single_pulse_dec
Experiment	1D
Probe	2692
Number of Scans	1024
Receiver Gain	58.0
Relaxation Delay	2.0000
Pulse Width	3.0694
Presaturation Frequency	
Acquisition Time	1.3841
Acquisition Date	2018-04-15T16: 18:00
Modification Date	2018-04-15T16: 55:54
Class	
Spectrometer Frequency	75.57
Spectral Width	18938.4
Lowest Frequency	-1912.4
Nucleus	13C
Acquired Size	32768
Spectral Size	26214

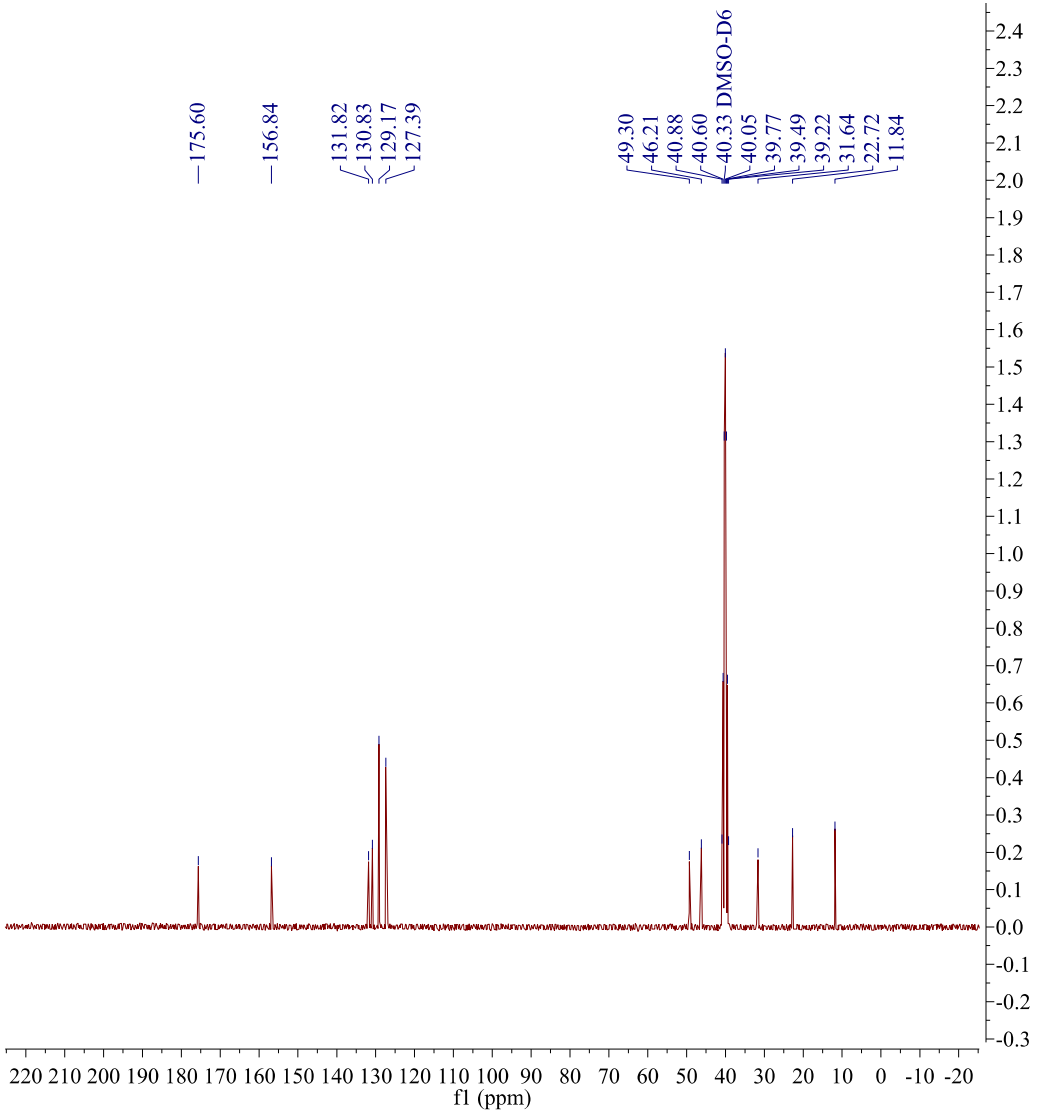

Parameter	Value
Data File Name	/ Volumes/ Lexar/ MH03_04_DEPT_DEPT135-3.jdf
Title	MH03_04_DEPT
Comment	
Origin	JEOL
Owner	
Site	
Instrument	ECX 300
Author	Delta
Solvent	DMSO-D6
Temperature	22.3
Pulse Sequence	dept.ex2
Experiment	1D
Probe	2692
Number of Scans	45
Receiver Gain	56.0
Relaxation Delay	2.0000
Pulse Width	9.2082
Presaturation Frequency	
Acquisition Time	1.3841
Acquisition Date	2018-04-15T16:21:28
Modification Date	2018-04-15T16:55:54
Class	
Spectrometer Frequency	75.57
Spectral Width	18938.4
Lowest Frequency	-1912.4
Nucleus	13C
Acquired Size	32768
Spectral Size	26214

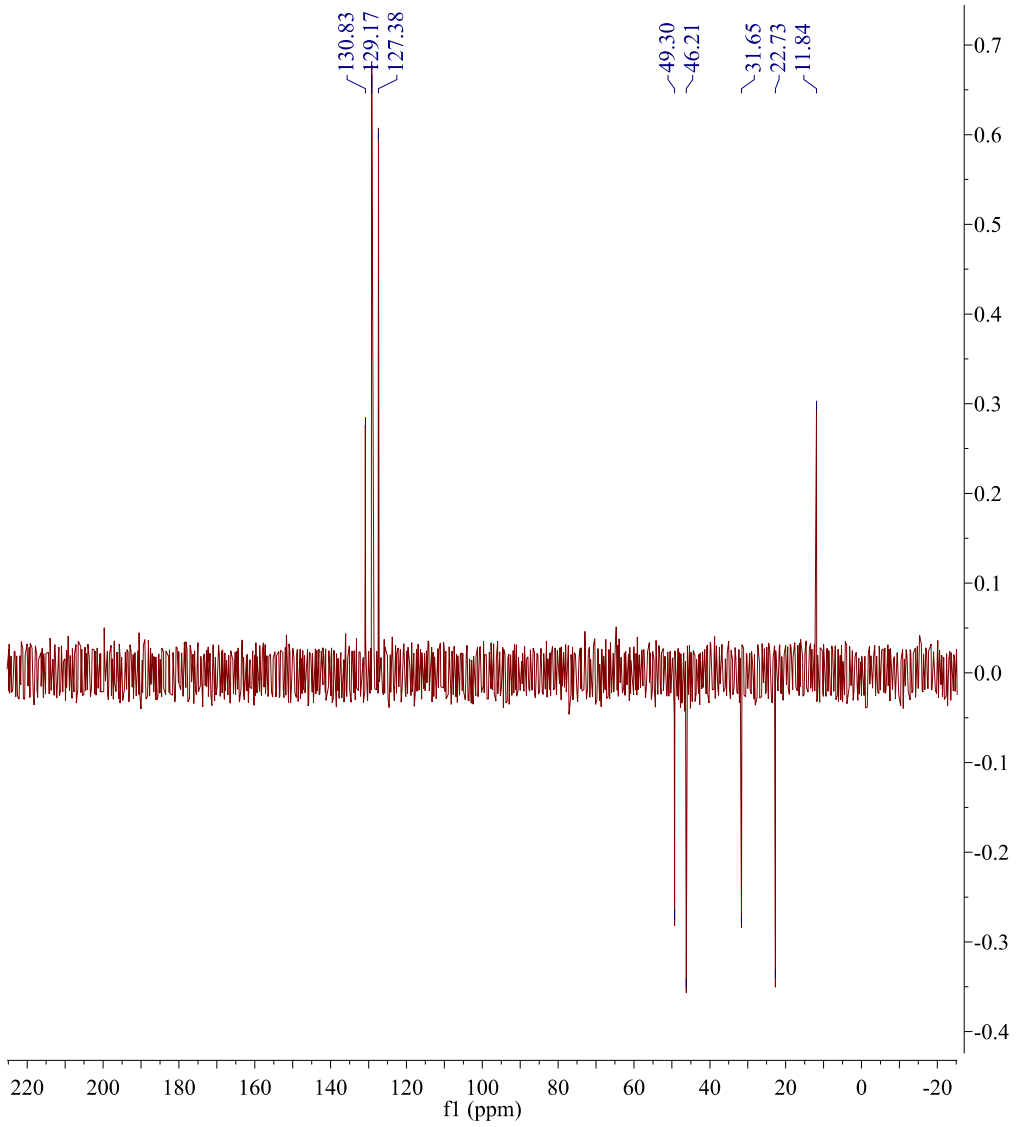

Who	What	When	Parameters	Comment
Organic Chem	Created as New Dataset	10/15/2017 3:08:14 PM		Sample 018 By organic lab Date Sunday, October 15 2017
Organic Chem	Atmospheric Correction	10/15/2017 3:08:14 PM		

Spectrum Graph

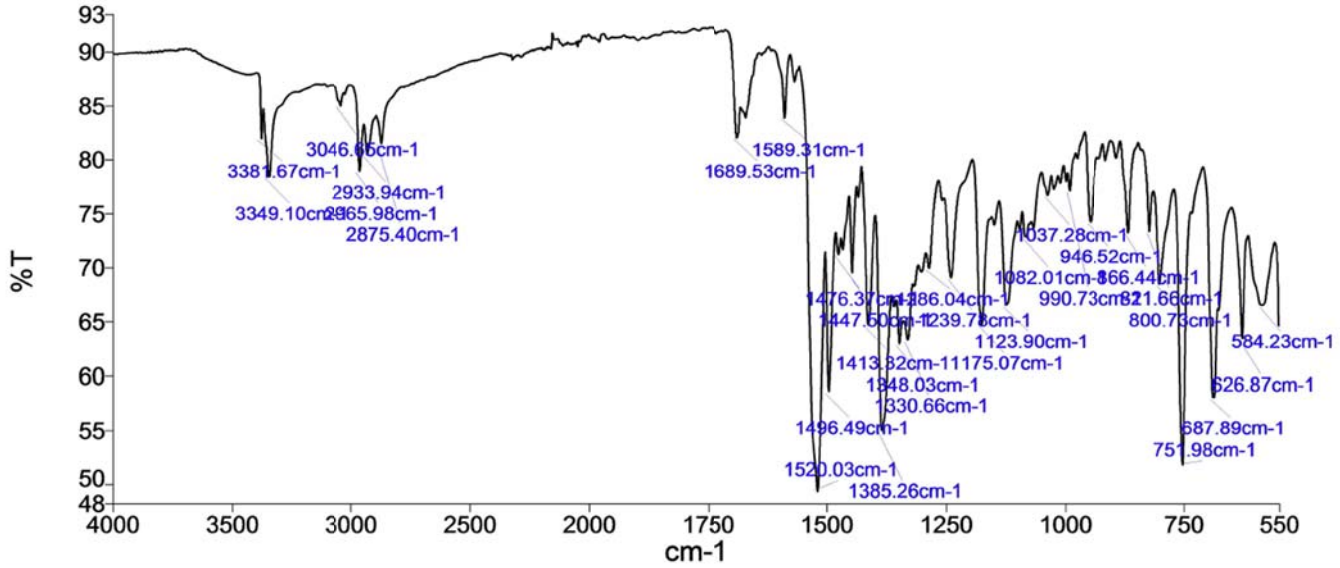

Name	Description
MH03_04	Sample 018 By organic lab Date Sunday, October 15 2017

Compound 20

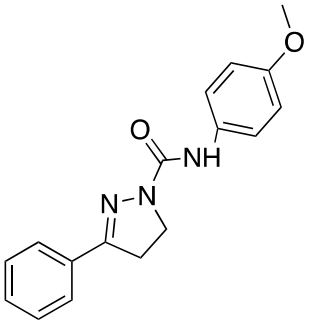

Synthesis of *N*-(4-methoxyphenyl)-3-phenyl-4,5-dihydro-1*H*-pyrazole-1-carboxamide:

3-phenyl-4,5-dihydro-1*H*-pyrazole (1.51 g, 12.0 mmol, 1.00 equiv.) was dissolved in 40.0 mL dry ether with three drops triethylamine and *p*-methoxyphenyl isocyanate (1.79 g, 12.0 mmol, 1.00 equiv.). This solution stirred for three days at room temperature and the resulting peach solid was filtered and dried, in 93.8% yield.

^{1}H NMR (300 MHz, $CDCl_3$) δ (ppm): 7.72 (t, *J*= 3.8Hz, 2H), 7.45 (dd, *J*= 5.4Hz, 2.2Hz, 3H), 6.87 (dd, *J*= 8.7, 1.6Hz, 2H), 4.09 (t, *J*= 9.3Hz, 2H), 3.79 (s, 3H), 3.31 (t, *J*= 10.5Hz, 2H).

^{13}C NMR (75.6 MHz, dmso-d_6) δ (ppm): 155.25, 153.9, 152.8, 132.9, 132.1, 130.3, 129.1, 127.2, 121.8, 114.2, 55.7, 45.3, 32.1.

DEPT-135 (75.6 MHz, dmso-d_6) δ (ppm): (+) 130.3, 129.1, 127.2, 121.8, 114.2, 55.7; (-) 45.3, 32.1.

IR (neat, cm^{-1}): 3392.0, 2958.1, 1657.7, 1594.9, 1535.8, 1419.8, 1240.8, 1099.9, 1032.4, 815.3, 688.2, 575.2.

Parameter	Value
Data File Name	/ Volumes/ TOSHIBA/ MH03_19_PROTON-1.jdf
Title	MH03_19
Comment	
Origin	JEOL
Owner	
Site	
Instrument	ECX 300
Author	Delta
Solvent	CHLOROFORM-D
Temperature	23.3
Pulse Sequence	single_pulse.ex2
Experiment	1D
Probe	2692
Number of Scans	16
Receiver Gain	50.0
Relaxation Delay	4.0000
Pulse Width	6.4750
Presaturation Frequency	
Acquisition Time	2.9072
Acquisition Date	2017-09-27T12:15:58
Modification Date	2017-09-27T12:47:38
Class	
Spectrometer Frequency	300.53
Spectral Width	4508.6
Lowest Frequency	-751.6
Nucleus	1H
Acquired Size	16384
Spectral Size	52430

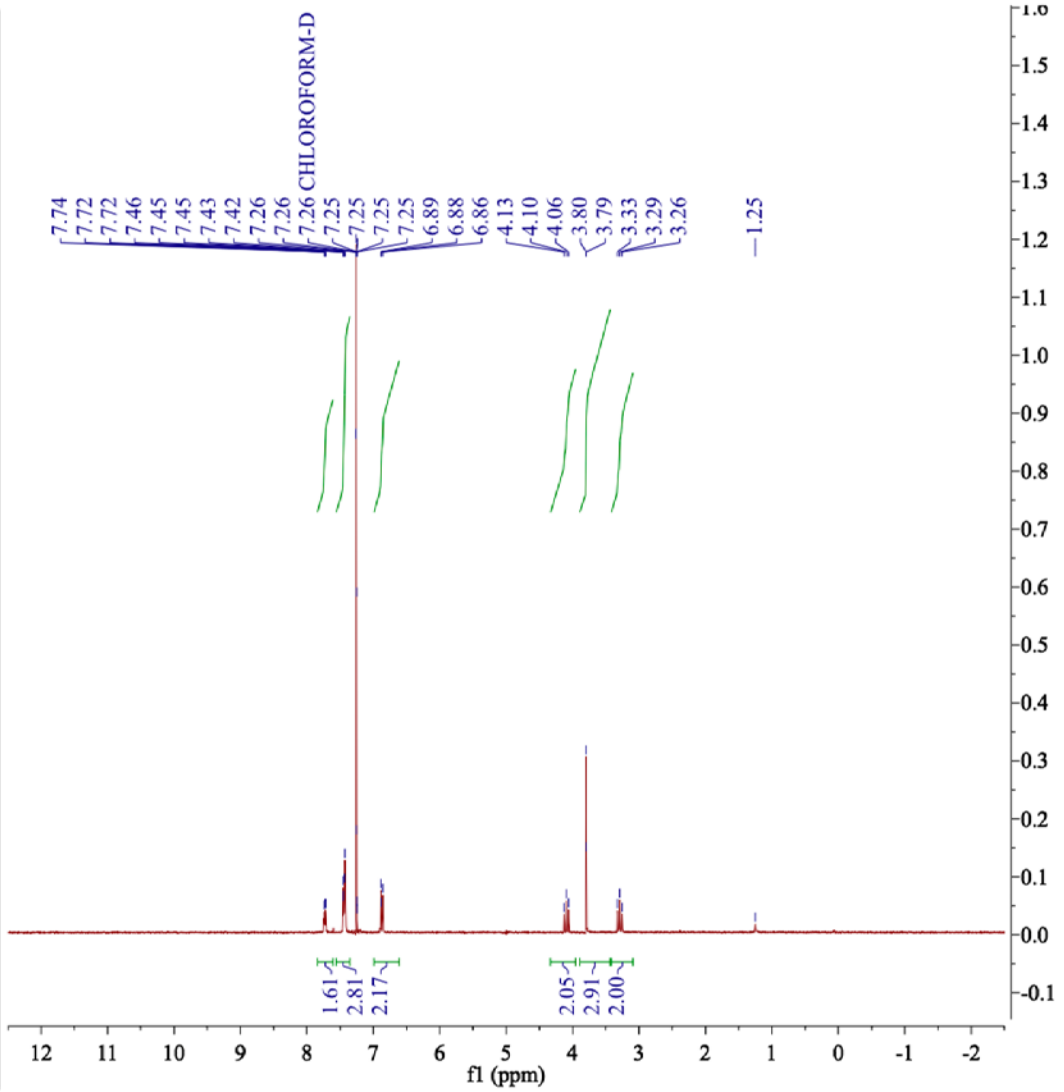

Parameter	Value
Data File Name	/ Volumes/ Lexar/ MH03_19_DEPT_CARBON-1.jdf
Title	MH03_19_DEPT
Comment	
Origin	JEOL
Owner	
Site	
Instrument	ECX 300
Author	Delta
Solvent	DMSO-D6
Temperature	22.3
Pulse Sequence	single_pulse_dec
Experiment	1D
Probe	2692
Number of Scans	1024
Receiver Gain	60.0
Relaxation Delay	2.0000
Pulse Width	3.0694
Presaturation Frequency	
Acquisition Time	1.3841
Acquisition Date	2018-04-15T17:22:59
Modification Date	2018-04-15T17:57:23
Class	
Spectrometer Frequency	75.57
Spectral Width	18939.4
Lowest Frequency	-1912.9
Nucleus	13C
Acquired Size	32768
Spectral Size	52430

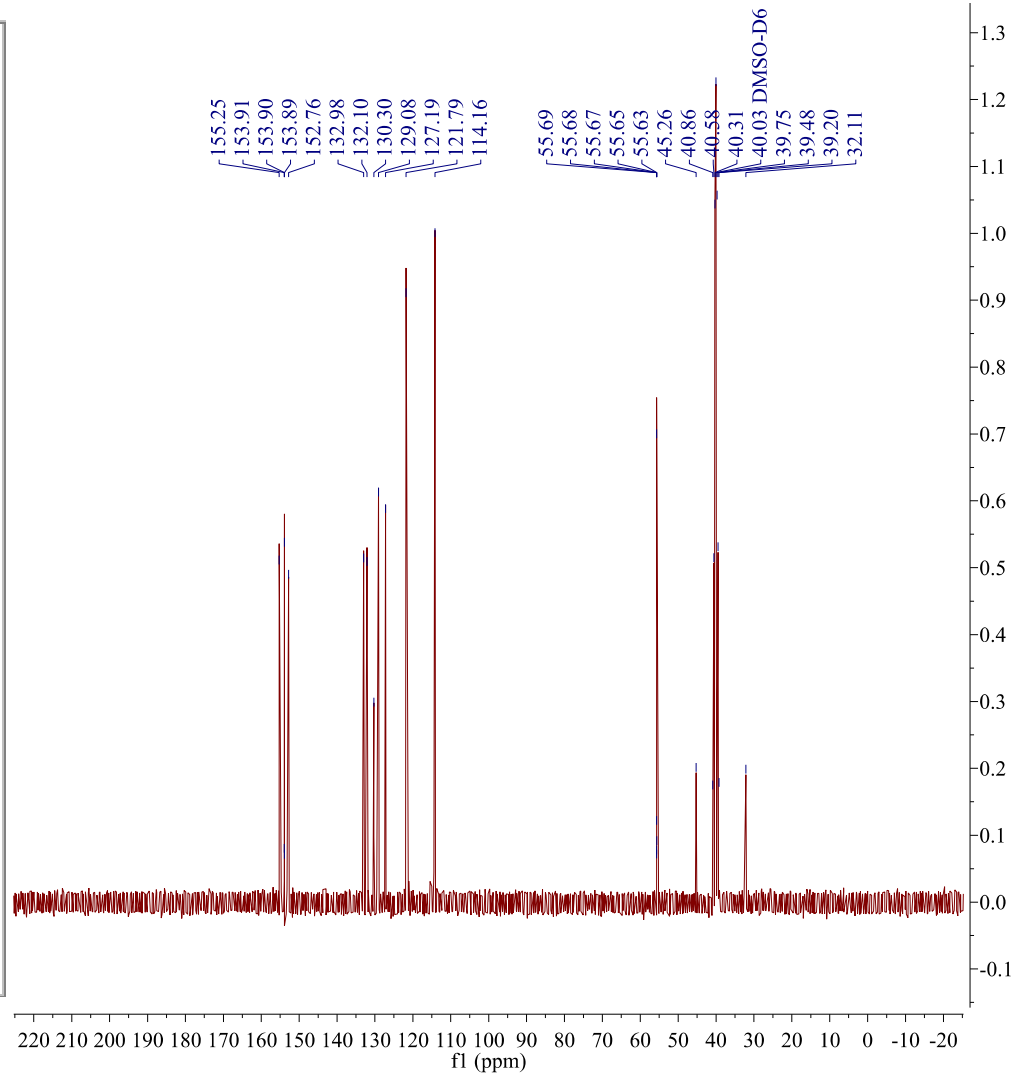

Parameter	Value
Data File Name	/ Volumes/ Lexar/ MH03_19_DEPT_ DEPT135-3.jdf
Title	MH03_19_DEPT
Comment	
Origin	JEOL
Owner	
Site	
Instrument	ECX 300
Author	Delta
Solvent	DMSO-D6
Temperature	22.2
Pulse Sequence	dept.ex2
Experiment	1D
Probe	2692
Number of Scans	21
Receiver Gain	56.0
Relaxation Delay	2.0000
Pulse Width	9.2082
Presaturation Frequency	
Acquisition Time	1.3841
Acquisition Date	2018-04-15T17: 25:06
Modification Date	2018-04-15T17: 59:31
Class	
Spectrometer Frequency	75.57
Spectral Width	18938.4
Lowest Frequency	-1912.4
Nucleus	13C
Acquired Size	32768
Spectral Size	26214

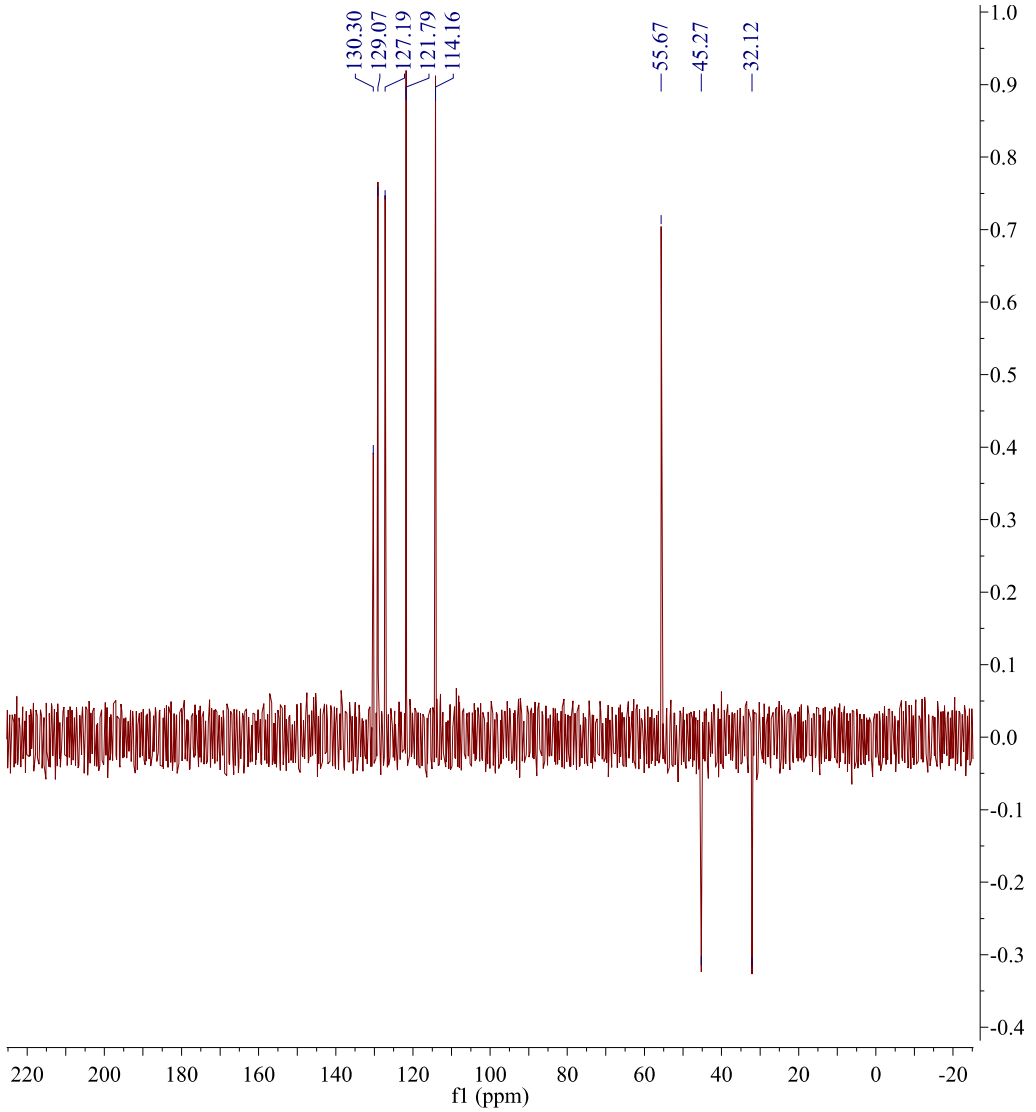

Who	What	When	Parameters	Comment
Organic Chem	Created as New Dataset	10/15/2017 3:03:47 PM		Sample 016 By organic lab Date Sunday, October 15 2017
Organic Chem	Atmospheric Correction	10/15/2017 3:03:47 PM		

Spectrum Graph

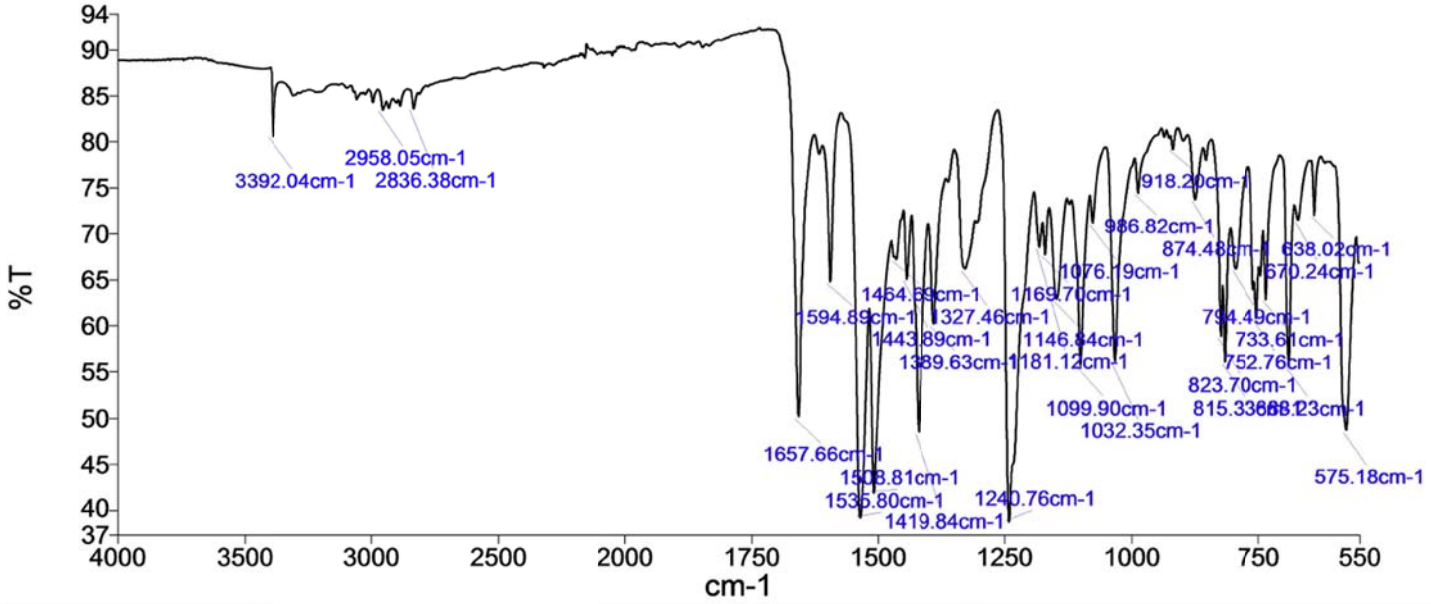

Name	Description
MH03_19	Sample 016 By organic lab Date Sunday, October 15 2017

Compound 21

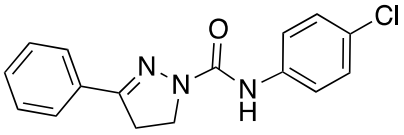

Synthesis of *N*-(4-chlorophenyl)-3-phenyl-4,5-dihydro-1*H*-pyrazole-1-carboxamide:

3-phenyl-4,5-dihydro-1*H*-pyrazole (1.51g, 12.0 mmol, 1.00 equiv.) was dissolved in 40.0 mL anhydrous ether with three drops triethylamine and 4-chlorophenyl isocyanate (1.84 g, 12.0 mmol, 1.00 equiv.). This solution stirred for three days at room temperature and the peach solid product was filtered and dried, in 94.0% yield.

^{1}H NMR (300 MHz, $CDCl_3$) δ (ppm): 7.99 (bs, 1H), 7.67 (dd, *J*= 3.4, 1.9Hz, 2H), 7.53 (d, *J*= 8.9Hz, 2H), 7.41 (t, *J*= 2.4Hz, 3H), 7.32 (q, *J*= 9Hz, 3H), 4.11 (t, *J*= 12Hz, 2H), 3.27 (t, *J*= 9.1Hz, 2H).

^{13}C NMR (75.6 MHz, CD_2Cl_2) δ (ppm): 154.0, 137.7, 131.4, 130.2, 128.8, 128.7, 126.5, 120.1, 100.0, 44.4, 32.5.

DEPT-135 (75.6 MHz, CD_2Cl_2) δ (ppm): (+) 130.2, 128.8, 128.7, 126.5, 120.1; (-) 44.4, 32.5.

IR (neat, cm^{-1}): 3383.0, 2887.6, 1690.7, 1590.0, 1530.9, 1339.4, 822.4, 683.2, 601.7.

Parameter	Value
Data File Name	/ Volumes/ TOSHIBA/ MH03_21_recrys_ PROTON-1.jdf
Title	MH03_21_recrys
Comment	
Origin	JEOL
Owner	
Site	
Instrument	ECX 300
Author	Delta
Solvent	CHLOROFORM-D
Temperature	23.8
Pulse Sequence	single_pulse.ex2
Experiment	1D
Probe	2692
Number of Scans	16
Receiver Gain	46.0
Relaxation Delay	4.0000
Pulse Width	6.4750
Presaturation Frequency	
Acquisition Time	2.9072
Acquisition Date	2018-01-10T15: 02:44
Modification Date	2018-01-10T15: 36:16
Class	
Spectrometer Frequency	300.53
Spectral Width	4508.6
Lowest Frequency	-751.6
Nucleus	1H
Acquired Size	16384
Spectral Size	52430

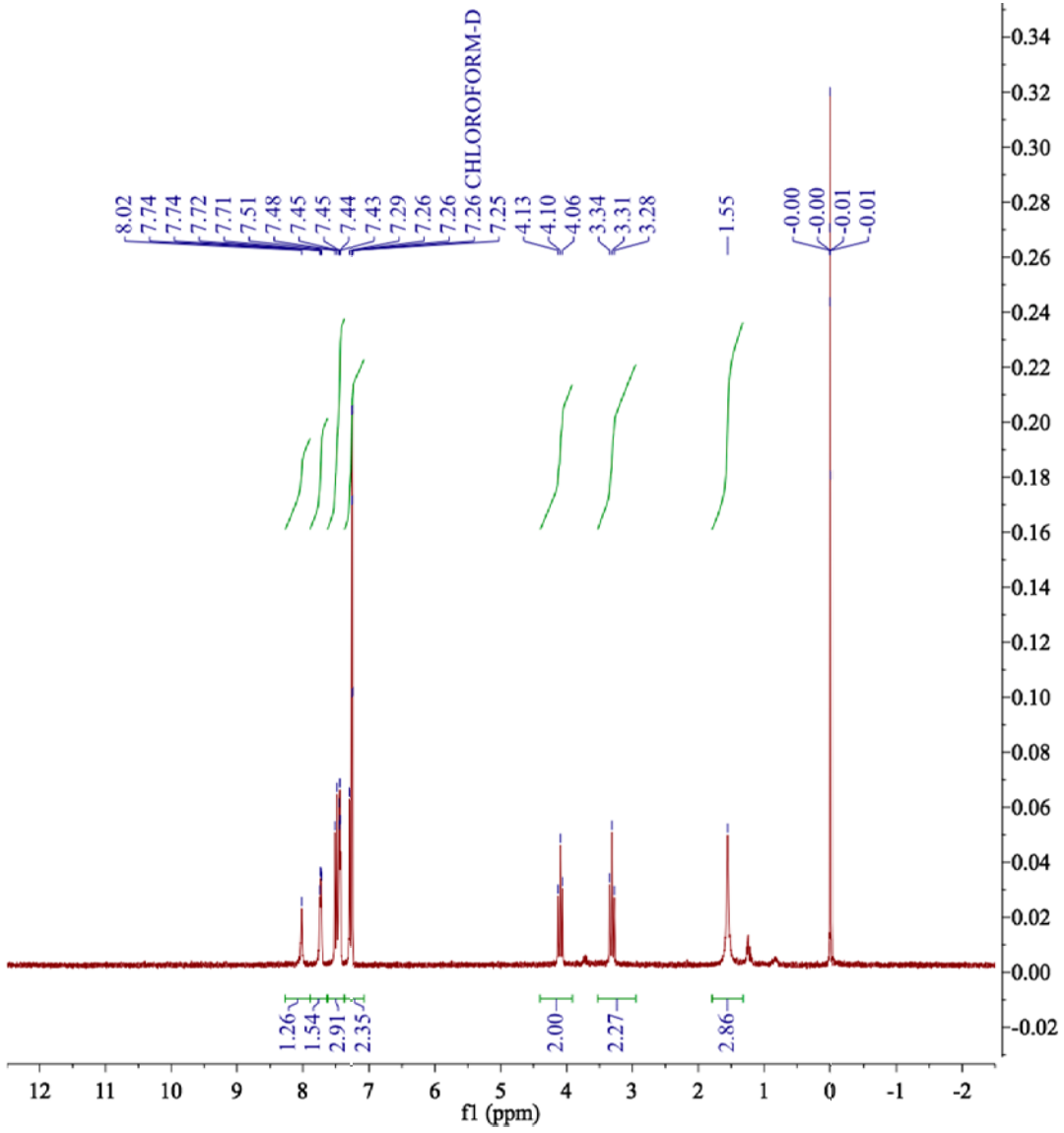

Parameter	Value
Data File Name	/ Volumes/ Lexar/ MH03_21_DEPT_CARBON-1.jdf
Title	MH03_21_DEPT
Comment	
Origin	JEOL
Owner	
Site	
Instrument	ECX 300
Author	Delta
Solvent	METHYLENE-CHLORI
Temperature	22.3
Pulse Sequence	single_pulse_dec
Experiment	1D
Probe	2692
Number of Scans	1024
Receiver Gain	60.0
Relaxation Delay	2.0000
Pulse Width	3.0694
Presaturation Frequency	
Acquisition Time	1.3841
Acquisition Date	2018-04-15T22:08:50
Modification Date	2018-04-15T22:43:14
Class	
Spectrometer Frequency	75.57
Spectral Width	18939.4
Lowest Frequency	-1912.9
Nucleus	13C
Acquired Size	32768
Spectral Size	52430

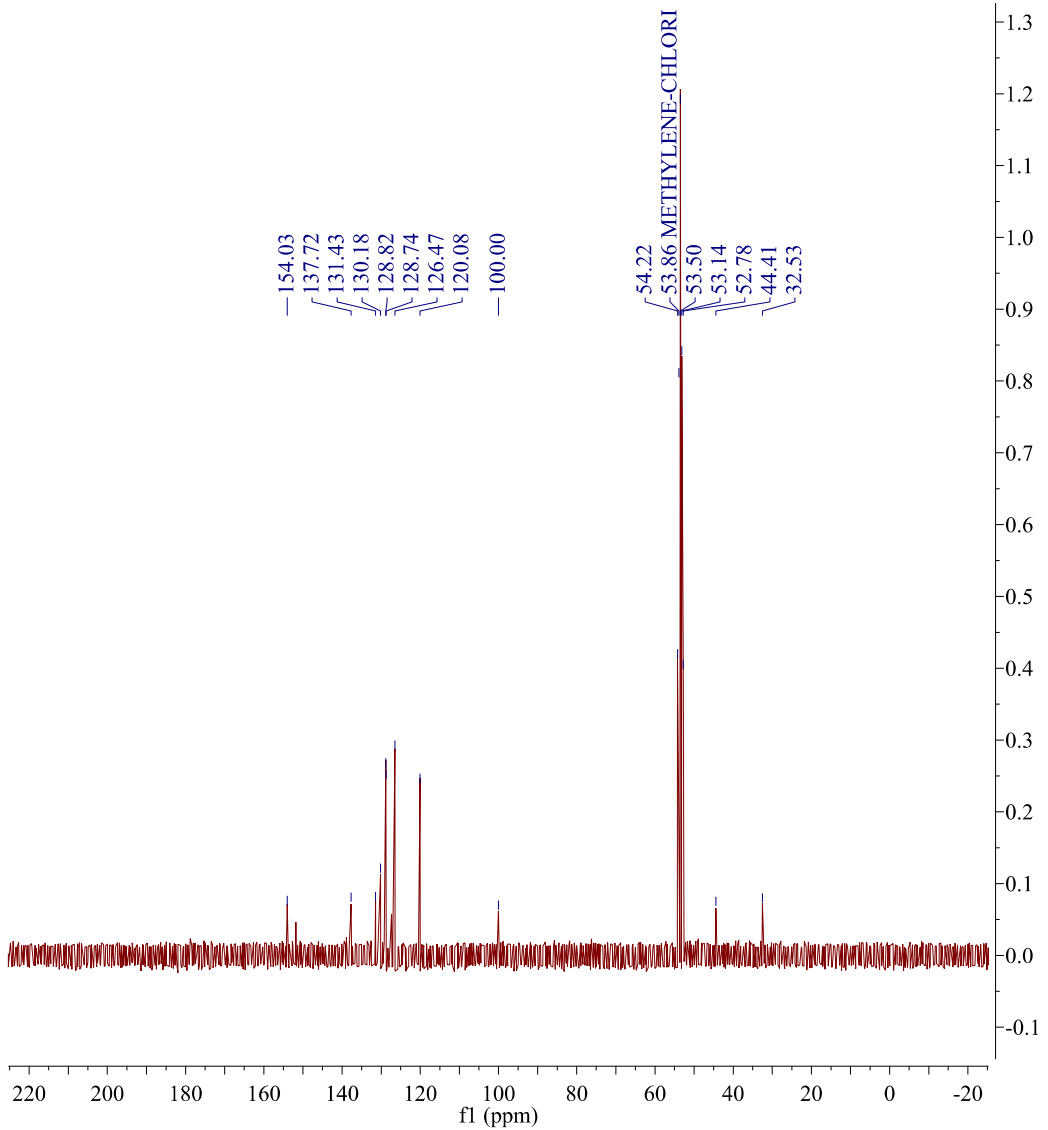

Parameter	Value
Data File Name	/ Volumes/ Lexar/ MH03_21_DEPT_ DEPT135-3.jdf
Title	MH03_21_DEPT
Comment	
Origin	JEOL
Owner	
Site	
Instrument	ECX 300
Author	Delta
Solvent	METHYLENE-CHLORI
Temperature	22.2
Pulse Sequence	dept.ex2
Experiment	1D
Probe	2692
Number of Scans	416
Receiver Gain	60.0
Relaxation Delay	2.0000
Pulse Width	9.2082
Presaturation Frequency	
Acquisition Time	1.3841
Acquisition Date	2018-04-15T22: 33:04
Modification Date	2018-04-15T23: 07:28
Class	
Spectrometer Frequency	75.57
Spectral Width	18938.4
Lowest Frequency	-1912.4
Nucleus	13C
Acquired Size	32768
Spectral Size	26214

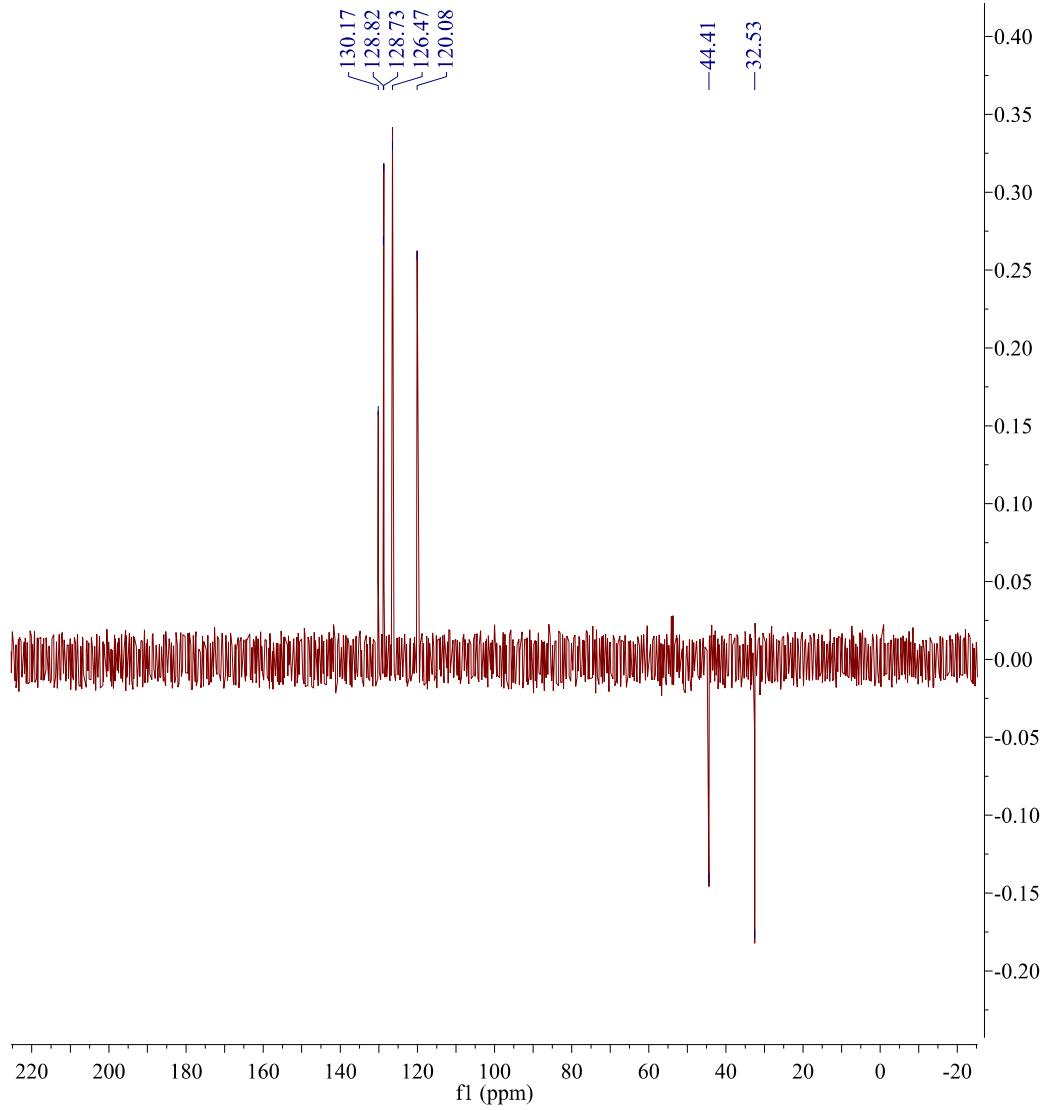

Who	What	When	Parameters	Comment
Organic Chem	Created as New Dataset	10/15/2017 3:05:46 PM		Sample 017 By organic lab Date Sunday, October 15 2017
Organic Chem	Atmospheric Correction	10/15/2017 3:05:46 PM		

Spectrum Graph

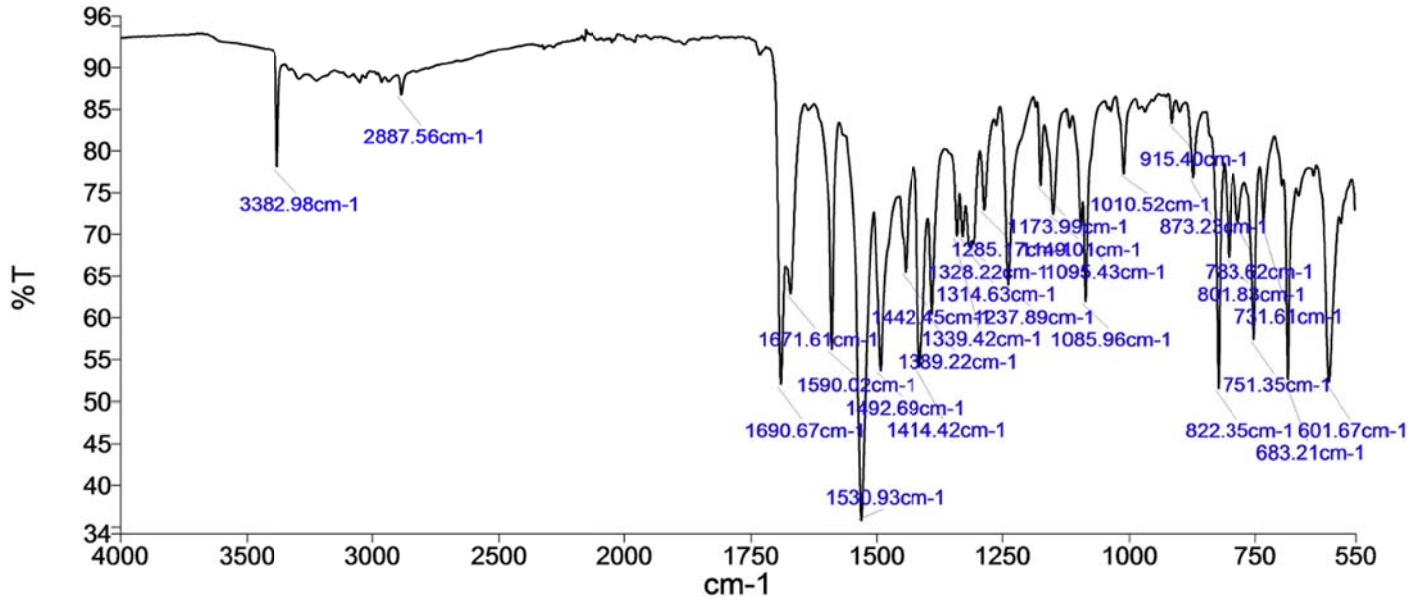

Name	Description
MH03_21	Sample 017 By organic lab Date Sunday, October 15 2017

Compound 22

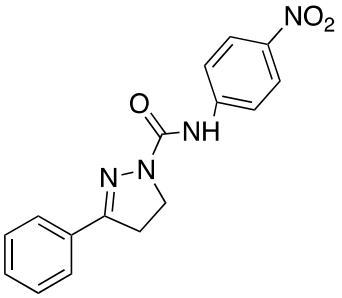

Synthesis of *N*-(4-nitrophenyl)-3-phenyl-4,5-dihydro-1*H*-pyrazole-1-carboxamide:

3-phenyl-4,5-dihydro-1*H*-pyrazole (1.51 g, 12.0 mmol, 1 equiv.) was dissolved in 40.0 mL anhydrous ether and three drops of triethylamine with *p*-nitrophenyl isocyanate (1.97 g, 12.0 mmol, 1.00 equiv.). This solution stirred for three days at room temperature and the resulting brown solid was filtered and dried, in 83.2% yield.

^{1}H NMR (300 MHz, $CDCl_3$) δ (ppm): 8.22 (d, *J*= 9.3Hz, 2H), 7.73 (m, *J*= 9.0Hz, 3H), 7.47 (t, *J*= 6.0Hz, 3H), 4.12 (t, *J*= 9.8Hz, 2H), 3.34 (t, *J*= 9.9Hz, 2H)

^{13}C NMR (75.6 MHz, dmso-d_6) δ (ppm): 155.4, 151.7, 146.9, 141.7, 131.8, 130.7, 129.1, 127.4, 125.3, 119.0, 45.2, 32.3.

DEPT-135 (75.6 MHz, dmso-d_6) δ (ppm): (+) 130.7, 129.1, 127.4, 125.3, 119.0; (-) 45.2, 32.3.

IR (neat, cm^{-1}): 3357.7, 3069.6, 1681.5, 1596.9, 1530.2, 1490.9, 1328.4, 1235.1, 1111.5, 1086.0, 852.6, 750.5, 690.9.

Parameter	Value
Data File Name	/ Volumes/ TOSHIBA/ MH03_20_PROTON-1.jdf
Title	MH03_20
Comment	
Origin	JEOL
Owner	
Site	
Instrument	ECX 300
Author	Delta
Solvent	CHLOROFORM-D
Temperature	23.3
Pulse Sequence	single_pulse.ex2
Experiment	1D
Probe	2692
Number of Scans	16
Receiver Gain	50.0
Relaxation Delay	4.0000
Pulse Width	6.4750
Presaturation Frequency	
Acquisition Time	2.9072
Acquisition Date	2017-09-27T12:10:32
Modification Date	2017-09-27T12:42:12
Class	
Spectrometer Frequency	300.53
Spectral Width	4508.6
Lowest Frequency	-751.6
Nucleus	1H
Acquired Size	16384
Spectral Size	52430

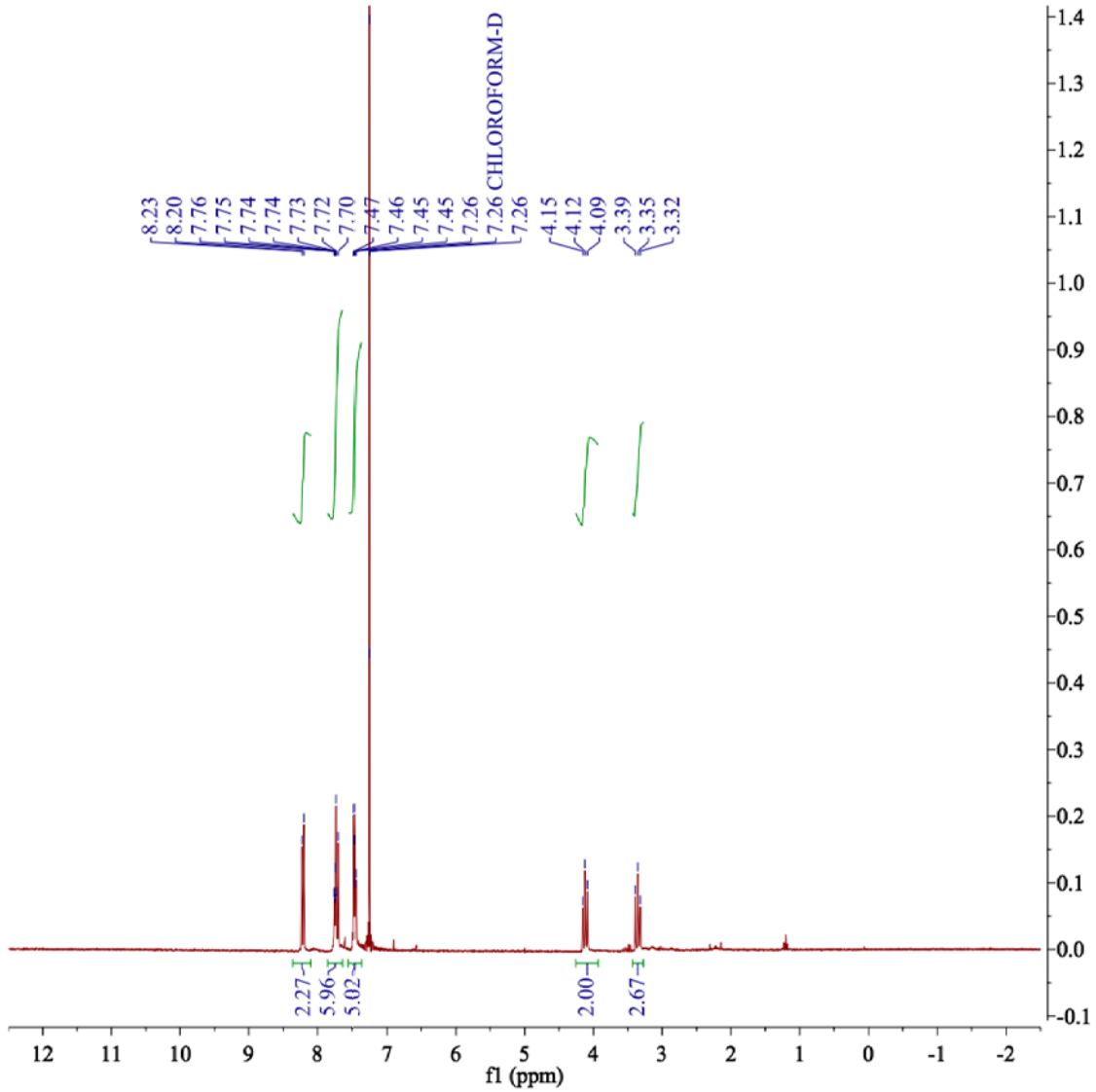

Parameter	Value
Data File Name	/ Volumes/ Lexar/ MH03_20_DEPT_CARBON-3.jdf
Title	MH03_20_DEPT
Comment	
Origin	JEOL
Owner	
Site	
Instrument	ECX 300
Author	Delta
Solvent	DMSO-D6
Temperature	22.4
Pulse Sequence	single_pulse_dec
Experiment	1D
Probe	2692
Number of Scans	1024
Receiver Gain	60.0
Relaxation Delay	2.0000
Pulse Width	3.0694
Presaturation Frequency	
Acquisition Time	1.3841
Acquisition Date	2018-04-15T18:26:49
Modification Date	2018-04-15T19:12:50
Class	
Spectrometer Frequency	75.57
Spectral Width	18938.4
Lowest Frequency	-1912.4
Nucleus	13C
Acquired Size	32768
Spectral Size	26214

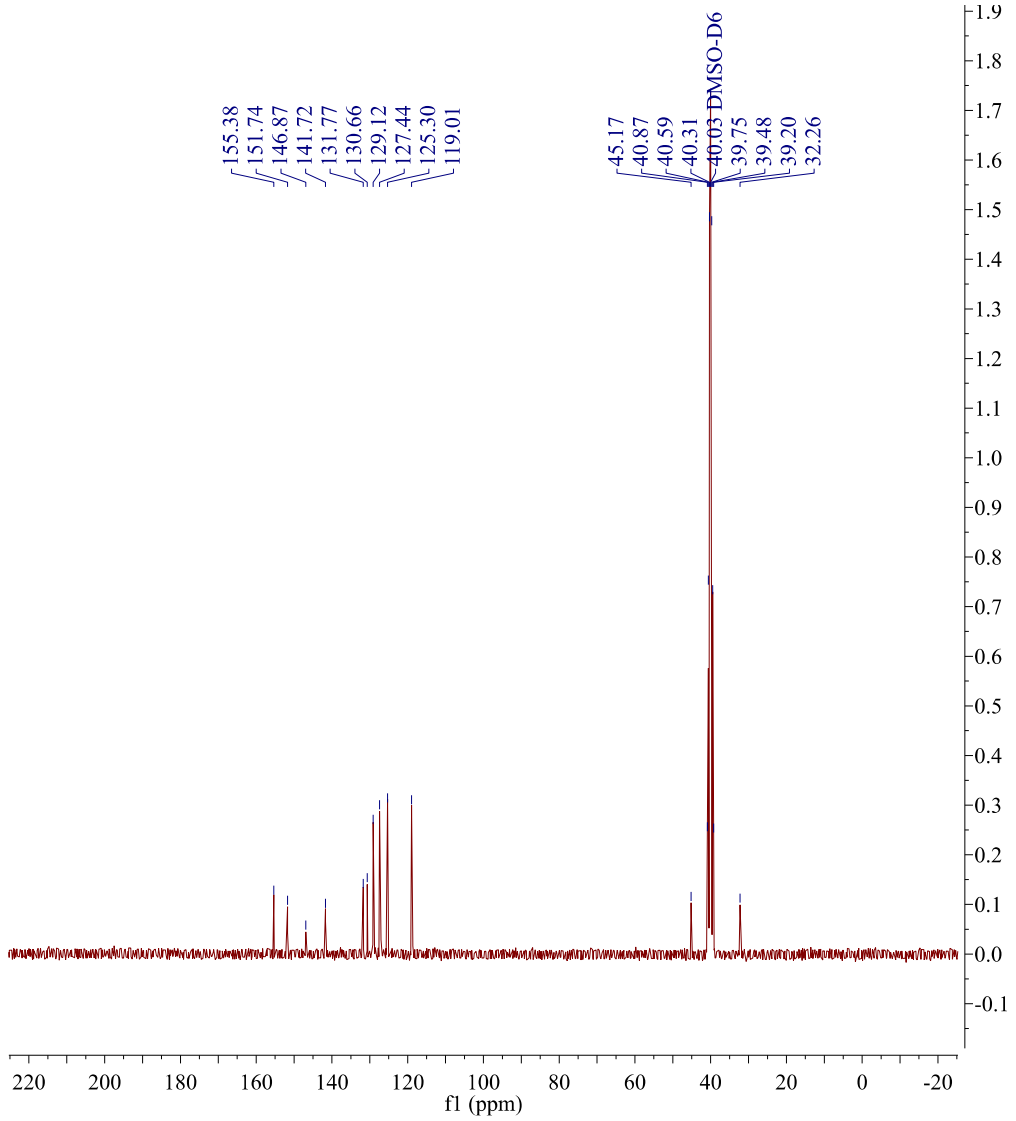

Parameter	Value
Data File Name	/ Volumes/ Lexar/ MH03_20_DEPT_ DEPT135-3.jdf
Title	MH03_20_DEPT
Comment	
Origin	JEOL
Owner	
Site	
Instrument	ECX 300
Author	Delta
Solvent	DMSO-D6
Temperature	22.3
Pulse Sequence	dept.ex2
Experiment	1D
Probe	2692
Number of Scans	191
Receiver Gain	58.0
Relaxation Delay	2.0000
Pulse Width	9.2082
Presaturation Frequency	
Acquisition Time	1.3841
Acquisition Date	2018-04-15T18: 38:25
Modification Date	2018-04-15T19: 12:50
Class	
Spectrometer Frequency	75.57
Spectral Width	18938.4
Lowest Frequency	-1912.4
Nucleus	13C
Acquired Size	32768
Spectral Size	26214

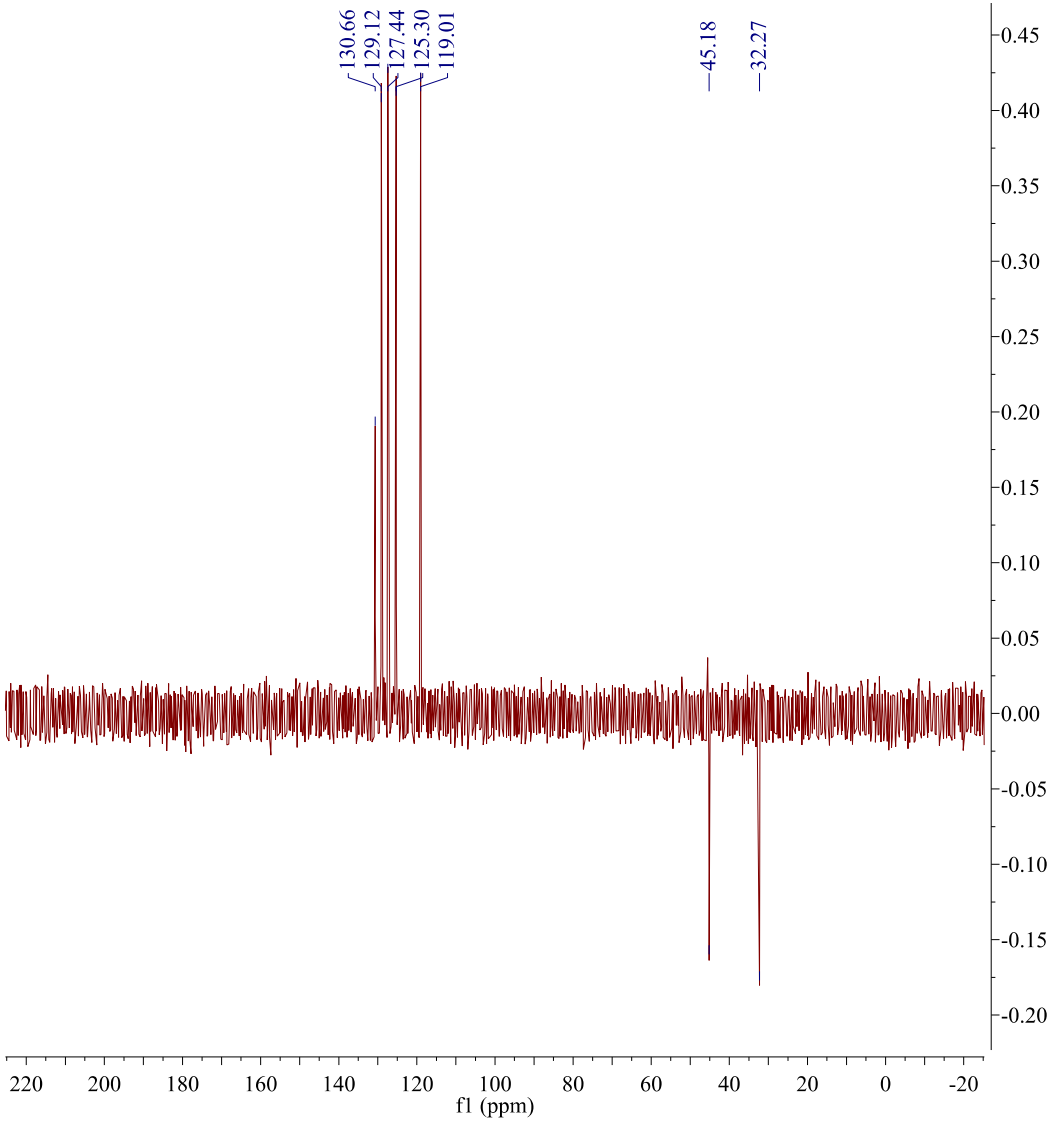

Who	What	When	Parameters	Comment
Organic Chem	Created as New Dataset	10/15/2017 2:59:19 PM		Sample 014 By organic lab Date Sunday, October 15 2017
Organic Chem	Atmospheric Correction	10/15/2017 2:59:19 PM		

Spectrum Graph

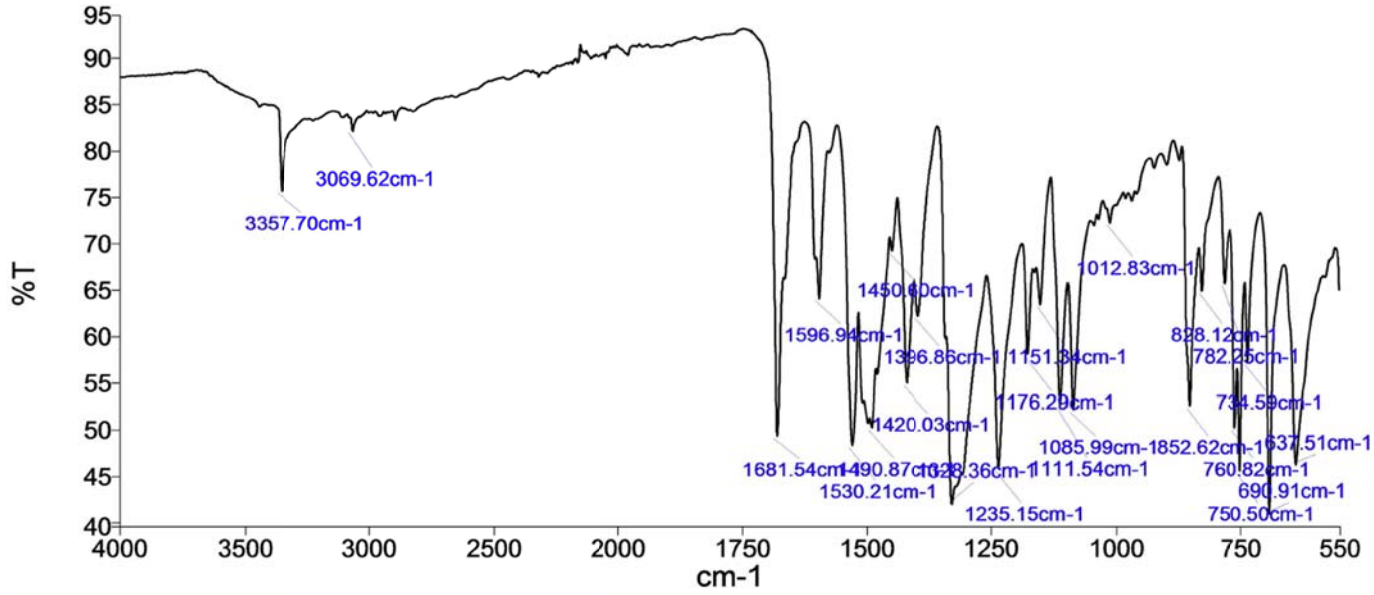

Name	Description
MH03_20	Sample 014 By organic lab Date Sunday, October 15 2017

Compound 26

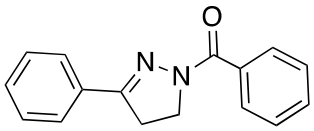

Synthesis of phenyl (3-phenyl-4,5-dihydro-1*H*-pyrazol-1-yl)methanone:

3-phenyl-4,5-dihydro-1H-pyrazole (0.92 g, 6.26 mmol, 1.00 equiv.) in 50.0 mL chloroform was chilled on ice before the addition of triethylamine (0.65 mL, 6.26 mmol, 1.00 equiv.) followed by benzoic anhydride (1.42 g, 6.26 mmol, 1.00 equiv.). This solution was warmed to room temperature and stirred for three hours, the resulting white solid precipitate was vacuum filtered and dried, in 85.4% yield.

This compound was not fully characterized and has not been screened for ADH inhibition.

IR (neat, cm^{-1}): 3199.1, 3001.1, 1665.5, 1628.7, 1486.7, 1284.8, 1028.1, 868.8, 703.7.

Who	What	When	Parameters	Comment
Organic Chem	Created as New Dataset	12/7/2017 3:16:26 PM		Sample 002 By organic lab Date Thursday, December 07 2017
Organic Chem	Atmospheric Correction	12/7/2017 3:16:26 PM		

Spectrum Graph

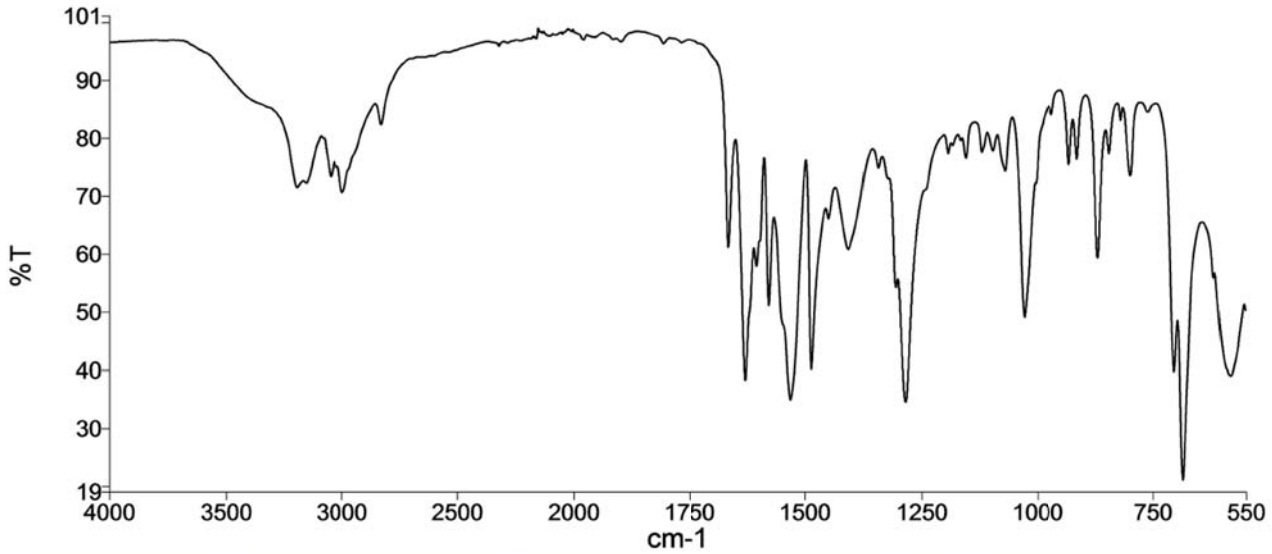

Name	Description
MH03_70	Sample 002 By organic lab Date Thursday, December 07 2017

Supplemental Information B

Horse Liver Alcohol Dehydrogenase FASTA Sequence (1HLD)[31]

Highlighted region indicates the substrate binding region of the active site. These residues (residues 49-67) are interacting with the substrate/positioned compound **1** as indicated by AutoDock analysis. Pink highlighted regions indicate charged residues. Green regions indicate nonpolar residues and yellow regions indicate polar residues.

>1HLD:A|PDBID|CHAIN|SEQUENCE
STAGKVIKCKAAVLWEEKKPFSIEEVEVAPPKAHEVRIKMVATGICRSDDHVVS
GTLVTPLPVIAGHEAAGIVESIGEGV
TTVRPGDKVIPLFTPQCGKCRVCKHPEGNFCLKNDLSMPRGTMQDGTSRFTCRG
KPIHHFLGTSTFSQYTVVDEISVAKI
DAASPLEKVCLIGCGFSTGYGSAVKVAKVTQGSTCAVFGLGGVGLSVIMGCKAA
GAARIIGVDINKDKFAKAKEVGATEC
VNPQDYKKPIQEVLTEMSNGGVDFSFEVIGRLDTMVTALSCCQEAYGVSVIVGV
PPDSQNLSMNPMLLLSGRTWKGAIFG
GFKSKDSVPKLVADFMAKKFALDPLITHVLPFEKINEGFDLLRSGESIRTILTF

>1HLD:B|PDBID|CHAIN|SEQUENCE
STAGKVIKCKAAVLWEEKKPFSIEEVEVAPPKAHEVRIKMVATGICRSDDHVVS
GTLVTPLPVIAGHEAAGIVESIGEGV
TTVRPGDKVIPLFTPQCGKCRVCKHPEGNFCLKNDLSMPRGTMQDGTSRFTCRG
KPIHHFLGTSTFSQYTVVDEISVAKI
DAASPLEKVCLIGCGFSTGYGSAVKVAKVTQGSTCAVFGLGGVGLSVIMGCKAA
GAARIIGVDINKDKFAKAKEVGATEC
VNPQDYKKPIQEVLTEMSNGGVDFSFEVIGRLDTMVTALSCCQEAYGVSVIVGV
PPDSQNLSMNPMLLLSGRTWKGAIFG
GFKSKDSVPKLVADFMAKKFALDPLITHVL PFEKINEGFDLLRSGESIRTILTF